

Laser Ablation -Inductively Coupled Plasma -Mass Spectrometry

(LA - ICP - MS)

I- Introduction

II - Instrumentation

- II-1- The Inductively Coupled Plasma (ICP)
- II-2- The Mass Spectrometer (MS)
 - A-Introduction
 - B-The Finnigan Element
- II-3- Laser ablation (LA)
 - A Description of the Laser ablation System
 - B Operating parameter
 - Laser wavelength
 - Pulse mode and repetition rate
 - Spatial resolution / crater shape
 - Calibration strategy
 - C Results on standards
 - Peak Shape
 - Element response factors
 - Limit Of Detection
 - Precision and accuracy

III- Applications of LA-ICP-MS on geological samples

- III-1- Sample preparation
- III-2 Trace elements determination
 - A- Introduction
 - B- In situ determination of trace element in minerals
 - C- Interference
 - D- Medium Resolution
 - E- Comparison with other analytical technique
 - F- Fluid inclusions
- III-3- Element fractionation
- III-4- Data Reduction software
- III-5- Future Improvements
 - Standard Quality
 - Time of Flight Instruments
 - Sample cell design
 - Mixed gas (Nitrogen and Helium)
 - Picosecond laser
 - The fifth harmonic
 - New Calibration Strategies

IV- Bibliography

V- Laser Ablation Pits (Merchantek LUV 266)

I- Introduction

Samples for trace element analysis are rarely in a form suitable for direct introduction to an Inductively Coupled Plasma Mass Spectrometer (ICP-MS; Longerich, et al., 1990; Jarvis and Jarvis, 1992; Falkner et al., 1995). They are dissolved to form solutions for aspiration into the spectrometer excitation source. In many cases, it would be desirable to analyse solid samples directly, without lengthy sample preparation procedures which sometimes leads to analytical problems (Totland, et al., 1992; Stotesbury, et al., 1989; Jarvis, 1990). Many analytical methods have been developed for direct solids analysis, each with unique strengths and weaknesses. Most recently, laser sampling, used in conjunction with ICP-MS, has been shown to be promising for direct trace element determinations in solids (Shibata et al, 1993; Richner et al 1994; Paul 1994; Perkins and Pearce, 1995; Arrowsmith, 1987; Denoyer, et al., 1991; Fryer, et al., 1995; Gray, 1985; Jackson, et al., 1992; Longerich, et al., 1993; Perkins, et al., 1993; Jarvis and Williams, 1993, Ludden, et al., 1995, Perkins and Pearce, 1995, Norman, et al., 1996, Longerich, et al., 1996, Hinton, 1997, Durrant 1999, Alexander et al 1998, Russo 1998, Durrant 1999; Günther et al, 2000).

After a description of the instrumentation, I will present some results obtain on synthetic Standard Reference Materials and on different geological samples using laser ablation in conjunction with a high resolution Inductively coupled plasma mass spectrometer.

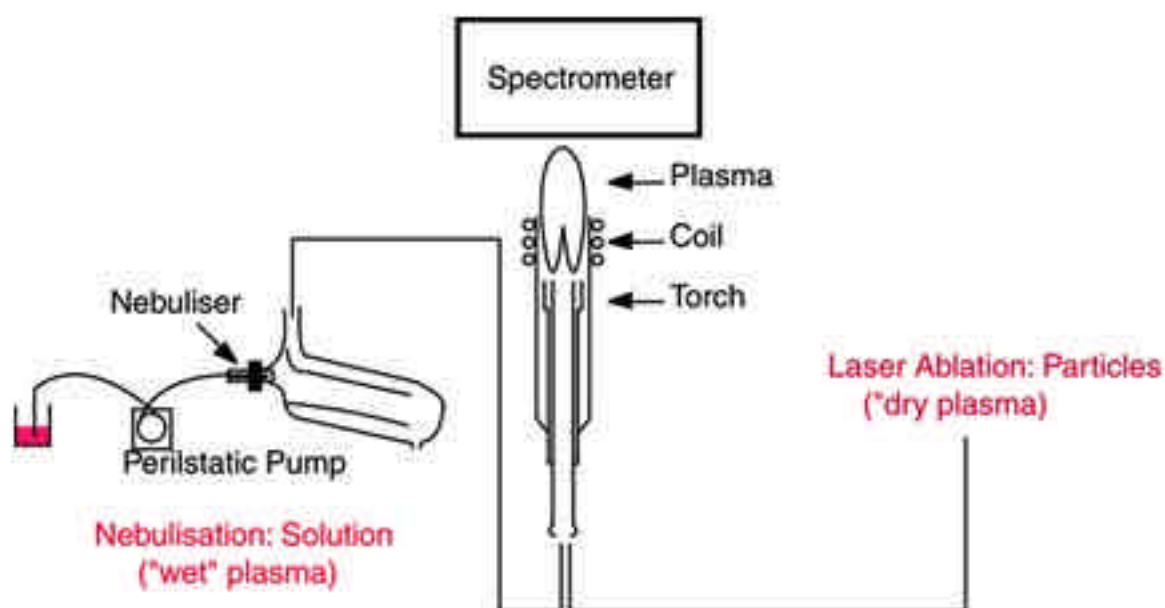


Fig. 1: Schematic representation of the sample introduction in ICP-MS (from Jarvis and Jarvis, 1992).

II- Instrumentation

II-1- The Inductively Coupled Plasma (ICP)

Inductively Coupled Plasma are used as emission sources for the mass spectrometer. Usually sample introduction for plasma spectrometry is generally accomplished using solution nebulisation. Sample is aspirated by a nebuliser using a peristaltic pump (a typical Scott type spray chamber limits the size of the droplets (<10 micron) that reach the plasma). Solutions or vaporised particles from a laser sampling device may be swept with a flow of argon into the plasma. In ICP spectrometry, the plasma (luminous volume of partially ionised gas) is generated from radiofrequency magnetic fields induced by a copper coil, which is wound around the top of a glass torch (Fig. 1). The plasma could be "wet" if solution is introduced into the torch, which produces a large amount of interference by oxides formation. This plasma could also be "dry" by using a laser ablation sampling device which leads to a reduction in the level of oxide interference. Hot argon and sample ions (8000K) are accelerated through the sample cone orifice to produce a supersonic jet of gas in the expansion chamber. The skimmer cone pierces the back of the supersonic jet and extracts a small proportion of the plasma gas. Ions extracted from this gas are focussed and shaped in the mass spectrometer interface using ions lenses. The proportion of ions, sampled from the plasma, that reach the detector is very small (1 in 10^6 - 10^8) and usually a high gain ion detection system is essential if low limits of detection are to be achieved. The problem is exacerbated in the case of laser sampling because of the competitive factor between lower spatial resolution (less volume ablated) and lower limit of detection (which needs higher volumes of ablation). This problem might be in part resolved by (a) a modification of the interface between the ICP and the quadrupole based mass spectrometer. By adding a larger pumping in the expansion chamber region of the interface, more material from the plasma is drawn to the mass spectrometer which improves the sensitivity ((Günther, et al., 1995). (b) using small aperture sample cone and probably larger aperture torch. Günther, et al. (1996) have shown that a reduction of the sample cone orifice diameter from 0.7 mm to 0.5 mm limit the air entrainment (H, C, N, O and Ar) and thus lower the background by a factor of ca. 100 in the low mass range and by a factor of ca. 10 in the higher mass range (using a Quadrupole mass spectrometer) (c) Using the CD option from Finnigan. A grounded platinum electrode (GuardElectrode™) is inserted between the quartz ICP torch and the RF load coil to prevent capacitive coupling from the load coil into the ICP. The ICP is then sustain by "pure" inductive coupling, and the secondary discharge between the ICP and mass spectrometer sampling cone is eliminated. This process leads to a higher (10 fold improvement) transmission for ions of all m/z (Wiederin and Hamester, 1997). Unfortunately only a slight improvement (1.5 fold improvement) has been observed under dry plasma conditions. (d) increasing the ion extraction energy (2000 eV instead of a few eV for a quadrupole type) using a double focussing mass spectrometer.

II-2- The Mass Spectrometer (MS)

A- Introduction

Two types of mass spectrometers are used in ICP-MS.

The most popular is the quadrupole mass filter (Fig. 2). By varying the electric signals to a quadrupole it is possible to transmit only ions within a very small m/z ratios (other ions are neutralised and carried away as uncharged particles). A quadrupole mass filter consists of four parallel metal rods. Two opposite rods have an applied potential of $(U+V\cos(\omega t))$ and the other two rods have a potential of $-(U+V\cos(\omega t))$, where U is a dc voltage and $V\cos(\omega t)$ is an ac voltage. The applied voltages affect the trajectory of ions travelling down the flight path centred between the four rods. For given dc and ac voltages, only ions of a certain mass-to-charge ratio pass through the quadrupole filter and all other ions are thrown out of their original path. A mass spectrum is obtained by monitoring the ions passing through the quadrupole filter as the voltages on the rods are varied.

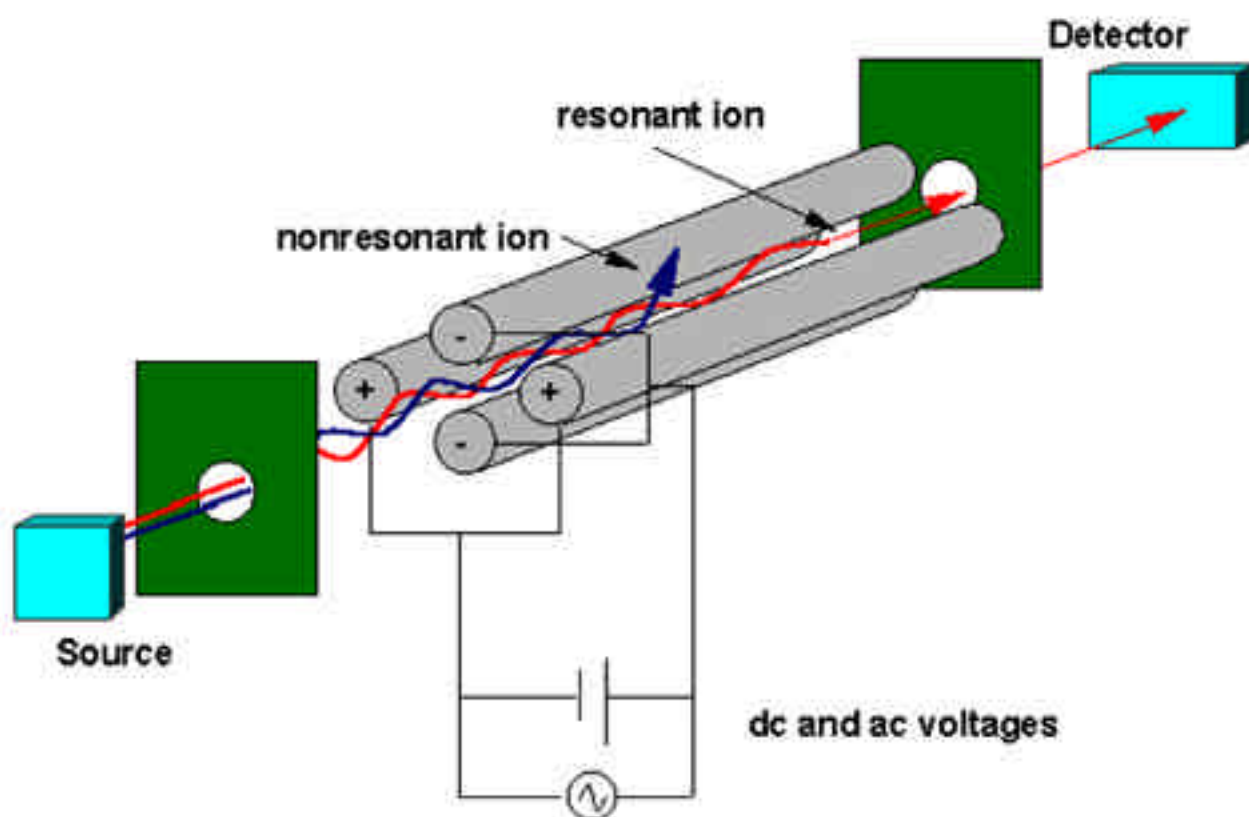


Fig. 2: Schematic of a quadrupole filter (picture from <http://www.scimedia.com/chem-ed/ms/quadrupo.htm>)

The other type of instrument is a magnetic sector (with a radii of r_1) which simultaneously disperses ions (of charge = e and velocity = v) by a magnetic field (field strength = H) as a function of their m/z ratio between the poles of a magnet (first focus).

Most magnetic sector mass spectrometer are usually single focussing but recent mass spectrometers, are double focussing by adding an electrostatic analyser (with a radii of r_2 and a field strength of E/d) to separate ion (with a charge = e) with differences in kinetic energies (KE, second focus).

When the magnetic sector is located before the electrostatic analyser the instrument is in Reverse Geometry (RG) in comparison to Nier-Johnson Forward Geometry. The ion beam generated at the interface is transmitted into a magnetic sector where it undergoes

mass dispersion. Then the electrostatic sector bring the ion beam of filtered kinetic energy into focus through the exit slit. Moreover double focussing mass spectrometers have a Higher Resolution (HR) in comparison to quadrupole mass filters which is important for reducing the level of polyatomic ion interference introduced to the mass spectrometer by the ICP.

Doubly focussed ions are counted using a secondary electron multiplier, which consists of a series of biased dynodes that eject secondary electrons when they are struck by an ion. They therefore multiply the ion current and can be used in analog or digital mode. Other types of double focussing mass spectrometers use a multi-collector assembly, which consists of eight independently adjustable Faraday collectors and one fixed axial Faraday collector (multiple collector mass spectrometry; Halliday, et al., 1995; Christensen, et al., 1995; Lee and Halliday, 1995; Taylor, et al., 1995; Walder, et al., 1993; Walder, et al., 1993; Walder and Furuta, 1993; Hirata, 1996; Balaram, 1995; Thirlwall and Walder, 1995; Hirata, 1997; Blichert-Toft, et al., 1997). The disadvantage of this system is the high ion count rate required by the Faraday collector. Since a Faraday cup can only be used in an analog mode it is less sensitive than secondary electron multiplier that are capable of operating in pulse-counting mode. Hence, limit of detection are high.

B- Double focussing mass spectrometers (The Finnigan Element TM)

The use of the magnetic sector mass spectrometers offer lots of advantages in terms of (1) resolution; (2) peak shape (3) background.

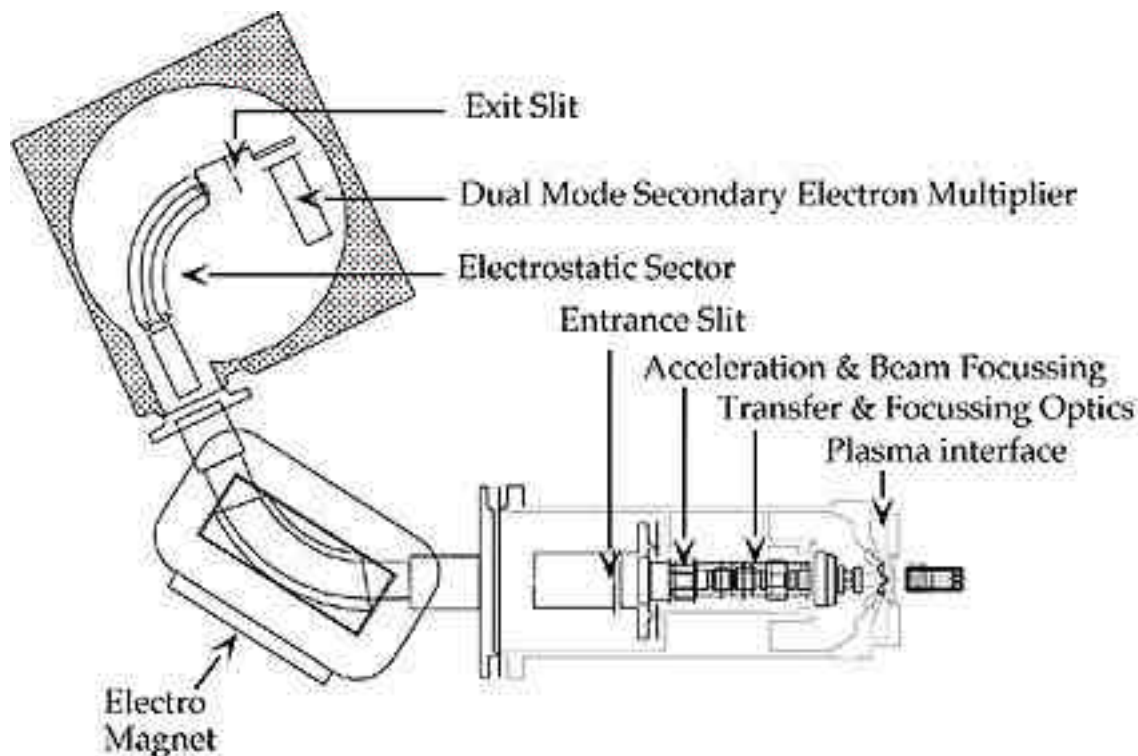


Fig. 3: Schematic diagram of a Reverse Geometry High Resolution-ICP-MS instrument (the Finnigan ELEMENT, (Feldmann, et al., 1994) divided into three main parts: (1) the ICP with the interface (cones and ion optics); (2) the analyser (magnetic sector and electrostatic analyser); (3) the detector (secondary electron multiplier: SEM).

(1) In comparison to quadrupole mass filters, double focussing mass spectrometers permit variable resolution using three sets of slit positions ($M/\Delta M = 300, 3000, 7500$) which is important for reducing the level of polyatomic ion interference introduced to the mass spectrometer by the ICP. This is critical for the accurate quantification of elements such as P, S, As, K, Ca and the transition elements that can exhibit significant isobaric interference (Giebmann and Greb 1994, Moens et al. 1994, Tittes et al. 1994, Moens et al. 1995, Vanhaecke et al. 1997).

(2) The flat topped peak shape obtained using stable magnetic sector instruments allows better precision for isotope ratio measurements in comparison to the gaussian peak shape produced by quadrupole-based instruments designed for scanning over a relatively large mass range (e.g. Begley and Sharp 1997).

(3) The curvature of the optical axis of the double-focussing geometry greatly reduces the photon background derived from the ICP torch without reducing sensitivity. For heavy masses, the background counting rate is negligible (< 0.2 cps) which significantly increases signal/noise and provides enhanced limits of detection in comparison to quadrupole-based instruments which tend to have a high background (~ 10 cps). Background is only significant for light

elements, due to spectroscopic interference from the argon carrier gas. However, molecular oxides and hydroxides are significantly reduced under the dry plasma conditions encountered during laser ablation analysis.

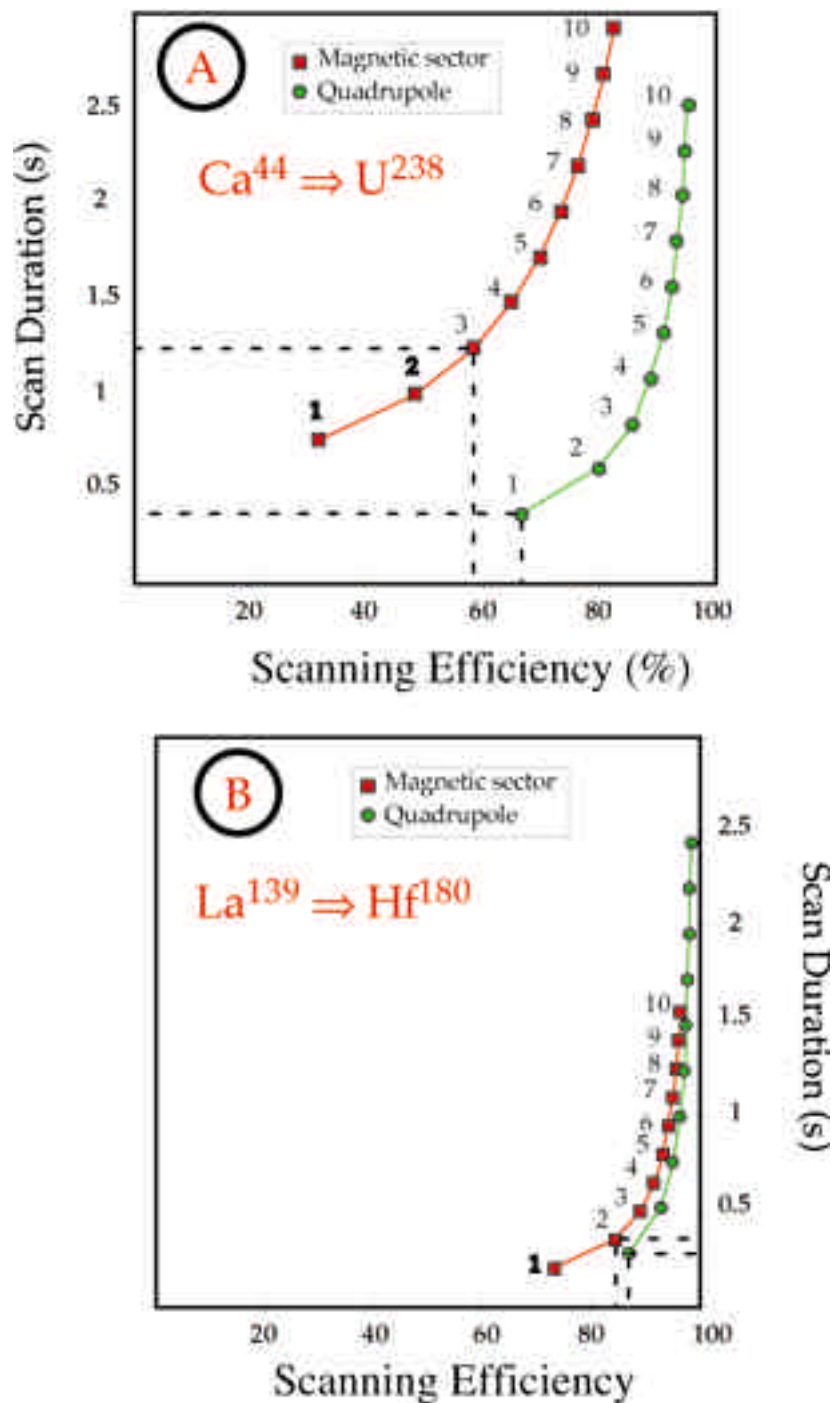


Fig.4: Scanning efficiency vs scan duration for different scan range when comparing a magnetic and a quadrupole instrument (see text for detail)

The particular design of the ion source of the ELEMENT (Plasma, torch, skimmer, sampler and all other mechanical parts including the pumping system operate at ground potential; (Giebmann and Greb, 1994) allows rapid electric scanning of up to 30% from its nominal

starting magnet mass without excessive loss of ion energy and subsequent beam defocussing. (i) Elements are divided into small groups in order to minimise the use of the magnet which has a longer jump time. The total scan thus comprises a series of large magnetic jumps using 1 ms per amu of travel plus 5 ms for the magnet to settle. (ii) The mass window is reduced over the peak top, in order to acquire only three or four channels per peak top with a dwell time of 10 ms. Using four channels per peak top and a menu of 30 elements which cover nearly the entire mass range (from ^{44}Ca to ^{238}U), the total scan duration is less than 1.7 s. This scan duration can be decreased to 1.4 s using three channels per peak top. Assuming a scan time of 0.5-1 s for a quadrupole mass filter, the total scan duration of the HR-ICP-MS is only about 50% to three times slower than the quadrupole mass filter.

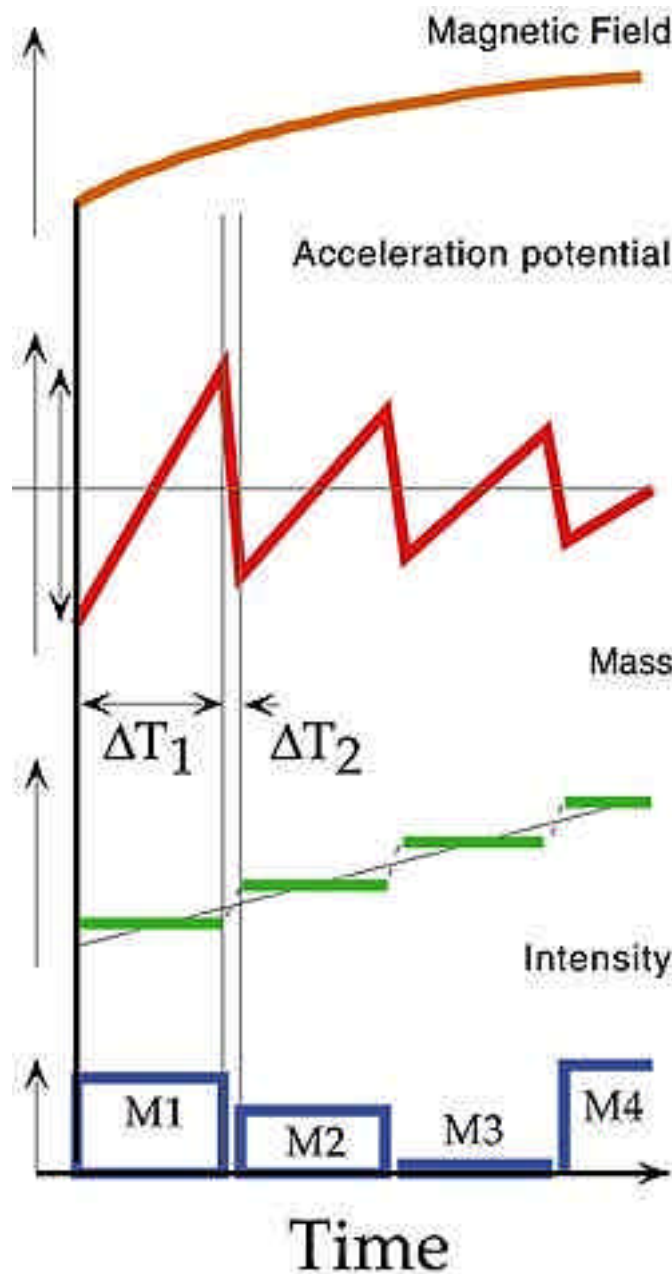


Fig.5: Principal of Synchroscan. M_x = mass registered; ΔT_1 = measurement time; ΔT_2 = jump time. This figure is adapted from Giebmann & Greb (1994).

Figure 4 illustrate a comparison of the scanning efficiency of a magnetic sector instrument and a quadrupole instrument using from 1 to 10 channel per peak with a dwell time of 10 ms. The settling time of the quadrupole has been set at 5 ms. For a magnetic sector instrument, the scanning efficiency is dependant on the element menu i.e. the mass range covered by the magnet. Figure 4A illustrate a typical scanning range from Ca44 up to U238. This figure shows an optimal and lower efficiency (57%) for magnetic sector at 3 points per peak. Using the same element menu, the quadrupole is more efficient with one (66%) or three (85%) channel per peak. However, in some other applications, such as the measurement of the REE in zircon using Hf180 as an internal standard, a magnetic sector instrument can have an efficiency similar to a quadrupole mass filter as illustrate in Figure 4B.

Although we have used a succession of magnetic (B) and electric (E) scan in our experiment, another scanning strategy, currently under investigation, is called SynchroScan. As illustrate in figure 5, by allowing magnetic and electrostatic fields to change at the same time, on-peak duty cycle of the instrument should be improved. While the magnet continuously scan at a constant speed from lower to higher masses, the electric field scans in opposition to the magnetic field which "freezes" the mass that pass through the analyser. Because the ELEMENT can scan over the full mass range in less than 0.6 s the efficiency should increase. Based on our calculated drilling rate of the laser at optimum configuration (1 micron per second), this new scanning strategy should allow an acquisition every 0.6 microns. However this new scanning facility is still in development and no method created through the ICP software could support this scanning tool at the moment.

II-3- Laser ablation (LA)

Principle of Laser

Laser is an acronym for **L**ight **A**mplification by **S**timulated **E**mission of **R**adiation. As a consequence of its light-amplifying property, a laser produces spatially narrow and extremely intense beams of radiation having identical frequency, phase, direction and polarisation properties. According to the resonance condition ($E = h\nu$) and to the rules of quantum mechanics, an atom can change its energy level, which leads to the absorption or emission of a photon. Stimulated emission is the basis of laser behaviour. Stimulated emission leads to the emission of a coherent radiation with the incoming radiation. In order to have light amplification in a laser it is necessary that the number of photon produced by stimulated emission exceed the number of photons lost by absorption. This light amplification is only achieved when a population inversion from the normal distribution of energy state exists. This population inversion (activation of a laser material) is created by an external pumping source, so that a few photons of proper energy will trigger the formation of a cascade of photons of the same energy. This cascade of photons is focussed on a sample. Interaction between the laser beam allows the conversion of photon energy into thermal energy, which is responsible for the vaporisation of most of the exposed solid surface. The material ablated is swept away with an argon stream to an Inductively Coupled Plasma Mass Spectrometer (ICP-MS) and analysed.

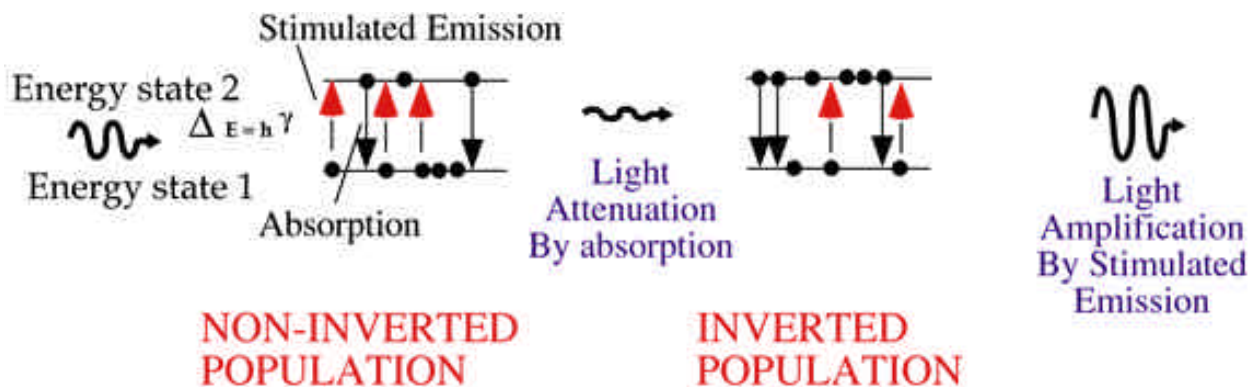


Fig.6: Principle of Light amplification. Passage of radiation through a non-inverted population and an inverted population.

Two main types of UV lasers are widely used in Earth Sciences:

(1) **Excimer gas** lasers in which light is emitted by a short-lived molecule made up of one rare gas atom (Kinsley, et al. 1997; Balhaus, et al. 1997; Gahderi, et al. 1997; Sinclair and McCulloch 1997; Bea, et al. 1996; Ducreux-Zappa and Mermet 1996; Eggins, et al. 1998; Günther, et al. 1997; Sylvester and Ghaderi 1997; Sylvester 1997) This type of laser is beginning to be used in LA-ICP-MS. Its operation depends on electronic transitions in molecules.

(2) **Solid state** lasers such as the frequency-quadrupled Nd:YAG in which the atoms that emit light are fixed within a crystal or a glassy material. Lasers are characterised mainly by their wavelength (1064 nm for a Nd:YAG), output power and pulse length fixed by the design of the laser (nanosecond or picosecond)

NB:

$$\text{PULSE LENGTH} = 2Ln / C(1-R)$$

L = cavity length

c = speed of light in vacuum

n = laser medium refractive index

R = output mirror reflectivity

Solid interaction:

Laser - material interaction is a complex process resulting in (1) vaporisation or ablation; (2) ejection of atoms, ions, molecular species and particulate; (3) shock waves. Power density is a critical parameter which allows the separation of two different processes; (1) vaporisation and (2) ablation.

Laser ablation of a solid sample consists of several stages, in which different kinds of 'vapor-products' are ejected. The initial stage is electronic excitation inside the solid, accompanied by the

ejection of electrons at the sample surface, due to photoelectric and thermionic emission. During this time, the energetic electrons in the bulk of the solid transfer energy to the lattice through a variety of scattering mechanisms; the sample target then undergoes melting and vaporization, followed by ionization and the formation of a plasma plume consisting of the sample constituents. The expanding plume interacts with the surrounding gas to form a shock wave, causing the ambient gas to become further ionised. The expanding high-pressure plasma exerts a force back to the target, which flushes out the melted volume. This recoil pressure and flushing mechanism can produce large-sized particles (several micrometers, Borisov et al, 2000). The transport efficiency to the ICP is typically low for small diameter particles <5nm, which tend to be lost by diffusion, and is also low for large particles > 3 μm, which will settle out owing to gravity. Particles with diameters between these extremes are carried with an efficiency of >80%.

NB: Power density is calculated according to the energy of the beam, the spot size and the pulse width. The power density is calculated following the formula below:

$$[(\text{Energy} / \text{Area}) * \text{Correction Factor}] / \text{Pulse Width}$$

with a correction factor of 2.3 for Gaussian beam and a correction factor of 1.5

A- Description of the Merchantek Laser ablation System

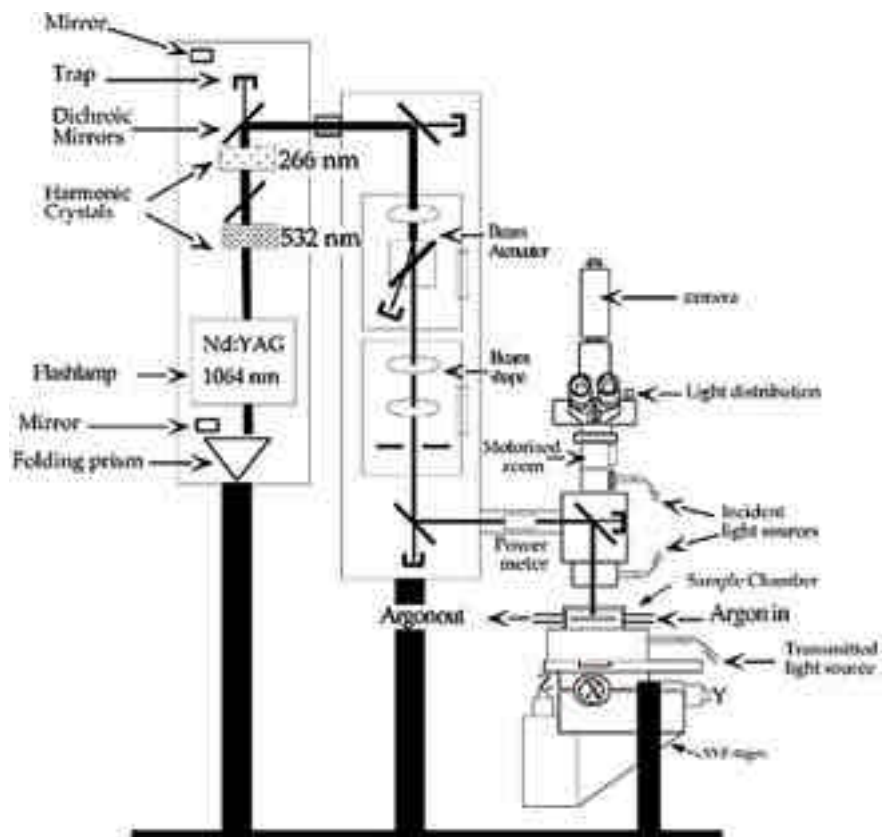


Fig.7: Sketch of the First version of the petrographic laser ablation system from Merchantek.

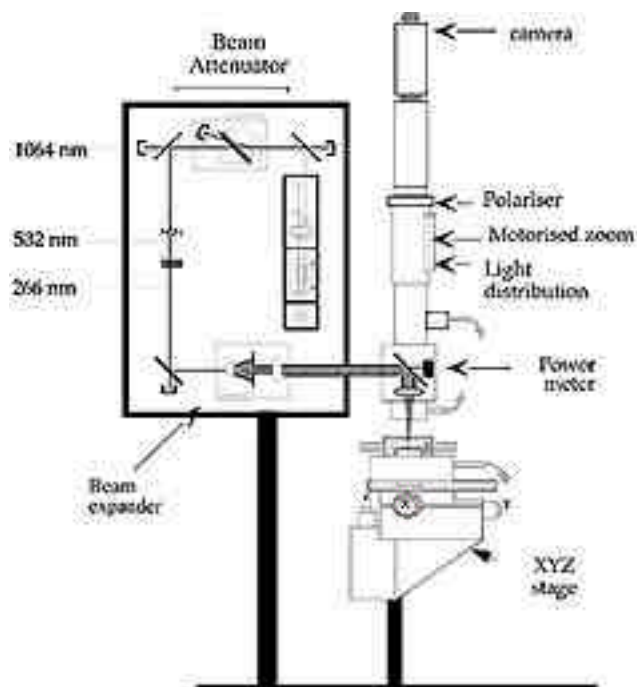


Fig.8: Sketch of the third generation of the petrographic laser ablation system from Merchantek.

The Merchantek laser is a Nd:YAG laser which comprises a rod of Yttrium aluminium garnet ($Y_3Al_5O_{15}$) doped with approximately 3wt% Nd_2O_3 , providing a wavelength of 1064 nm. The wavelength of the beam generated by the laser within the resonator cavity is frequency quadrupled to the Ultra Violet (UV) range using two harmonic crystals. The maximum output energy is about 10 mJ with a pulse length of 4 ns with the first design of the laser system (Fig. 7). This first system failed several times, mainly due to the inefficiency of the optics to match the high power density generated by the laser. The third generation is less powerful with a maximum of 5mJ output (Fig. 8). The output energy can be changed by varying the voltage applied to the flashlamp of the cavity resonator or by using a beam attenuator. The size and shape of the beam is also monitored by a beam expander. The beam is finally focussed on a sample through the objective lens of a microscope. The sample is observed through a microscope using three different light sources (incident, transmitted and reflected). The sample is contained within a sample cell and connected to an XYZ motorised stage. This laser sampling use electronic stepper motors to move the stage on which the sampling cell is mounted. Remote control X, Y and Z axes stages allow you to move the sample under the laser beam in different manners: single point, along a line or within an area (raster).

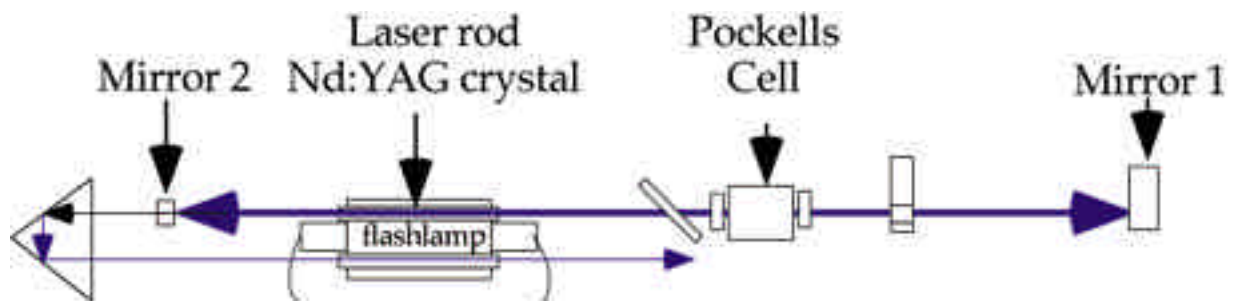


Fig.9 : Schematic of the Merchantek laser cavity.

Laser cavity:

When a discharge occurs in the xenon flashlamp, the atoms Nd^{3+} of the Nd:YAG laser are raised from the ground state to the pumping level. This optical pumping produces an overpopulation of excited-state Nd. The system becomes unstable and a photon will stimulate the emission of a cascade of photons. The light pulse is reflected from the two mirrors and is amplified each time it passes through the laser rod. Because of the design of the cavity resonator, light produced is amplified until it reaches a threshold and emission can occur. By placing an optical switch (Pockells Cell, Fig 9) between the laser rod and one of the mirrors, the laser run in a Q-switched mode which leads to the formation of a single large output pulse.

Harmonic Crystals:

The large output pulse generated within the cavity resonator has a fundamental wavelength of 1064 nm (Infra Red) characteristic of the Nd:YAG laser rod. The Infra Red wavelength can be frequency-quadrupled to 266 nm using two harmonic generating crystals which provide second and fourth harmonics in the visible (532 nm) and ultraviolet (266 nm). Two dichroic mirrors are also necessary to reflect the initial wavelength of the laser after the first harmonic crystal and finally reflect the UV beam toward the beam attenuator.

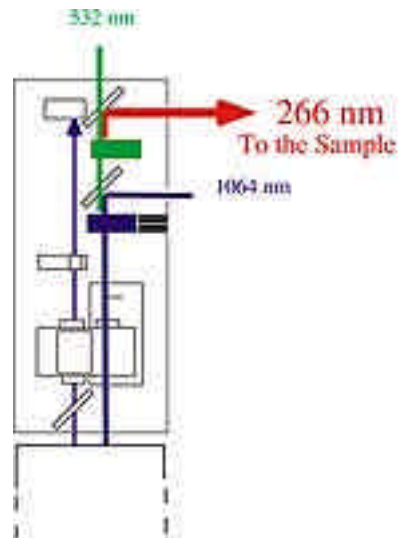


Fig.12 : Schematic of the harmonic crystals from the first design of the laser

Beam Attenuator:

The initial output energy is reduced using a half wave retardation plate and a calcite polarising prism. By rotating the half wave plate with angular velocity w (the output polarisation rotates at an angular velocity of $2w$) the polarised beam emerges from the prism with different irradiance I_s and I_p . Depending on the orientation of the prism, the laser beam can be reflected by the prism to a trap ($w = 45^\circ$, $I_s \sim 100\%$, Fig 13b) or pass through the prism without any attenuation ($w = 0^\circ$, $I_p \sim 100\%$, Fig 13a)

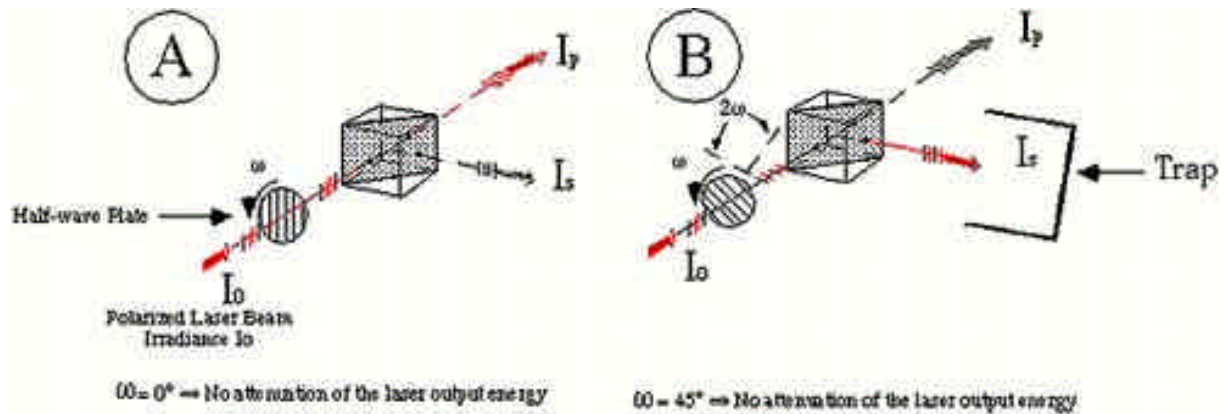


Fig.13 : Schematic of the beam attenuator

Beam Expander:

By moving the beam expander lenses from one to another, the beam size can be changed from 400 μm to 10 μm . An aperture can also change the energy profile of the beam from gaussian to a "top hat" beam profile.

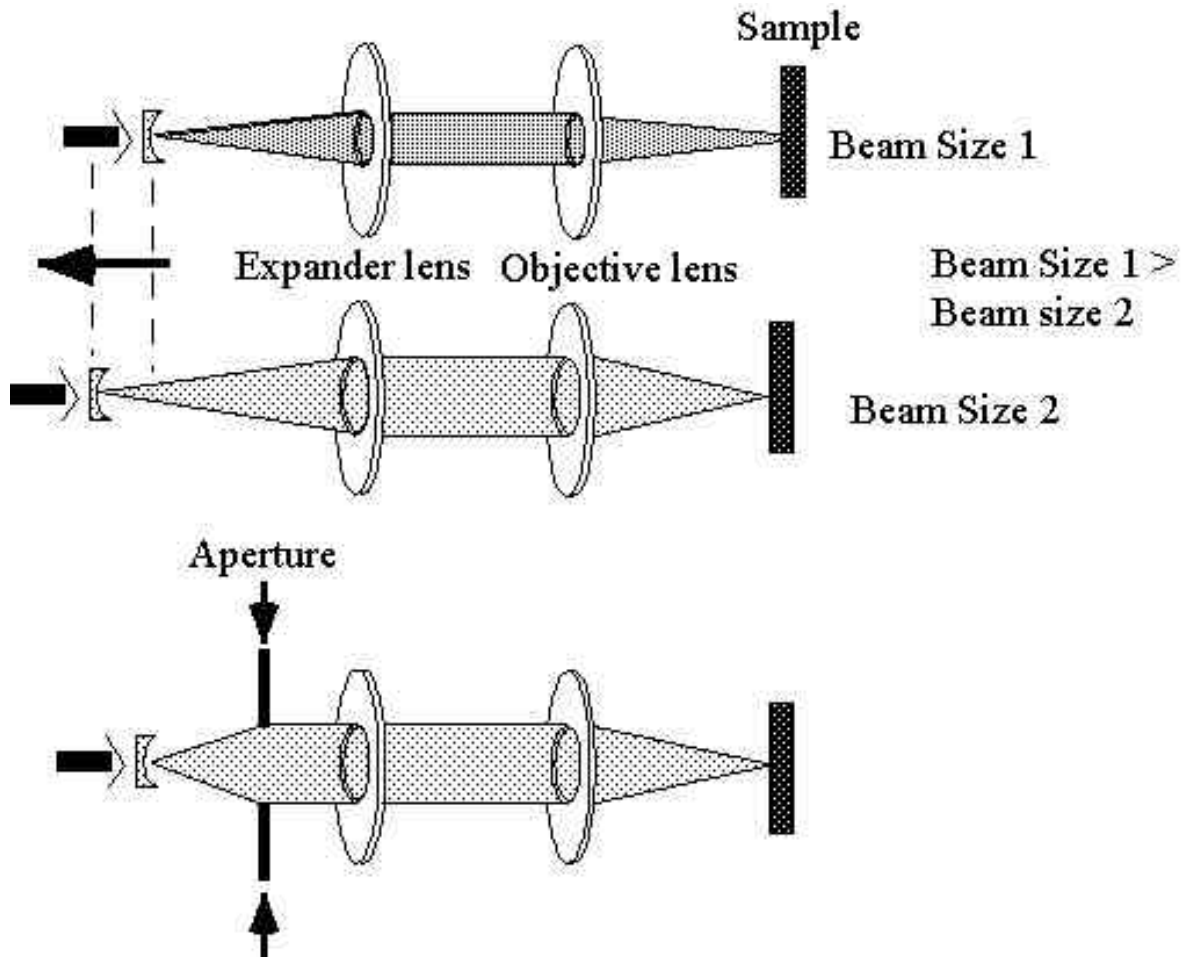


Figure 14: Schematic of the beam expander. The movement of the two lenses from one to another is responsible for the modification of the spot size and the closure of the aperture is responsible for the change in the energy beam profile.

B- Operating parameter

With laser sampling, several operating parameters that affect the sampling event are at the control of the analyst:

- (1) pulse mode and repetition rate;
- (2) spatial resolution and peak shape;
- (3) calibration strategy:

Laser wavelength

Pioneer work on laser ablation used a ruby laser (Cr³⁺, 694 nm) mounted in a binocular microscope (Gray 1985; Moenke-Blankenburg 1989). Efficiency of ablation is related to the wavelength of the laser. Ablation at 1064 nm, 694 nm and 532 nm radiation produced elemental fractionation that relates to the melting point of the elemental oxide, whereas with 266 nm ablation is independent of the elemental oxide melting point (at least at the beginning, Outridge, et al. 1996; Figg and Kahr 1997; Figg, et al. in press). Using the fundamental IR wavelength of the Nd:YAG laser, ablation of material such as quartz or synthetic silicate glasses (NIST 612) results in a catastrophic failure because of a lack of absorption of the laser beam of this wavelength by these materials (Feng 1994; Morrison, et al. 1995). Absorption of the laser beam is dependant on the chemical composition and the orientation of minerals (Hazen, et al. 1977; Jeffries, et al. 1995).

Pulse mode and repetition rate

There are two modes of operation: (1) Fixed-Q, and (2) Q-switched (Q indicating the Quality of the resonant cavity).

(1) Fixed-Q: When a discharge occurs in the flashlamp, the light pulse passes through the laser rod and is reflected from the two mirrors. The light interacts with the Nd in the laser rod, raising it to an excited state. Any beam of light not parallel with the optical axis or with a wavelength other than 1064 nm is destroyed by interference. The optical pumping from the xenon flashlamp raises the atoms from the ground state to the pumping level. The purpose of the optical pumping is to produce an overpopulation of excited-state Nd as a precursor to laser operation. When such an overpopulation occurs, the system becomes unstable and a photon will stimulate the emission of other photons. Because of the design of the resonator, light produced from such transitions is amplified until it reaches a threshold and emission can occur. When this process is repeated (duration of the flashlamp discharge: ~ 150 ms), it leads to a single laser pulse. In this mode the laser is said to be in free-running or fixed-Q operation.

(2) Q-switched: By placing an optical switch between the laser rod and one of the mirrors of the laser, the Q-switched pulse mode can be executed as either a single pulse or a series of pulses. The higher the Q, the lower the loss. A high loss cavity can store more energy than a one with a low loss. By blocking one laser mirror and excite the laser medium, a population inversion is produce but the laser can't oscillate because the mirror does not reflect light. Stimulated emission will quickly drain the stored laser energy from the cavity in a short pulse with peak power much higher than the laser could otherwise produce. In Q-switched mode, a microplasma is generated at the surface of the sample and the ablation produces a large and more shallow crater.

NB: Early work on ruby lasers (Thompson, et al. 1990) and IR laser (Outridge, et al. 1996) has demonstrated that, depending of the pulse mode and the nature of the ablated material, different types of particle material can be identified in the ejecta after ablation; (a) spherical droplets (0.1-10 μm) during ablation of metallic targets, (b) sharp-edged spall-breccia during ablation of brittle materials, (c) amorphous condensate from the vapour phase all types of material. The formation of these particulate depend on the elemental composition and refractoriness of the sample. Only the smaller size range ($< 2 \mu\text{m}$) is likely to be transported very efficiently by gas flows. In Q-switched mode, one population of particles with the right composition is found but in free-running, two populations of particles are produced with different and unrepresentative compositions. Because of the better ablation efficiency and the representative composition of the material ablated in the Q-switch mode, this mode of operation is more convenient and preferable (e.g., Arrowsmith 1987).

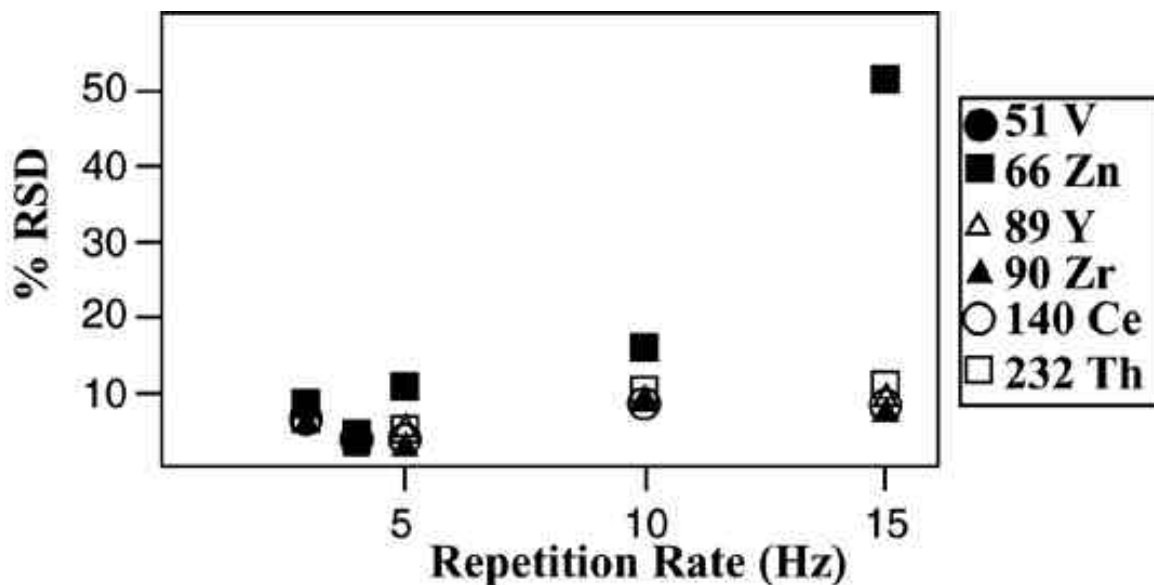


Fig.14: Signal variation (%RSD) for Ca-normalised trace element isotopes (51V, 66Zn, 89Y, 90Zr, 140Ce, 232Th) versus increasing repetition rates (3, 4, 5, 10, 15 Hz) at the same energy (2 mJ) when ablating NIST 612 synthetic glass with a 50 μm wide spot.

A single laser pulse provides a transient signal, however multiple pulses may be used to produce a near steady-state signal analogous to that obtained with continuous solution aspiration. Norman et al. (1996) have shown that selective elemental fractionation is greatly reduced by using a low repetition rate. Figure 14 illustrates the signal variation for Ca-normalised trace element data obtained when ablating the NIST 612 synthetic glass standard reference material in different site at 2 mJ and various repetition rates. This figure demonstrates limited fractionation for first row transition elements with low melting point such as Zn at 4 Hz but more extensive fractionation at 15 Hz. Other elements with higher melting points, such as V, Th, the rare earth elements (REE = Ce, Y) and high field strength elements (HFSE = Zr), do not show the same behaviour, thus a repetition rate up to 15 could be used without any significant decrease in signal stability. See the paragraph about elemental fractionation for more details below.

Spatial resolution and crater shape

Focussing of the laser is a critical parameter which control inter-element fractionation (behaviour of volatile versus refractory elements during ablation-volatilisation) as well as the stability of the signal through time (Hirata and Nesbitt 1995). The ablation efficiency of most UV lasers drops off as the depth of ablation in the sample increase dependant on the focal length of the objective objective. Various spatial resolutions can be achieved. Using common Nd-YAG infra red lasers the spot size may vary from 10 to 500 μm . Larger spot sizes can be achieved by removing the focussing lens so that the spot size is similar to the laser beam (~ 6 mm). However, in order to work on polished thin sections (thickness ~ 30 μm) and at the mineral scale, geochemist try to reduce the spot size as much as possible even if the limit of detection increases dramatically (Limit of detection is inversely proportional to the square of the ablated area). By replacing the single plano-convex focussing lens with a compound objective, the spatial resolution can be routinely decreased down to 20-50 μm or even lower in some specific applications (Chenery and Cook 1993; Pearce, et al. 1992; Jeffries, et al. 1995; Jackson, et al. 1992). Laser systems, such as the Merchantek laser microprobe used here are thought to provide a similar spatial resolution while maintaining a more "top-hat"-shaped rather than Gaussian beam energy profile. This produces a flatter-bottomed and shallower crater morphology appropriate for thin section or layer analysis.

Calibration strategy

Once microparticulate material has been transported by the stream of argon to the plasma, the number of ions which reach the detector depends on (a) the atomic proportions of the element in the source mineral, (b) the amount of material removed during ablation, (c) the ionisation potential of the element in the plasma, and (d) isotopic abundance. Assuming no fractionation during ablation between volatile and other more refractory elements, it is possible to overcome these problems using an internal standard (known concentration of one element in the unknown using another analytical technique). Electron microprobe analysis is usually used to measure the concentration of the element chosen as the internal standard in the unknown. Calibration can then be achieved by comparing the response for the internal standard element in a reference material and the unknown. This element response for the internal standard allows the analyst to apply a correction for other elements included in the selected menu. In order to perform this correction, the geochemist must: (a) assume that the element response in the unknown is similar to that of the reference material (i.e., both matrices are matched); (b) assume that the reference material has a homogeneous trace element composition and distribution; and (c) correctly choose the internal standard in the material analysed (usually a minor isotope of a major element). Once these several operating parameters has been controlled, a typical analytical sequence comprises; (a) analysis of the argon blank; (b) analysis of the reference material; (c) analysis of the unknown; (d) second analysis of the reference material in order to monitor the drift (sensitivity variation of the instrument through time); (e) analysis of other unknowns.

C - Results on standards

In order to test the performance of a LA-HR-ICP-MS, we have examined key parameters including peak shape, sensitivity, element response factors, limits of detection, inter-element fractionation, precision and accuracy, using a series of experiments on NIST and USGS glass standards (Lahaye et al, 1997; Shuttleworth and Kremser, 1998).

Peak Shape

Figure 16 represents an average of 50 scans using a 1 second scan duration which translates to 1000 UV laser shots at the surface of the sample using a magnetic sector ICP. The typical flat topped peak shape produced for La during ablation of NIST 612 (~37 ppm) is characteristic of magnetic sector instruments and should allow the precise measurement of isotope ratios. The precision should be higher to that of a quadrupole instrument which is characterised by a more gaussian peak shape.

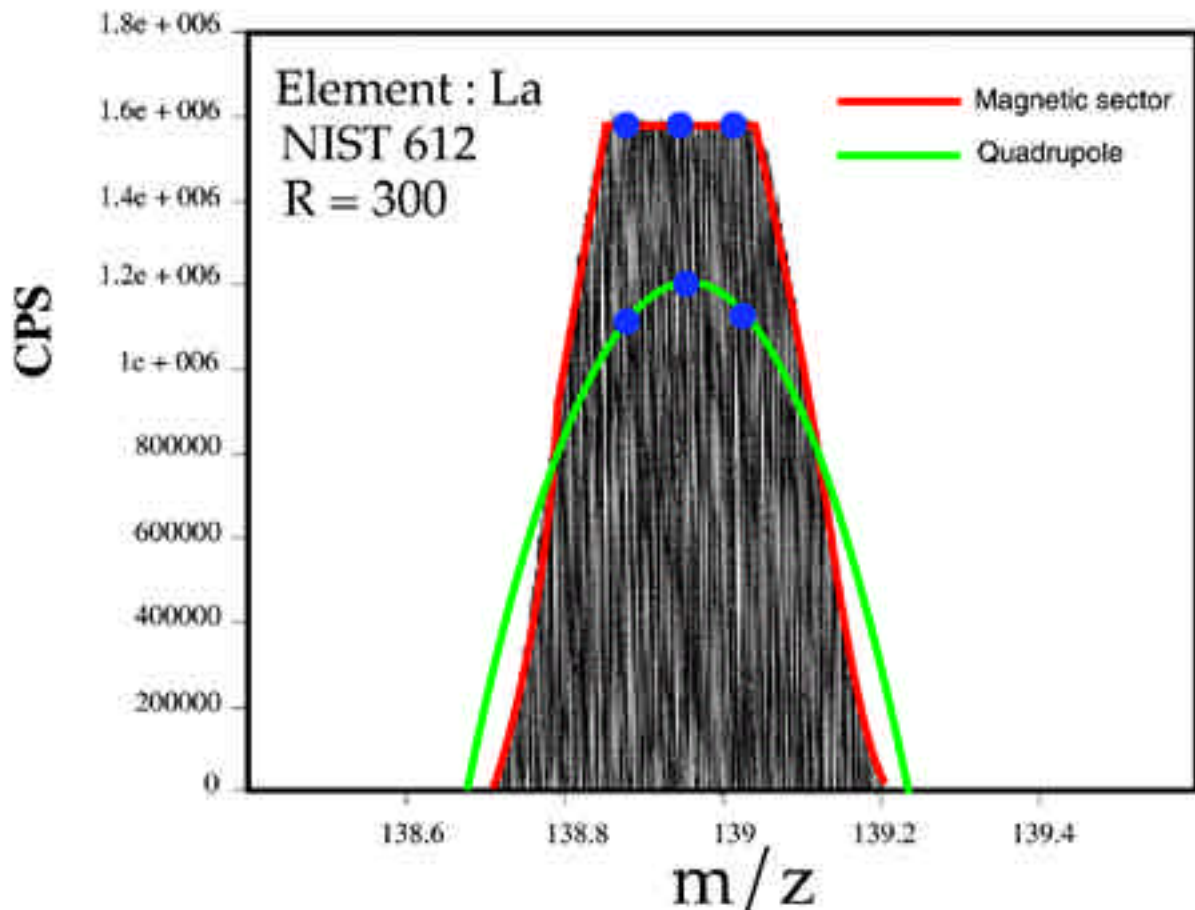


Fig.16: Peak shape of La (~37 ppm) when ablating the NIST 612 synthetic glass at 1 mJ and 20 Hz. This figure represents an average of 50 scans (1s scan duration) or a thousand shots at low resolution ($M/\Delta EM = 300$). A typical quadrupole peak shape is also shown for comparison.

Element response factors

Figure 17 shows element response factors obtained when ablating the NIST 612 standard reference

material using a menu of 30 element which covers nearly the entire mass range. A linear increase in

signal intensity at the multiplier is observed throughout the mass range with a minimum response for light elements and a maximum for heavier elements. Low element response factors are observed for major and light elements, such as calcium, which is usually used for internal standardisation and have high concentrations in many geological samples. Higher element response factors are observed for the heavier and geochemical important elements, such as the REE, Pb and U. Linearity of the element response curve also suggests a significant improvement in comparison to IR laser ablation systems where inter-element fractionation is observed during ablation (Morrison et al. 1995, Jeffries et al. 1996). Selective enhanced vaporisation efficiency of volatile elements (e.g., Hg and Pb) compared to more refractory elements which is frequently observed with IR laser ablation systems is minimised (but still present) with lower UV wavelength.

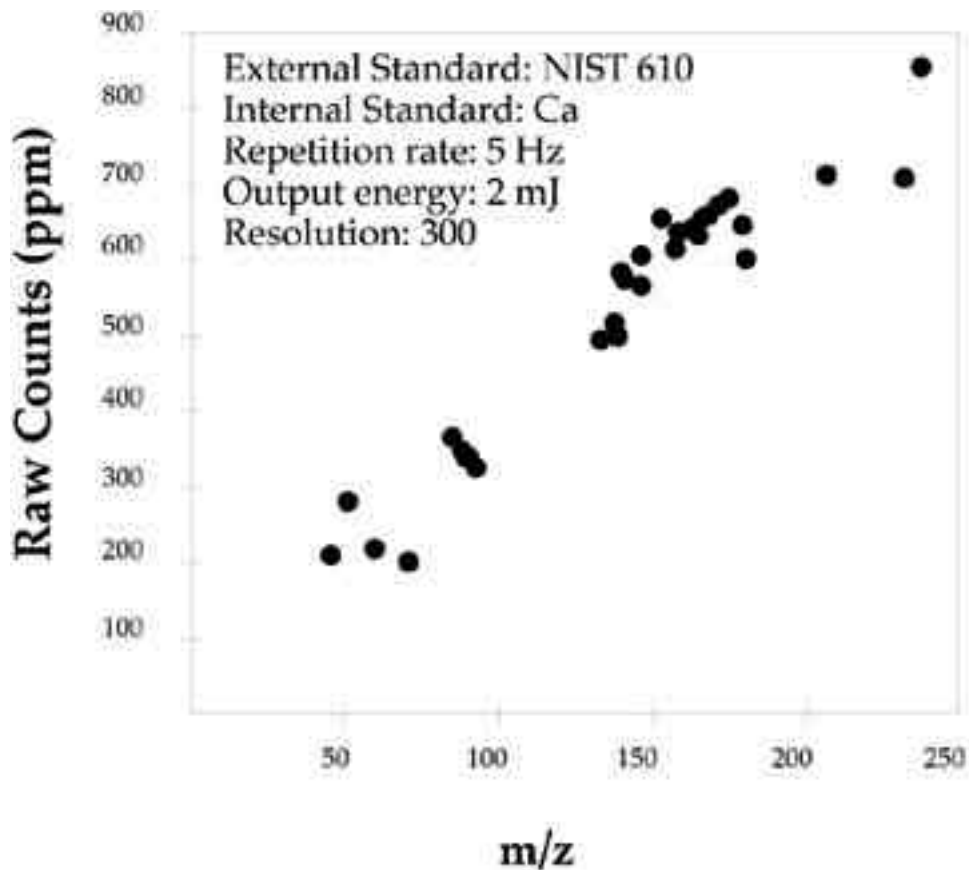


Fig.17: Element response curve when ablating the synthetic glass NIST 612 with a 50 μm wide spot.

Limit Of Detection

Figure 18 represent a comparison of the limits of detection (LOD) between different analytical techniques such as PIXE, Synchrotron XRF, Ion Probe, IR laser ICPQuadMS (with quadrupole mass filter), solution ICP-MS and UV ICPsectorMS (with a double focussing Magnetic Sector). LOD have been calculated as three standard deviations from the background when ablating a synthetic glass from NIST (NIST612) at 5Hz, 1.5mJ and a crater size of 50 μm . LOD vary from 3 ppb for Sc to 300 ppt for heavier masses such as Pb and U. These LOD can be significantly reduced to the lower ppt range by reducing the size of the element menu or by using a higher laser output energy or repetition rate when analysing elements such as the REE and HFSE which show less fractionation as a result of higher laser pulse energies.

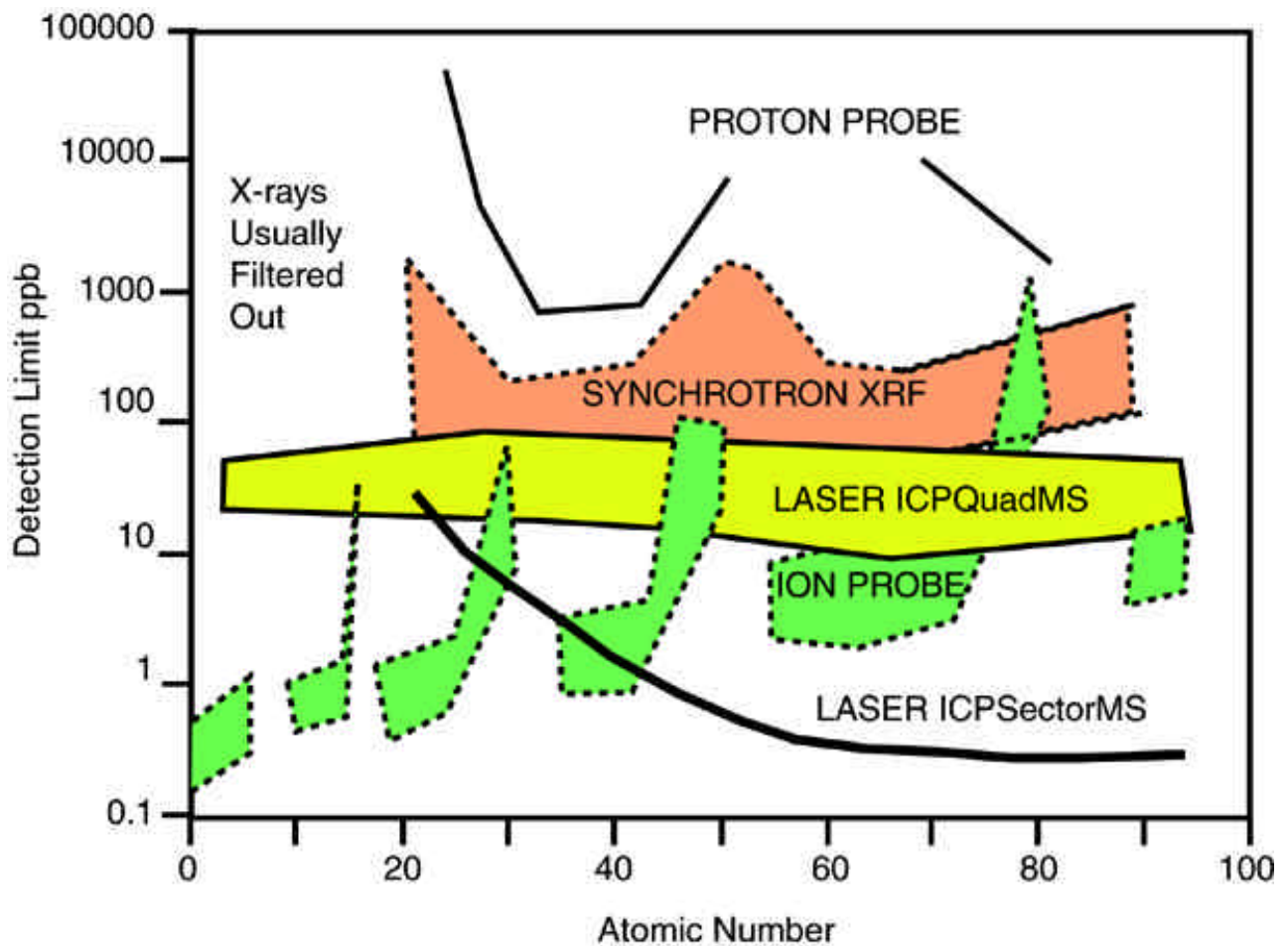


Fig.18: Comparison of Limit of detection between Proton Probe (PIXE), Synchrotron XRF, Ion Probe, IR laser ICPQuadMS (with quadrupole mass filter), solution ICP-MS and UV ICPsectorMS (with a double focussing Magnetic Sector) for a range of trace element from m/z 44 to 248 in NIST 612, using a 50 μm wide spot (adapted from Federowich, et al., 1995 and Hinton, 1997).

Precision and accuracy

On Figures 19 and 20 are shown results when ablating and analysing synthetic glasses from NIST and the USGS (Lahaye et al, 1997). These results are compared with solution mode analyses. All of these results have been calculated using the standard reference material NIST 612 as an external standard and CaO concentration as an internal standard.

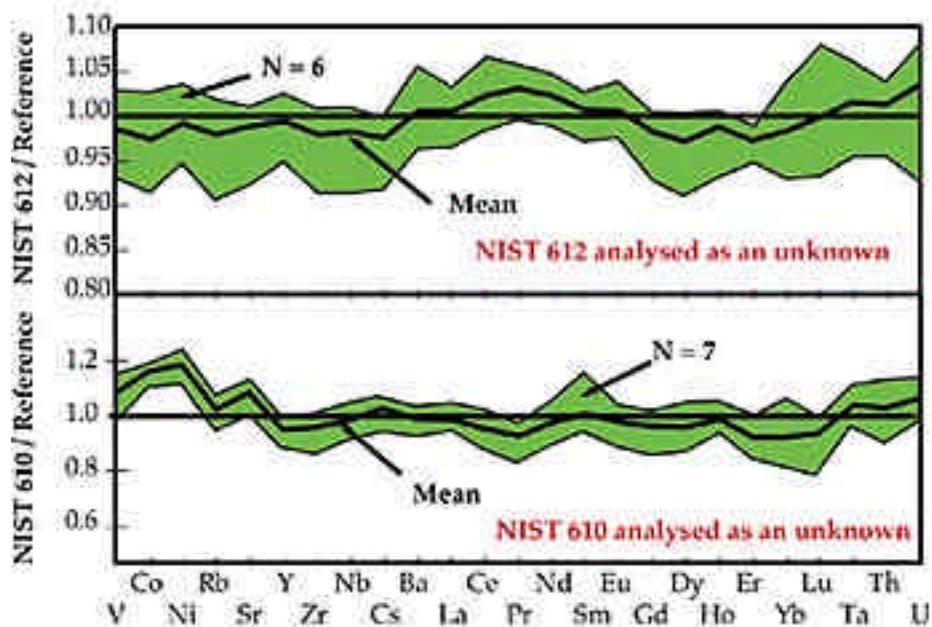


Fig.19: Results of laser ablation versus solution mode of analysis using NIST 612 and 610, expressed as a percentage deviation from solution analysis.

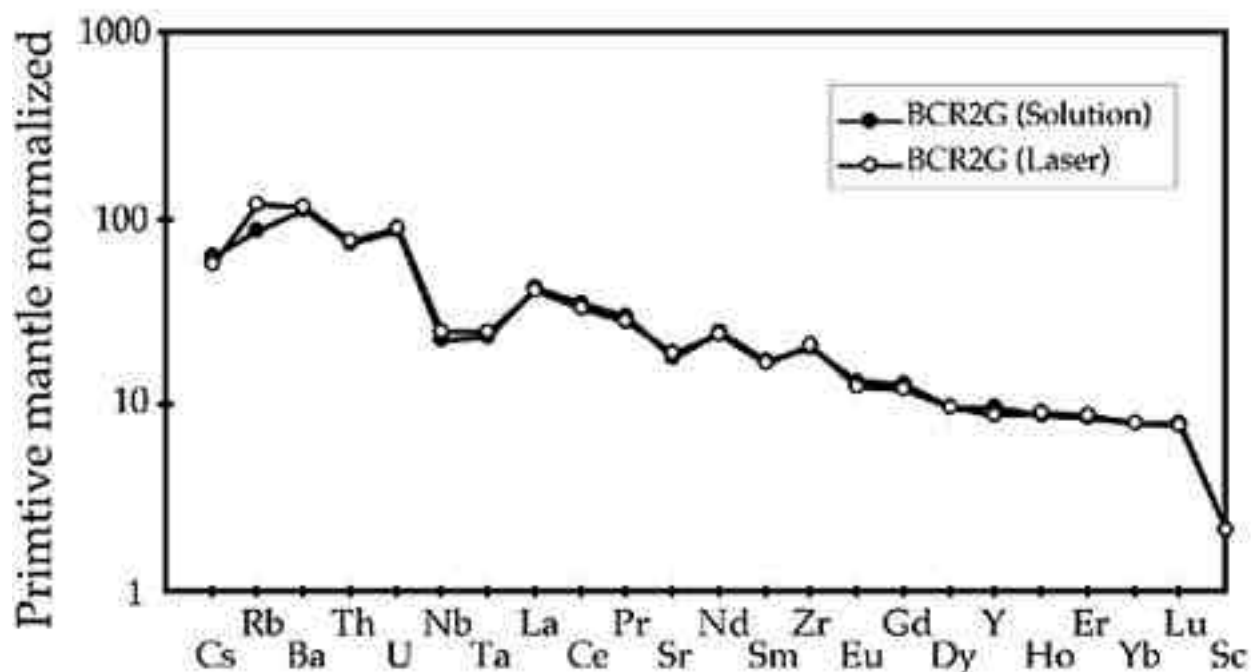


Fig.20: Primitive mantle-normalised multi-element diagram showing a comparison between laser ablation mode of analysis (white circle) and solution mode of analysis (black circle). Primitive mantle values are from Hofmann et al. (1988).

Results of multiple analyses of the NIST 612 glass calibrated against itself are shown on Figure 19. The shaded area represents the range of results obtained on 9 determinations of this standard reference material and the thick line represents the average of these 9 determinations.

Precision relative to the mean are between 3 and 10 % (1s). The mean concentration of these different elements is less than 5% (1s) different from solution analysis considered in this study to be reference values for comparison purposes only. Accuracy increases up to 10% for V and 7% for Cs, but accuracy for other elements is better than 5% (1s). Precision and accuracy are similar for the highly enriched NIST 610 glass but increase for the depleted NIST 614 glass, especially for Sc, V and Rb (up to 25%). Figure 20 is a multi-element diagram normalised to the primitive mantle (Hofmann 1988) showing a comparison between results obtain by laser ablation and solution mode on the new BCR-2G glasses. BCR-2G was prepared by remelting of BCR-2 powder, a new USGS basalt standard collected from the Columbia River Basin in north eastern Oregon. The trace element diagram is smooth and both results show an enrichment in light rare earth and alkali elements as well as a depletion in Nb, Ta and Sc, characteristic of BCR samples. Using the solution mode, as data reference values, most of the elements agree to within 10% RSD , except for Rb, Nb and Co which give up to 25% higher concentrations.

III- Applications of LA-ICP-MS on geological samples

Analyses of solids by lasers requires little or no sample preparation. The result is a high sample throughput and the determination of trace element content or isotopic composition in almost all types of materials at high spatial resolution.

IV1- Sample preparation

In general sample preparation is straightforward. Polishing is usually necessary if the electron microprobe is to be used before loading the sample into the sample cell. Because the laser sample cell is not under vacuum, outgazing of the support material is not a problem. Powdered samples should be treated in a similar way to XRF analysis and stabilised either by

(a) compacting the sample into a pellet with or without a binding agent,

or

(b) fusing the sample to a borate glass or using a strip heater.

IV-2- Trace elements determination

A- Introduction

Laser ablation has been applied to the determinations of the trace element concentrations in a wide range of materials such as :

Polymer: Hemmerlin and Mermet 1996; Marshall, et al. 1991; Wolf et al 1998;

Particule: Lüdke, et al. 1994; Tanaka et al 1998; Chin et al 1999;

Press pellets: Gray 1985; Imai 1990; Morrison, et al. 1995; Perkins, et al. 1991; Perkins, et al. 1993; Raith and Hutton 1994; Scholze, et al. 1994; Van Heuzen and Morsink 1991; Baker et al 1999;

Alloy - Metals: Goodal, et al. 1995; Raith, et al. 1995; Kogan, et al. 1994; McCandless, et al. 1997; Watling, et al. 1994, 1997; Outridge, et al. 1998;

Fused glasses: Chen, et al. 1997; Lichte 1995; Perkins, et al. 1991; Perkins, et al. 1993; Ødegård and Hamester 1997; Ødegård et al 1998;

Fe-Mn crust: De Carlo and Pruszkowski 1995; Garbe-Schönberg 1994; Hoffmann, et al. 1997;

Meteorite: Hirata and Nesbitt 1997; Campbell and Humayun 1999;

Volcanic glass shards: Perkins, et al. 1997; Westgate, et al. 1994; Bryant et al, 1999;

Melt inclusions: Taylor, et al. 1997;

Fluid Inclusion: Ghazi, et al. 1996; Irwin and Roedder 1995; Moissette, et al. 1996; Shepherd and Chenery 1995; Stalder, et al. 1997; Wilkinson, et al. 1994; McCandless, et al. 1997; Shepherd et al 1997; Fabre, et al 1999; Boué-Bigne, et al 1999 and new references from the ETH group (Günther and Heinrich and Audétat...);

Marble crusts: Ulens, et al. 1994;

Leaves: Scholze, et al. 1996;

Mussels: Pearce and Schettler 1994;

Coral: Sinclair and McCulloch 1997; Sinclair et al 1998;

Wood - Tree ring: Alteyrac, et al. 1995; Garbe-Schönberg, et al. 1997; Hoffmann, et al. 1994, 1996, 1997; Watmough, et al. 1997, 1998;

Teeth: Cox, et al. 1996; Evans, et al. 1995; Outridge and Evans 1995;

Biological organism: Durrant and Ward 1994; Evans, et al. 1994; Hoffmann, et al. 1996;

Shell: Fuge, et al. 1993; Imai and Shimokawa 1993; Imai 1992; Price and Pearce 1997; Vander Putten et al 2000; Bellotto and Miekeley 2000; Raith et al, 1996;

Plant ashes: Hoffmann, et al. 1996;
Stalactite: Imai 1992;
Foraminifers: Wu and Hillaire-Marcel 1995;
Cannabis: Watling 1998;
Fire assay beads: Shibuya, et al 1998; Jarvis et al, 1995;
SiC crystals: Hofmann, et al 1999;
Sediments: Baker, et al 1999;
Fremdlinge: Campbell, et al 1999;
Antique: Devos, et al 1999;
Tungsten Carbide: Kanicky et al 2000;
Hair and nails: Rodushkin and Axelsson 2000;
Coal: Rodushkin et al 2000;
Fish: Thorrold and Shuttleworth 2000

and minerals such as:

Zircon: Barbey, et al. 1995; Bédard, et al. 1997; Feng, et al. 1993; Imai and Yamamoto 1994; Jackson, et al. 1992; Pearce, et al. 1992; Perkins, et al. 1992; Nesbitt, et al. 1997;
Plagioclase: Bea, et al. 1996; Pearce, et al. 1992;
Amphibole: Bea, et al. 1996; Dalpé and Baker 1994; Dalpé, et al. 1995; Zack, et al. 1997; Ionov 1998;
Anthophyllite: Bea, et al. 1996;
Apatite: Chen, et al. 1997; Chenery, et al. 1996; Fryer, et al. 1995; Jackson, et al. 1992;
Monazite: Chen, et al. 1997; Chenery and Cook 1993, Poitrasson et al 1996, 2000a, b;
Clinopyroxene: Chenery and Cook 1993; Foley, et al. 1996; Fryer, et al. 1995; Günther, et al. 1997; Jeffries, et al. 1995; Zack, et al. 1997; Ionov 1998; Mason et al, 1999;
Chromite: Chen, et al. 1997; Eggins, et al. 1998; Horn, et al. 1994;
Olivine: Chen, et al. 1997; Eggins, et al. 1998; Jeffries, et al. 1995; Norman 1998; Pearce, et al. 1992;
Orthopyroxene: Eggins, et al. 1998; Jackson, et al. 1992; Norman 1988; Kurat and Dobosi 2000;
Sulphide: Chenery, et al. 1995; Watling, et al. 1995, 1998)), (Alard, et al (1999));
Carbonate: Feng 1994; Pearce, et al. 1992; Pearce, et al. 1992; Perkins, et al. 1991; Kontak and Jackson 1995; Kontak and Jackson 1999; Ionov 1998; Craig et al 2000;
Phlogopite: Foley, et al. 1996; Fryer, et al. 1995;
Garnet: Günther, et al. 1997; Jackson, et al. 1992; Zack, et al. 1997; Bea, et al. 1997; Kurat and Dobosi 2000;
Magnetite: Horn, et al. 1994;
Dolomite: Imai and Yamamoto 1994;
Titanite: Jackson, et al. 1992;
Uraninite: Jackson, et al. 1992;
Spinel: Norman 1988;
Ilmenite: Raith and Hutton 1994;
Rutile: Raith and Hutton 1994;
Scheelite: Sylvester and Ghaderi 1997; Gahderi, et al. 1997; Ghaderi et al, 1999, Brugger et al 1999, 2000;
Diamond: Watling, et al. 1995;
Experimental Petrology: Veksler et al 1998, Thompson & Nalpas 2000;
Glass: Ionov 1998;
Biotite: Yang & Rivers 2000; Yang et al 1999;
Muscovite: Yang & Rivers 2000; Yang et al 1999;
Tourmaline: Garofalo et al 2000;
Bark samples: Narewski et al 2000;

Zeolites: Pickhardt et al 2000

B- In situ determination of trace element in minerals

Thin section

We have applied the laser ablation technique in the analysis of the REE in clinopyroxene (cpx) from a komatiite lava flow of Alexo in Canada. Alexo is one of the best preserved komatiite flows in the world. The sample analysed is characterised by well preserved cpx needles in a matrix of chlorite plus 30 μm grains of sphene. This figure presents REE data for the cpx and from the sphene, normalised to the chondritic values of (Evensen, et al. 1978). Three conclusions could be drawn from these experiments:

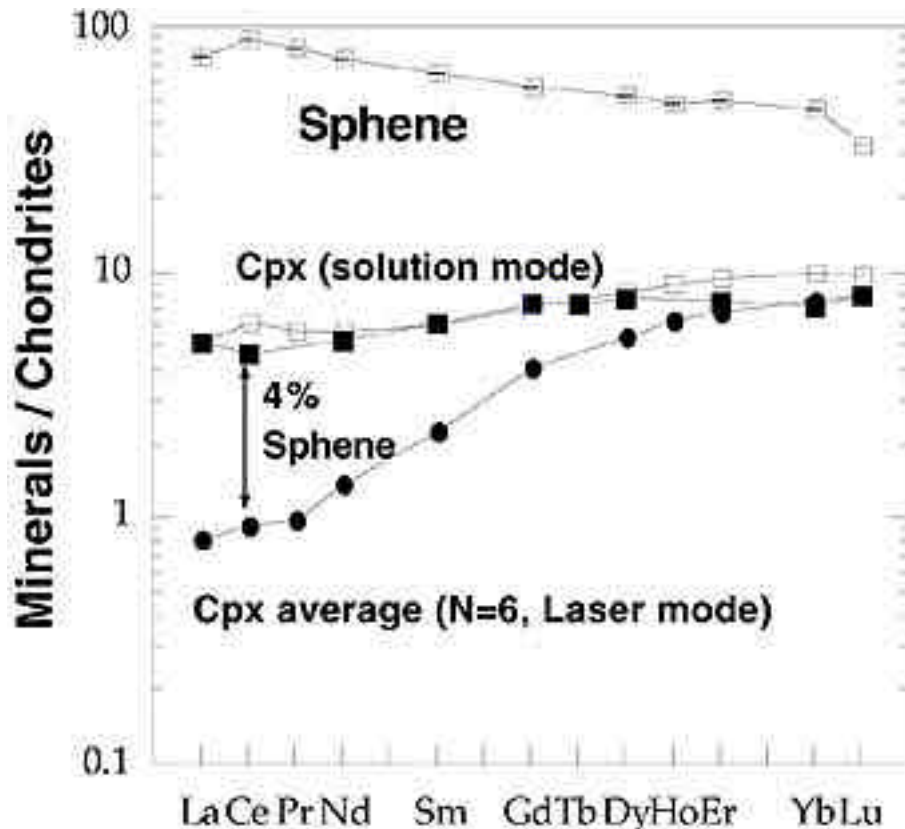


Fig.21: Chondrite normalised diagram of clinopyroxene and sphene from the Alexo komatiitic flow (sample M668; Lahaye and Arndt 1996).

1. This configuration allows the acquisition of a signal for as much as one minute using a 30 μm thin section and generates data at the chondritic level. However significant differences in the ablation rate has been observed, dependant on the mineral matrix (see ablation pits in the last page). For example, ablation of apatite is characterised by the quick removal of at least the 10 first micron within the first seconds of the initiation of the ablation. Once a hole has been drilled, the ablation rate greatly decrease to a normal rate (~ 1 micron/s). In order to monitor the drilling process on a thin section, it has been suggested that the araldite use to make the thin section should be enriched in an unusual element (such as In; see U. Memorial publications, Jackson et al).
2. Comparison between solution-based ICP data and laser ablation-based HR-ICP-MS data demonstrate a better accuracy by laser ablation and shows that the cpx crystallised in equilibrium with a LREE-depleted komatiite lava. Mass balance calculations suggest that as

little as 4% of sphene in the mineral separate may explain the LREE enriched pattern of the cpx analysed in solution.

3. The REE budget of well preserved komatiitic sample is stored in small secondary grains of sphene which cast some doubt on the ability of komatiites to fingerprint the geochemistry of the Archaean mantle.

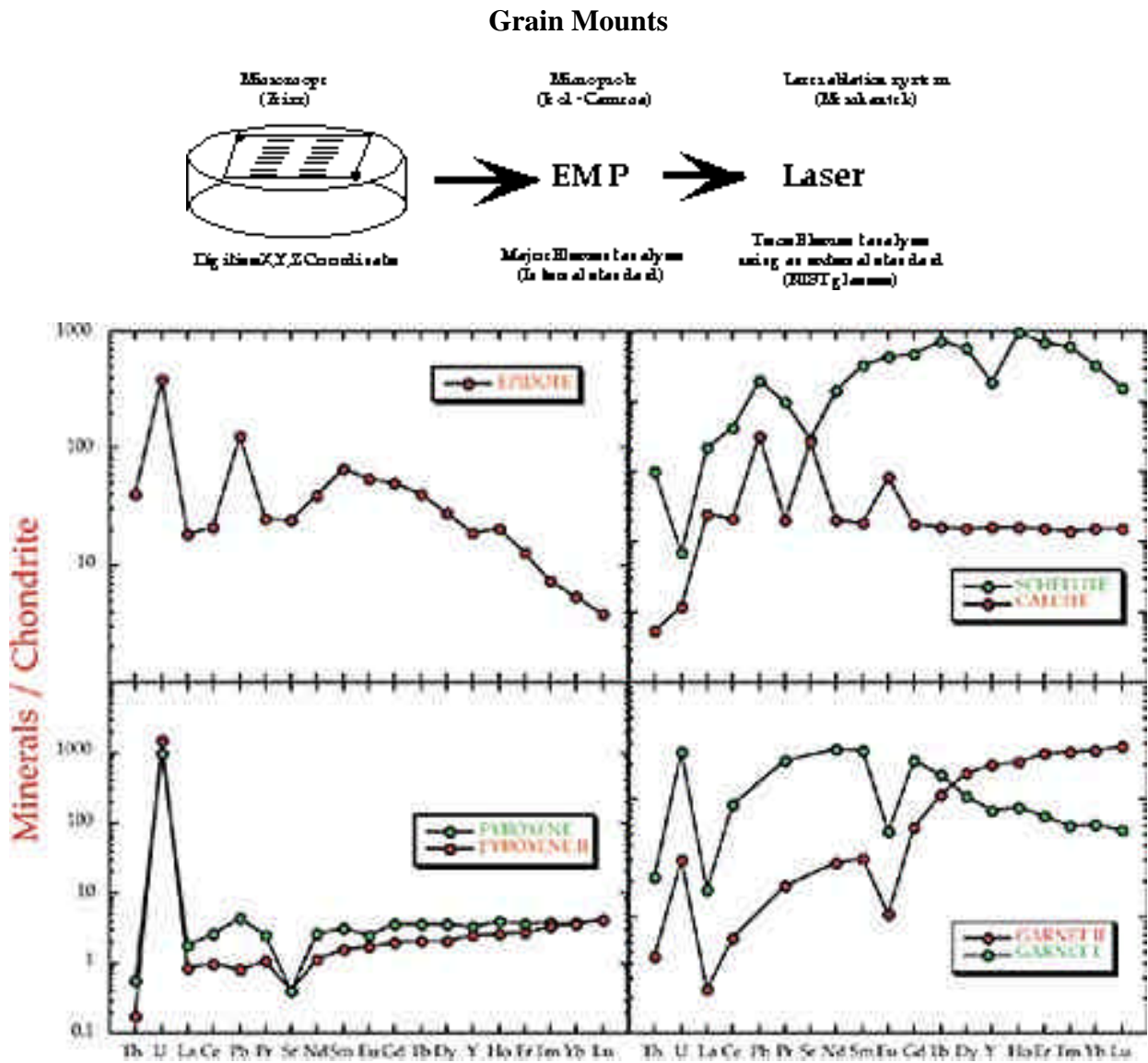
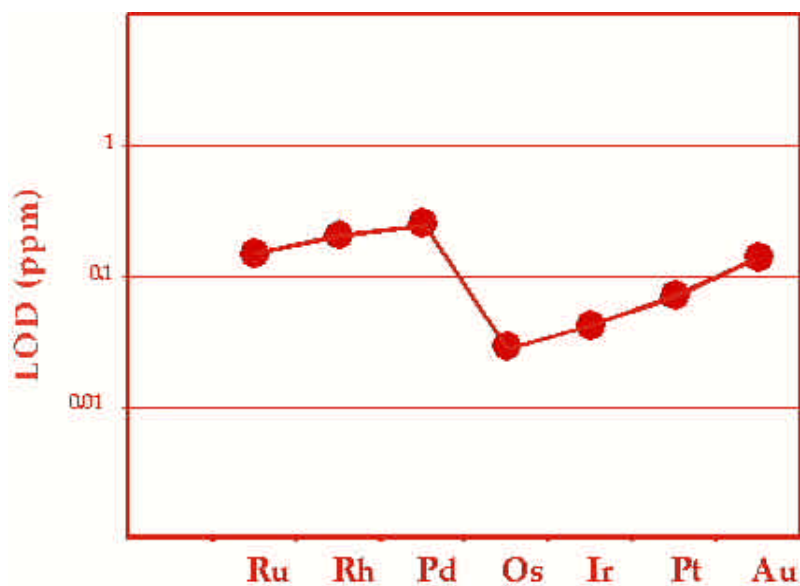


Fig.22: Multi-element diagram normalised to the primitive mantle (Hofmann 1988) of different minerals using a 50 μm spot size at 5Hz and 0.1-0.2 mJ output energy. Ca44 and Si29 have been used as an internal standard for the respective quantification of the epidote, scheelite, calcite, pyroxene I, garnet I, pyroxene II, and garnet II. NIST 610 and 612 has been used for external quantification using data from (Norman, et al. 1996).

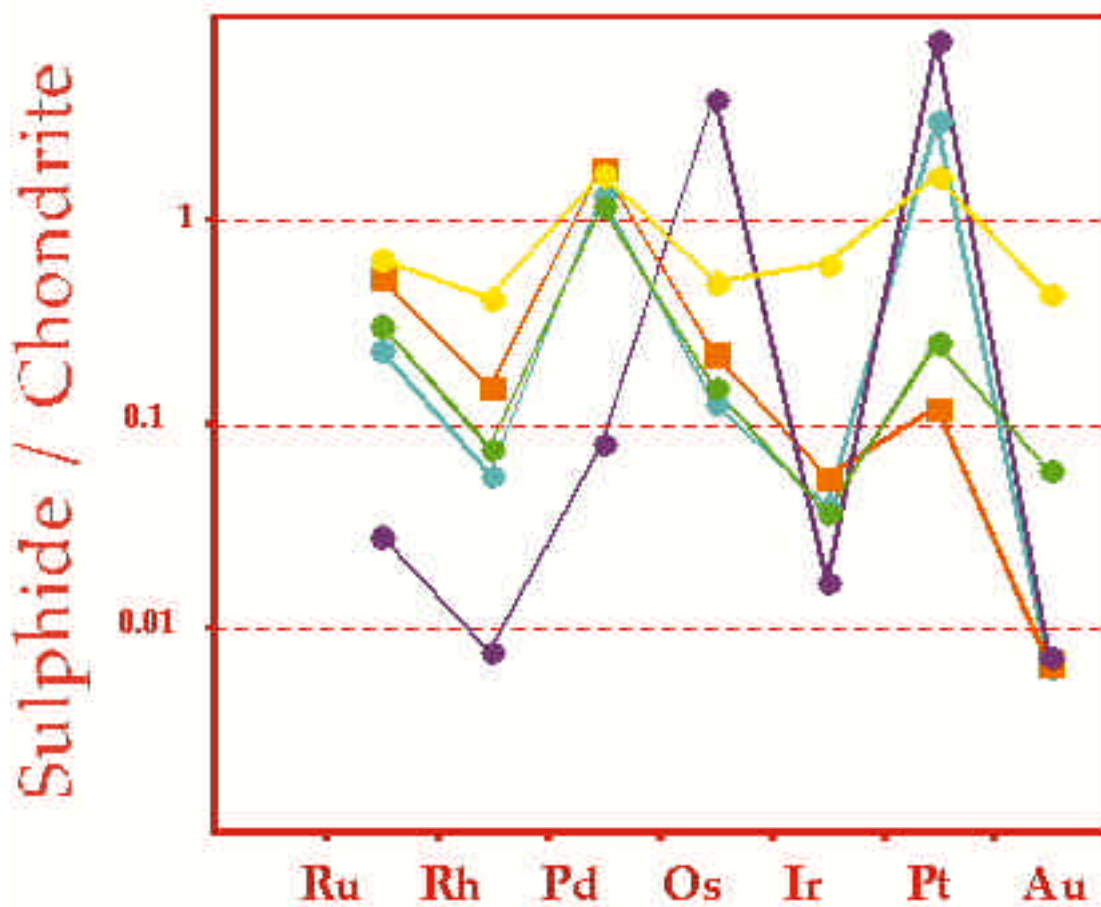
In order to improve the sample output, a new 3D recoordination technique has been developed at Monash university. This technique imply the separation and deposition of a large number of grains into an epoxy mount (2 inches by 1). These samples are located within a rectangular frame define by two recoordination marks located in the middle of a copper and nickel grid. These two marks allow a recoordination in 2 dimension (X and Y) of the sample using a digitising stage and a software developed by Microbeam (Contact Graham Hutchinson for further details: beamm@mail.enternet.com.au). Instead of developing an autofocus system (Cousin, et al. 1995; Chen et al, 2000) for the third axes, this software calculate a third recoordination mark based on the location of the further sample from the diagonal define by the first and second recoordination mark. This third recoordination mark define a plane and thus the third dimension. The position of each samples (X, Y and Z) are stored in a file. This file is used by the electron microprobe which found the location of the sample and analyse it for its major elements content. This file is also used by the laser ablation system to recover the location of the sample and analysed them for its trace elements content. One of the major element analysed by the electron microprobe is used as an internal standard and excellent recoordination allow us to avoid zonation problems. Figure 22 represent some samples analysed by laser ablation from grain mounts.

Platinum Group Element in Sulphides

We have recently analysed PGE from sulphides associated with komatiitic volcanism in Kambalda (see (Heath et al submitted) for analytical details). The next figures represent the Limit Of Detections and the results normalised to the chondritic values (McDonough and Sun 1995).



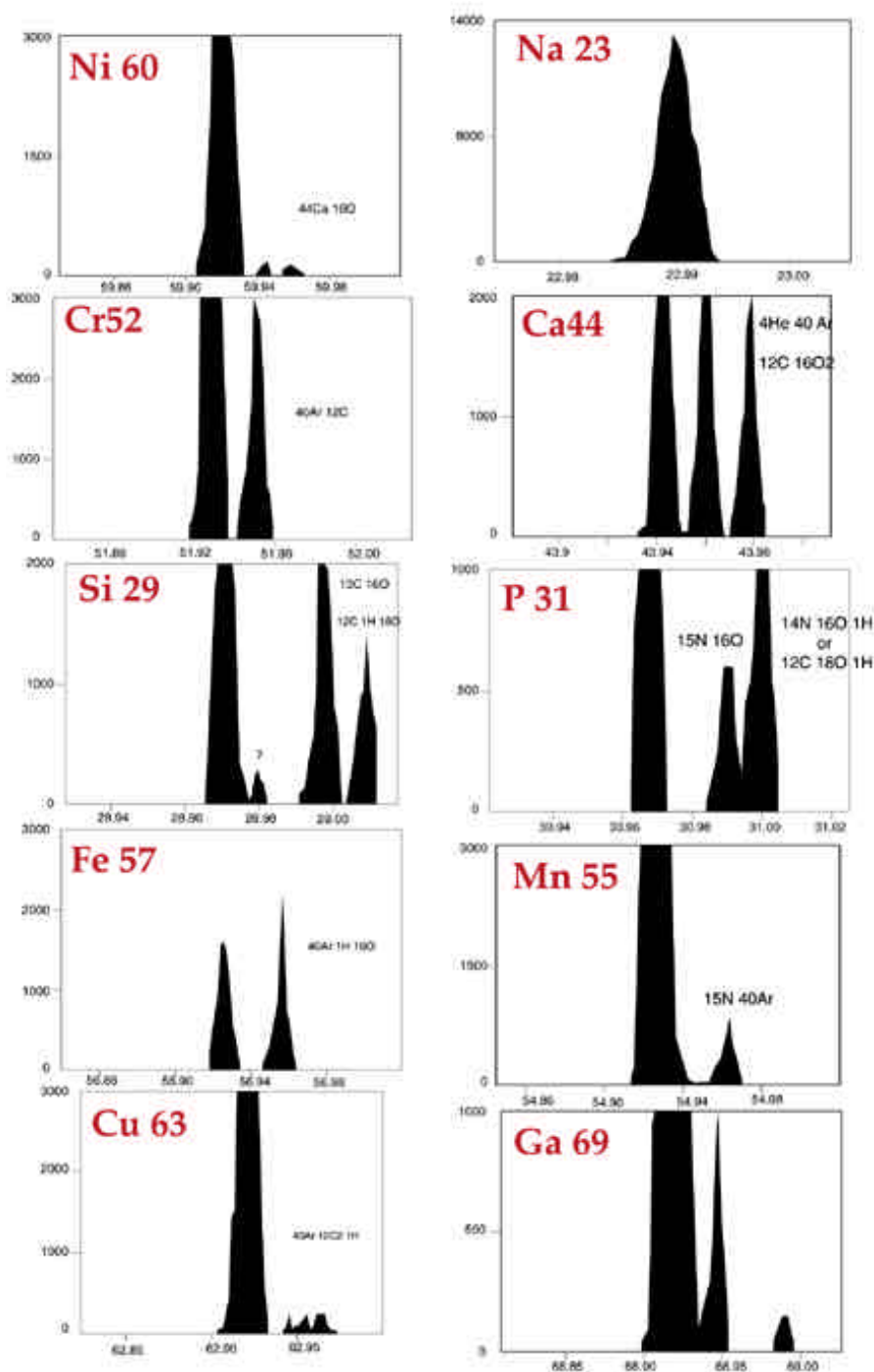
Calculated Limit of Detection for the Platinum Group Element in sulphides



Calculated PGE concentrations, normalised to the primitive mantle values (McDonough and Sun 1995), for some major sulphides from massive ore associated with komatiitic volcanism (Heath et al, submitted)

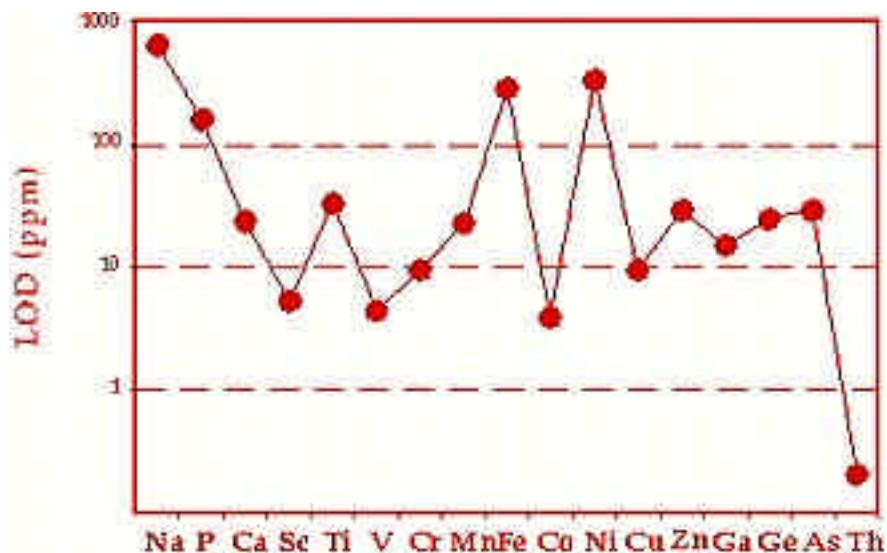
C- Interference

The next figures represent some classic interference mainly due to air entrainment (Si29, P31, Ca44, Fe57, Mn55). The interference are minimal for Ni, Cu and Cr are result mainly from source contamination. Those interference may be reduce by using a special bonnet or using the medium resolution setting of a high resolution magnetic sector ICP.

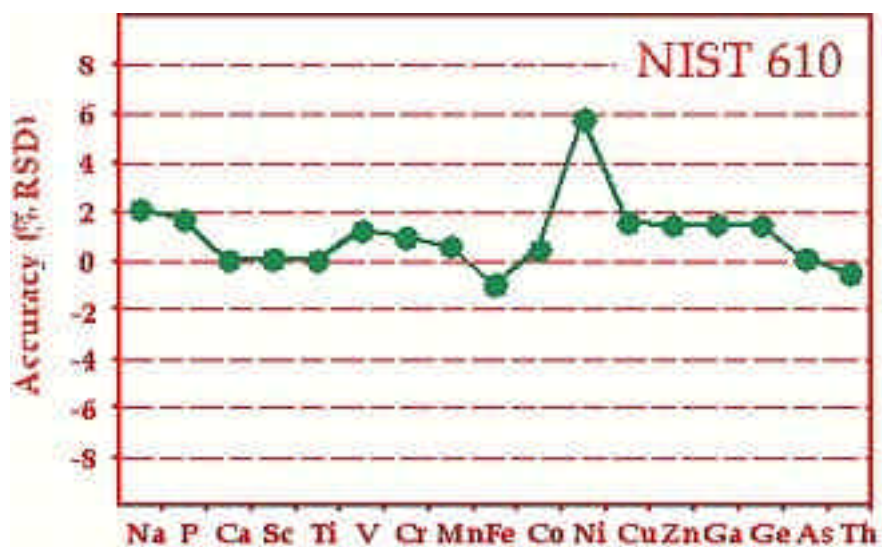


D- Medium Resolution

We have recently analysed the trace element content of NIST 610 in medium resolution and compare those values with results at low resolution. The next figures represent the calculated Limit Of Detections and the accuracy (%RSD relative to Norman et al 1996). Accuracy are mainly within 2% RSD except for Ni. Medium resolution has been very useful recently for the measurement of trace element in high purity glass at ppm level.



Calculated Limit of Detection for some light and transition elements (ppm)



Calculated accuracy (%RSD) during the measurement of NIST 610 in medium resolution for some light and transition elements.

E- Comparison with other analytical techniques

Different test has been performed in order to compare the accuracy of our laser ablation system with other analytical technique. Here are two examples: The first (Figure 23) is a comparison between the trace element analyse of LREE rich apatite by laser ablation ICP-MS with LA-HR-ICP-MS. This comparison is presented on a multi-element diagram normalised to the primitive mantle and show a good agreement between the two techniques.

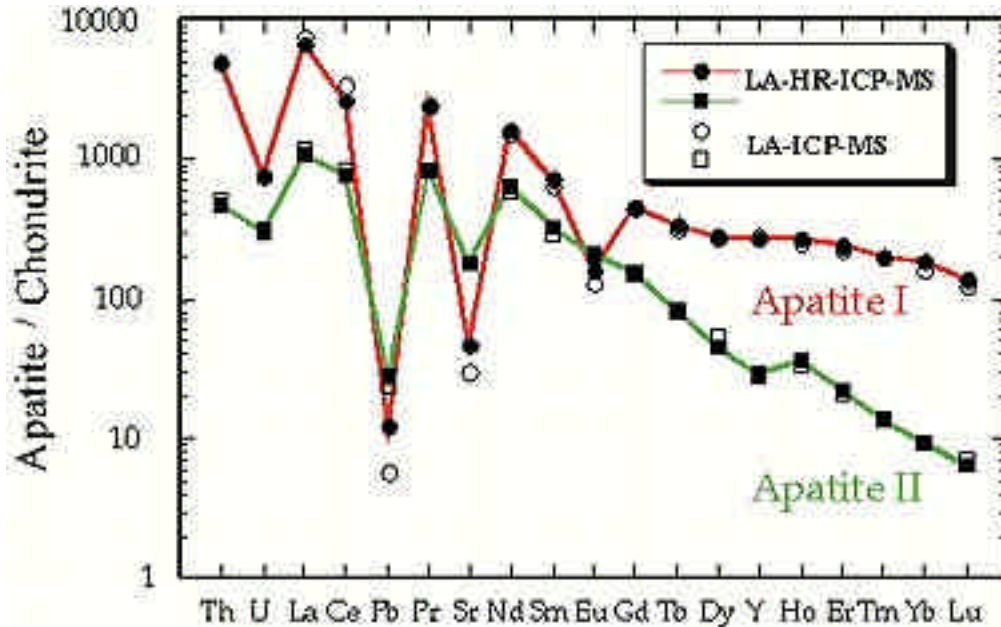


Fig.23: Multi-element diagram normalised to the primitive mantle values of Hofmann (1988) of apatite standard analysed by laser ablation ICP-MS (white symbols) and laser ablation HR-ICP-MS (black symbols).

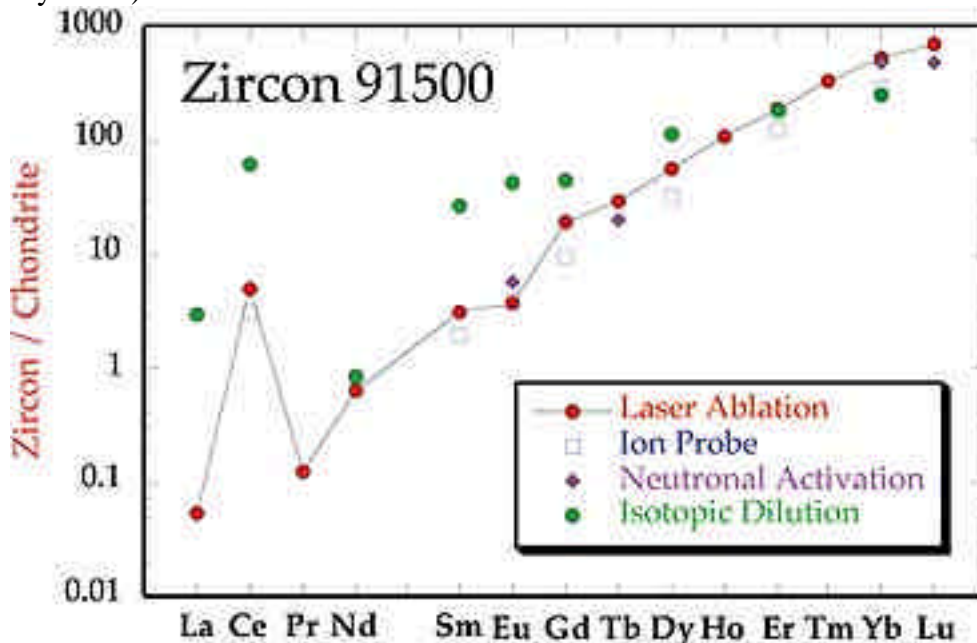


Fig.24: Chondrite-normalised REE data (Evensen et al, 1978) for a zircon standard (91500; Wiedenbeck, et al., 1995) analysed by different microanalysis techniques. Laser ablation data are in good agreement with neutron activation.

The second example (Figure 24) is a comparison between the trace element analyse of LREE poor mineral such as a zircon by ion probe, isotopic dilution, and neutrons activation. Ion probe data are significantly lower for the heavy REE. Isotope dilution gave systematically higher results for the light REE which may be related to incomplete dissolution of the standard. The results are presented on figure 24 on a chondritic normalised diagram. This figure highlights the good accuracy for in-situ microanalysis of refractory minerals versus dissolution techniques.

F- Fluid inclusions

Three main laboratories has already conducted some experiments on the ability of laser ablation to measure the concentrations of trace elements in fluid inclusions. In summary, after the pioneer work of Chenery and coworker from the British geological survey at Nottingham (Sheppherd and Chenery 1995; Moissette, et al. 1996) based on a calibration technique involving the encapsulation of microdroplets of standard solution in hydrophobic epoxy resin, Ghazi and coworkers (McCandless, et al. 1997; Ghazi, et al. 1996; Ghazi and Shuttleworth 2000) from the Georgia State University develop a new calibration technique using solutions sealed in microcappillary tubes. More recently Gunther and coworkers from ETH develop a quantification procedure using elements concentrations ratios calculated by referencing intensity integrals against signals from external standards (glass and solution) and using Na as an internal standard (Audétat, et al. 1998; Günther, et al. 1997; Günther, et al. 1998, Audétat and Günther 1999; Heinrich et al 1999). Following the introduction of a paper by Gahzi et al (1997), fluid inclusion are analysed by a variety of non-destructive and destructive techniques. Non destructive methods that have been used successfully for the analysis of major elements in single inclusions include mainly synchrotron X-ray fluorescence (Frantz, et al. 1988; Rankin, et al. 1992; Vanko, et al. 1993). Destructive techniques typically provide greater compositional information on the fluid inclusion and are more widely available than the non destructive techniques. The destructive methods can be divided in two groups:

- Single inclusion analysis method include laser microprobe noble gas mass spectrometry for the analysis of halogens and the noble gases (Irwin and Roedder 1995), ion microprobe analysis of frozen inclusions (Kelly and Burgio 1983; Ayora and Fontarnau 1990; Diamond, et al. 1990), laser ablation atomic emission spectroscopy (Rankin, et al. 1992; Ramsey, et al. 1992; Wilkinson, et al. 1994), and laser ablation inductively coupled plasma mass spectrometry.
- Bulk analysis, crush leaching or decrepitation used for extraction of fluid inclusions (Bottrell, et al. 1988; Channer, et al. 1992; Ghazi, et al. 1993) with different analytical techniques such as gas or ion chromatography, atomic absorption, ICP-ES and ICP-MS (Ghazi, et al. 1993; Banks, et al. 1994).

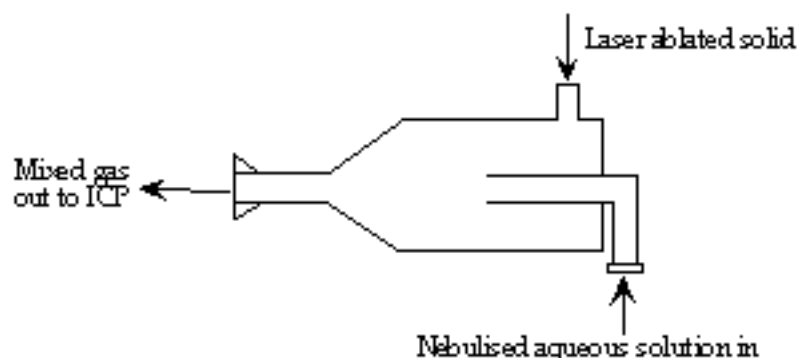


Fig.25: Schematic of the dual gas-flow mixing device, from Chenery, et al. (1995).

There are several problems related to the analysis of fluid inclusions by LA-ICP-MS. The main problems are:

(1) the use of an external and internal standard for quantification purposes. The method used by Chenery and coworkers is based on the use of (i) a dual gas flow system (Figure 25) that allowed use of standard solutions and NIST glasses for tuning the instrument, (ii) a high temperature ablation cell which improve the efficiency and reproducibility of fluid release and (iii) a new calibration technique involving the encapsulation of microdroplets of standard solutions in hydrophobic epoxy resins.

The method used by Ghazi and coworker is based on a set of artificial fluid inclusion standard prepared by drawing small volume (0.2-0.3 ml) of standard solution of known concentration into 4 ml volume glass microcapillary tubes . These synthetic external standard are used for the construction of a calibration curve (Cps vs concentration). More recently Gunther, et al. (1998) and Audétat, et al. (1998) have used a different technique (without a dual gas flow system) in which they integrate the counts, use NIST glasses and solutions in teflon beakers as external standard (Günther, et al. 1997) and Na as an internal standard from microthermometric measurements.

(2) the size of the inclusion and the ability to calculate the volume of the liquid ablated. The range of volume for fluid inclusion is between 10^{-3} and 10^{-7} ml. Using Ghazi and coworkers method, the volume of solution is perfectly known so that the volume per pulse is known as well. Spikes in element intensities were noted by McCandless et al (1997), Audétat et al (1998) and Shepherd & Chenery (1995), between first bleached fluids versus subsequent analysis, suggesting that accurate element concentration may not be determinate in small fluid inclusion when only one scan is obtained before the fluid is exhausted. In order to increase the acquisition, the sample gas flow has to be reduce once the inclusion is open.

(3) the presence of solid phases in the inclusions

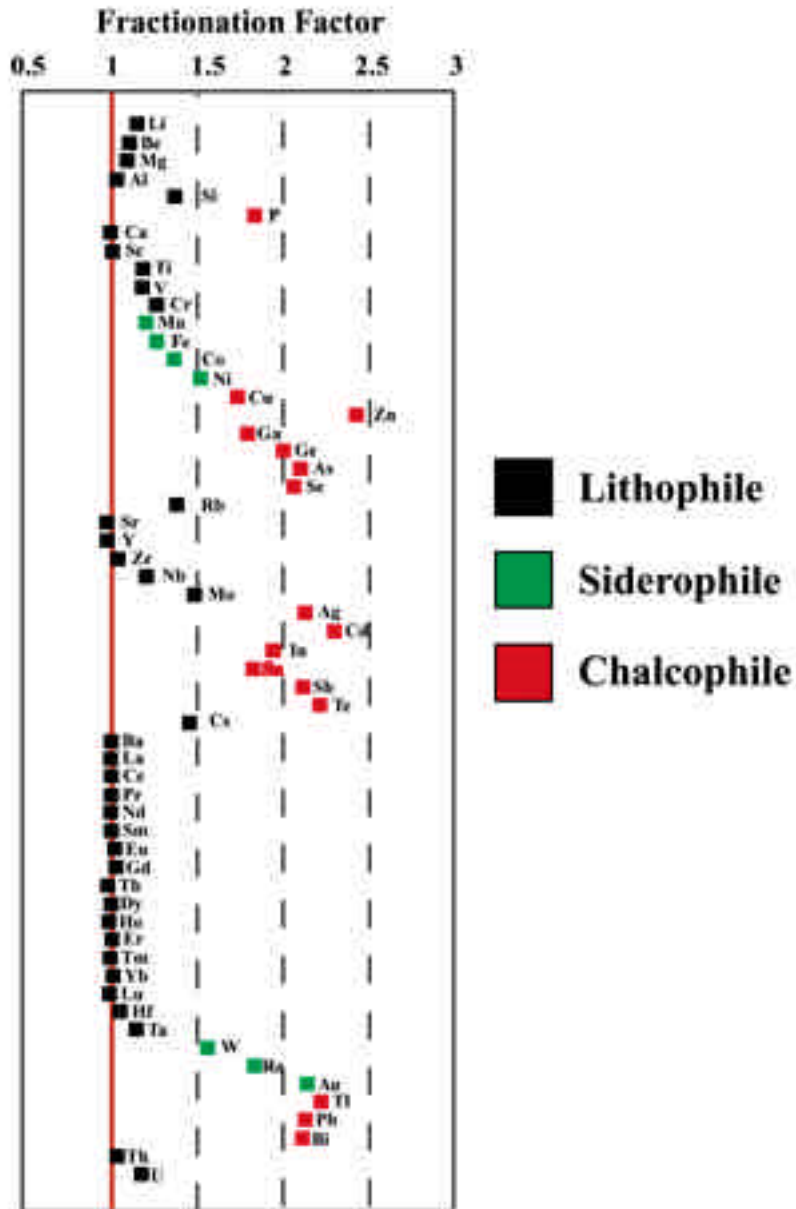
(4) thermal fracturing: Ablation is usually initiated by focussing onto the surface to create a shallow pit hole (2-5 μm). As the rate of ablation decrease due to beam defocussing, the power is slowly increase whilst continually adjusting the focus to achieve a steady rate of drilling. During this drilling step, an early thermal fracturation may occur which leads to the premature release of the fluid inclusion content (Sheppherd and Chenery 1995). Alternatively an active focussing should keep a constant drilling rate without increasing the power density and potential thermal fracturation.

(5) internal vapour pressure of the inclusion: Sheppherd and Chenery (1995) have also noticed that the rate and manner of liquid release are determinate by the volume and internal vapour pressure of the inclusion. A Continuous ablation of the liquid phase within a liquid inclusion is possible at room temperature, but the ablation of a CO₂-rich inclusion lead to an explosive release of the liquid phase. According to Sheppherd and Chenery (1995), for many two phases (liquid + vapour) inclusions, fluid release at room temperature is extended over 1-2 seconds and moreover ablation is often accompanied by the precipitation of salts at the surface, due to capillary attraction of the liquid. High temperature ablation minimise the unpredictable ablation response and the cell temperature used by Sheppherd and Chenery (1995) is always set close to the liquid-vapour homogenisation temperature for the inclusion.

(6) the high background in Na: Na is a mono isotopic element and its background with our system is around 2×10^6 cps. The contamination source of this high background has also been notice by Sheppherd and Chenery (1995) and remain unknown. It's everywhere !!

IV-3- Elemental fractionation

Fractionation between element has been highlighted by various IR laser ablation users (Cromwell & Arrowsmith, 1995; Jeffries et al, 1996; Otridge et al 1997) and described by Fryer et al (1995) who ratioed the signal from the first two minutes over the last two minutes and calculated a fractionation factor (figure below). The fractionation intensity seems to follow the Goldschmidt classification of elements (lithophile, chalcophile and siderophile). Why ??



Fryer et al (1995) Can. Miner.

This section is mainly a summary of outstanding papers from Eggins et al (1998); Mank and Mason (1999) and the research team of Rick Russo (see bibliography below).

Selective removal of some elements and material can be caused by the laser interaction with the sample, a process termed "elemental fractionation".

Several process contribute to the fractionation process between element during the ablation:

Plasma shielding:

Fractionation of the Cu/ Zn ratio at lower power density is related to plasma shielding, and thermal effect induce by the behaviour of the plasma from the laser on the sample below a critical power density (Mao, et al., 1996; Mao 1997; Mao, et al. 1993; Mao, et al. 1997; Russo 1995, Russo, et al. 1996; Chan et al 2000). The plasma consist of small liquid particles, clusters and a large amount of free ions, molecules, atoms and electrons. Electrons contained in this heterogeneous mass are capable of absorbing further incoming laser light ("inverse bremsstrahlung" effect) after more than 5ns after ablation starts. The plasma can effectively shield the sample and reduce the amount of laser light that reaches the sample surface. Heat may be transmitted from plasma to sample where low melting/vaporisation points elements may be selectively removed from the sample surface.

Crater size/depth ratio:

At a constant laser fluence, the principle parameter which appears to control fractionation behavior is the aspect ratio of the ablation pit. For the deeper craters the three structural regions of an ablation crater can be defined as follows:

-Regions A, at the base, The ablation front: The glass appears to have been removed cleanly from the surrounding sample and there is little evidence for the condensation or re-deposition of ablated material. However some very small melt globules (<10 μm) are sometimes seen in this region and the smooth nature of the walls may be due to re-melting by the plasma following ablation. When viewed under cross-polarised light the glass exhibit extensive pressure cracks around the crater walls but not at the base. Strain features are evident in the glass immediately beneath the base.

-Regions B: The intermediate region: Characterised by thermal cooling cracks on the walls of the crater. This part of the ablation crater is where particles escape from the ablation front, some of which are deposited on the walls where they may be re-ablated by reflected light and heated by the secondary plasma that penetrates into the ablation crater. Heating in this region may also lead to volatilisation of elements with the particles that are ablated from deeper in the crater.

-Region C: Crater opening: Where large amount of particles redeposition and melting have been taken place. Fracturing of the sample is most apparent in this region and may be related to stress during cooling or recrystallisation of thin molten layers. Deposition around the crater on the surface of the glass sample can be extensive and is dependant upon the amount of material removed during the ablation event, the viscosity or density of the gas in the sample cell and the dynamics of flow of the gas in the sample chamber. The model can be applied under all power density, repetition rate and static focus parameters that have been applied in this study. The formation and relative influence of each structural unit is controlled by the depth/diameter ratio of the ablation crater.(Mank and Mason, 1999) The change in elemental behavior was suggest as being related to a change from photothermal-dominated to a plasma dominated ablation mechanisms. Hence for minimal fractionation it is essential to maintain power density well above the ablation threshold giving a crater of similar diameter from the top to the base

Laser wavelength:

Ablation mechanisms are influenced by the photon energy of the laser. Shorter wavelengths offer higher photon energies for bond breaking and ionisation processes. The ablated volume in different matrix will be similar for shorter wavelength in the standard and the unknown which limit fractionation effect between the two and make quantification easier.

Gas medium

Significant reduction of mass fractionation has been observed using He instead of Ar as a sample gas carrier (see below).

Other parameter such as **power density** or **focusing conditions** have also an influence

NB: The degree of fractionation can be described by relevance to a fractionation factor, f . For a given power density, which is significantly higher than the material ablation threshold value, the fractionation factor for element a at a time t , $f_a(t)$, is the change in signal relative to a reference element r at a time t , normalised to an initial response for both elements, and can be represented as :

$$f = \frac{R_{at}R_{ro}}{R_{ao}R_{rt}}$$

R_{ao} = initial response for element a

R_{ro} = initial signal response for reference element r

R_{at} = signal response for element a at time t

R_{rt} = signal response for reference element r at time t

Fractionation effects are lower when ablating in He (see discussion on Mixed Gas below)

IV-4- Data Reduction software

To my knowledge there is only one data reduction software package commercially available for laser ablation system (GLITTER TM, Achterbergh et al, 1998). However, in order to match the characteristic file format and to facilitate the rapid analysis of large volumes of raw data gathered from the ELEMENT HR-ICP mass spectrometer using laser ablation, it has been proposed that a software package has to be developed at Monash University (Schonbein TM). The package consist of three major operational phases, (Phase 1) treatment of raw data, (Phase 2) calculations of elemental abundances of trace elements in both minerals and inclusions and (Phase 3) isotope ratio measurements. At the moment only phase 1 and 2 has been achieved. The following consist of a description of the possibilities of this software:

Phase 1 - Processing of Raw Data

1] Exported files from the ICP-MS software containing the raw data (*.dat files) will be able to be processed directly by the ICP-MS package. An *.asc file will be convert from a *.dat file using the ICP-MS software

2] Each time slice in a run will then be examined and a suitable functional form will be chosen to represent the flat-topped peak shapes typically encountered on sector mass spectrometer instruments. A spike remover function will select the spikes and correct them, based on an average of the channels for one slice of time and for each element.

3] The next phase of data processing concerns the time evolution of the analytical signal for a given isotopic species over a period of consecutive time slices. The data will typically show an initial induction period, followed by a rapid rise and then a gradual decay. A second model fitting function will be used and the resulting function integrated numerically to obtain a signal for the species over the whole run. The end result of these operations will be a summary table of each isotope detected in the sample, and an average signal, such as the blank, the matrix of a sample and eventual inclusion(s).

Phase 2 - Calculation of Elemental Concentrations and Isotopic Composition in Minerals and Inclusions

1] Establishment of standard reference materials (e.g., NIST, USGS, etc.) databases.

2] Quantification and normalisation to internal standard data derived via external analytical technique (EMP, solution HR-ICP-MS) to correct for differences in laser ablation characteristics between standards and unknowns. The samples are analysed according to a specific sequence. Usually It start with the analyse of 2 standards then 10 samples and start again with 2 standards, etc.....The software will recognise this sequence, average the four standard between the ten samples are calculate the concentrations following this equation

$$C_{Unk, \text{ mg ml}^{-1}} = ((Unk_{\text{peak}} - Unk_{\text{background}}) / (Cal_{\text{peak}} - Cal_{\text{background}})) * (C_{\text{cal}} \text{ mg ml}^{-1})$$

Is = an internal standard of choice

I(m, x) = intensity of mass x of the element

C(m, x) = Concentration of the element of mass x in the standard

Depending on the position of the sample the response may be different for an element within the sequence. The software should be able to fit a straight line through the four points define by the raw counts and calculate a drift correction coefficient in function of the position of the sample within the sequence for each element. This correction isn't critical since signal drift (within a sequence of 10 samples) is unusual, mainly because the amount of sample ablated is

very small. Bulk analyse of homogeneous sample during the rastering of a fused glasses may create some drift. Using the same laser parameter, the laser may drill hole of different sizes within different samples having different matrix. The ablation given by the standard will be 100%. Then during the analyse of a sample we will observe a decrease of the spot size and thus a different ablation yield. This ablation yield will be calculated in function of the ratio between the count rate and the known concentration of the internal standard. This difference of ablation characteristic will be use to recalculate a new count rate for the calculation of the LOD for the sample. The software should be able to calculate the Limit Of Detection for each of the samples and correct these LOD in function of the ablation yield. In order to calculate the LOD the software need to calculate the standard deviation of the blank before each sample and then follow this equation:

$$= (3 * \text{Std. Dev. Isotope A (blank before ablation)} * \text{Conc. Isotope A in standard}) / (\text{Mean Isotope A in the standard} - \text{Mean isotope A in the blank})$$

- Finally the software should produce a %RSD variation between the standard which will give us an idea of the precision during the run for each standard treated as unknown within a sequence and also a %RSD variation of the same standard versus the composition given by the standard database for the accuracy.

Phase 3 - Isotope ratio measurements

Laser ablation coupled to ICP-MS also allows the measurement of in-situ isotopic signatures for geochronological or isotopical geochemical purposes. Research has been essentially focussed on the measurement of Sr isotopic composition in carbonate (Christensen, et al. 1995) and the lead (Feng, et al. 1993; Walder, et al. 1993; Machado et al. 1996; Scott and Gauthier 1996), U/Pb (Hirata and Nesbitt 1995; Fryer, et al. 1993) and Hf (Thirlwall and Walder 1995) isotopic compositions of zircon using multicollector ICP-MS or UV and IR quadrupole ICP-MS. The possibility of high resolution ICP-MS such as the ELEMENT in combination with a UV laser remain unknown but are very promising. The data reduction software should be able to apply a spike correction and select a stable portion of the signal in the same manner as for trace element determination (see phase I and II). Moreover this software should be able to calculate external and internal precision as well as the accuracy after dead time and mass bias correction.

- Precision: The software should able to select a stable portion of the signal that will be use for the calculation of the isotopic ratio. The ratio should be display on the screen versus the time of acquisition or the number of runs. Once the zone has been selected, a mean of the mean calculation will be apply in order to improve internal precision. For example, if we have selected a stable zone of 1000 scans over a total of 2000 scans. If we calculate a straight average of these 100 scan, the precision we will obtain will be higher than an average of 10 blocks of 100 scans. The software user should have the possibility to tell to the software if he needs to reduce the data in a certain number of blocks of dependant on the number of scan selected. The internal precision should be calculate following this equation:

$$\%RSD = \sqrt{\frac{\sum (R_i - \bar{R})^2}{N_R * (N_R - 1)}} * \frac{100}{\bar{R}}$$

- R_i = individual ratio of one scan
- R = Mean of all individual ratios
- N_R = number of individual ratios

The external precision should also be calculated following this other equation on a batch of identical samples:

$$\%RSD = \sqrt{\frac{\sum(R_m - R_{mi})^2}{(N_m - 1)}} * \frac{100}{R_m}$$

Rmi = individual ratio of one analysis

Rm = Mean of all analyses means

Nm = number of analyses

-Accuracy:

-Dead time correction: although the ICP software has the ability to correct the raw data for a given dead time following the equation 5, this facility should also be include in this software. It may be interesting to observe the change in accuracy while changing the value for the dead time.

$$C_{true} = \frac{C_{obs}}{(1 - C_{obs} \tau)}$$

t = deadtime

Ctrue = true count rates

Cobs = observed count rates

- Mass bias correction: We will run once again the sample in sequence starting with a standard of known isotopic composition and followed by unknown samples. Specific ratio on the standard will give us information on the mass bias (or to be more precise, the difference between this specific calculated ratio and the real ratio). The mass bias is calculated following the equation below. The mass bias is used to recalculate other ratios.

$$R_{true} = R_{obs} (1 + C)^m$$

Rtrue = true ratio

Robs = observed ratio

Dm = mass difference

C = mass bias factor.

The accuracy and precision of trace element and isotope ratio Measurements will also depends on the level of inter-element fractionation which is one of the major limitation of the laser ablation technique. Recent studies have described in great details the process of volatile versus refractory element fractionation during the interaction between the laser beam and the sample surface (see summary above).

IV-5- Future Improvements

Standard quality

Improvement in the determination of the trace element content of widely used standard such as the NIST glasses (Garbe-Schönberg, 1993; Rocholl, et al., 1997; Hollocher and Ruiz, 1995; Norman, et al., 1996; Pearce, et al., 1997; Horn, et al., 1997; Sylvester and Eggins, 1997). And The production of a series of new USGS glass standard such as BCR2G (Lahaye, et al., 1997; Norman et al 1998; Becker et al, 2000) and the development of new technique for making homogeneous standards (Bédard, et al., 1997; Hamilton and Hopkins, 1995; Raith, et al., 1996; Odergard 1998) should also improve the standard quality and subsequent accuracy of the data generated by laser ablation ICP-MS.

Time of Flight instruments (TOF)

TOF appears to be the instrument of choice to coupled with a laser ablation system in the near future (once improvement with the sensitivity will be achieved). The main advantage of TOF mass analyser is that all ions that contribute to the mass spectrum are accelerated into a flight tube at the same time, and the mass is related to the time taken to reach the ion detector. TOF is thus very fast and offer simultaneous sampling mass analysis which eliminate the characteristic noise associated with transient signal generated by laser ablation (Moore et al 1998, Mahoney et al 1996; Bleiner et al 2000). Further information on the principle of TOF could be obtain from SCIMEDIA.

Sample Cell design

Sensitivity as well as stability is also expected by improving the sample cell design. There are two main types of sample chamber. (1) Sample cell with a large volume for a cyclonic gas circulation. The gas is injected from beneath at one end of the sample chamber while it is collected at the other end in the middle, on the edge of the sample cell. It is suppose to give a much stable signal since the gas and sample is well mixed before it reaches the ICP; (2) Sample cell with small volume and aerodynamically shape for a laminar flow. It is suppose to give a better sensitivity and higher sample transport of the sample to the ICP. Other features such as the ability to flash the flashlamp at a higher and more stable rate, while the sample is ablated at a different and lower rate, should also result in a stability improvement.

Mixed gas (Helium - Argon)

Sensitivity improvement are expected using mixed gas such as nitrogen. Durrant (1994) have shown that the addition of about 1% N₂ in the coolant gas increase the sensitivity by a factor of 3 for some elements. Addition of about 12% N₂ to the cell flow have a similar effect. An improvement by a factor of 5 is also claimed by (Hirata and Nesbitt, 1995) for heavy masses. Moreover, mixed argon-helium atmosphere retards condensation and reprecipitation of ablated material around the excavated crater (Louks, et al., 1995; Eggins et al 1998; Mao et al 1998; Leung et al 1998; Chan et al 1998; Günther and Heinrich 1999). By introducing He to the sample cell, in such a way as to exclude Ar for the ablation site, ablation can be conducted in an ambient gas with an order of magnitude lower mass density, allowing the plasma a plume to expand further before relaxation of the high pressure leading edge. This allow more time for material to condense out of the cooling plasma and also means that any material driven backwards must again travel further before encountering the sample surface, The dramatic

reduction in surface condensate built up in He vs. Ar is evident and is associated with a large increase in sensitivity seen at the ICP-MS (Eggins et al, 1998).

NB: The signal intensity is 2-3 times greater when ablating in He rather than Ar under the same conditions. The corresponding fractionation factors are similar in both cases. However the depth of penetration is 20-30% greater when ablating in a He atmosphere. Approximately 0.22 μm is removed per shot in NIST 610 glass by the 266nm Nd:YAG laser when ablating in Ar. When ablating in He this increases to 0.27 μm per shot. Hence in terms of a specific depth from the sample surface, fractionation effects are lower when ablating in He. The manner of deposition of material around the top of the crater is very different when ablating in He with a larger diameter blanket of deposited material. However, the material is deposited in a thinner layer of coalesce particles than in the case of the blanket observed when ablating in Ar. Ablating in He can therefore be advantageous as the overall volume of deposited material is lower. The overall reduction corresponds to a increase in signal intensity observed on the ICP-MS, as was confirmed on the basis of weighing experiments before and after the ablation of craters. Ablation craters continue to show the 3 stage structure when ablating in He but the height of region A, appears to be smaller. This suggests that the plasma extends much further in heights and heats the surface less. (Mank and Mason, 1999).

Picosecond laser

Experiment on signal intensity versus power density on nanosecond and picosecond laser has led the conclusion (related the basic process of ablation) that Picosecond laser are more efficient than nanosecond laser for removing sample. (Mao, et al., 1996; Mao, 1997; Mao, et al., 1993; Mao, et al., 1997; Russo, 1995; Russo, et al., 1996)

The fifth harmonic
Jeffries et al (1998)

New calibration strategy

Craig et al, 2000; Falk et al 1998; Masters and Sharp 1997;

IV - Bibliography

Alard, O., et al. (1999) Highly siderophile elements in mantle sulfides: in-situ LAM-ICPMS analysis. abstract in Golschmidt conference.

Alexander, M.L., et al. (1998) Laser ablation inductively coupled plasma mass spectrometry. *Applied Surface Science* 129, 255-261.

J. Alteyrac, S. Augagneur, B. Medina, N. Vivas and Y. Glories (1995) Mise au point d'une méthode de dosage des éléments minéraux du bois de chêne par ablation laser ICP-MS., *Analisis*, 23: 523-526.

P. Arrowsmith (1987) Laser ablation of solids for elemental analysis by inductively coupled plasma mass spectrometry, *Analytical Chemistry*, 59: 1437-1444.

A. Audétat, D. Günther and C.A. Heinrich (1998) Formation of a magmatic-hydrothermal ore deposit -insights with LA-ICP-MS analysis of fluid inclusions, *Science*, 279: 2091-2094.

Audétat, A. and Günther, D., 1999. Mobility and H₂O loss from fluid inclusions in natural quartz crystals. *Contrib Miner Petrol*, 137: 1-14.

C. Ayora and R. Fontarnau (1990) X-ray micro-analysis of frozen fluid inclusions, *Chemical Geology*, 89: 135-148.

Baker, S.A., et al. (1999) Analysis of soil and sediment samples by laser ablation inductively coupled plasma mass spectrometry. *Journal of Analytical Atomic Spectrometry* 1999, 19-26.

V. Balaram (1995) Developments and trends in inductively coupled plasma mass spectrometry and its influence on the recent advances in trace element analysis, *Current Science*, 69: 640-649.

C. Balhaus, P. Sylvester and D. Ellis (1997) Spatial distribution of platinum-group elements in magmatic sulphides, *RSES - Annual report*, 96-97.

D.A. Banks, B.W.D. Yardley, A.R. Campbell and K.E. Jarvis (1994) REE composition of an aqueous magmatic fluid: a fluid inclusion study from the Capitan pluton, New Mexico, U.S.A., *Chemical Geology*, 113: 259-272.

P. Barbey, P. Allé, M. Brouand and F. Alabarède (1995) Rare-earth patterns in zircons from the Manaslu granite and Tibetan Slab migmatites (Himalaya): insights in the origin and evolution of a crustally-derived magma, *Chem Geol*, 125: 1-17.

F. Bea, P. Montero, G. Garuti and F. Zacharini (1997) Pressure-dependance of rare earth element distribution in amphibolite- and granulite- grade garnets. A LA-ICP-MS study, *Geostandard Newsletter*, 21: 253-270.

F. Bea, P. Montero, A. Stoh and J. Baasner (1996) Microanalysis of minerals by an Excimer UV-LA-ICP-MS system, *Chemical Geology*, 133: 145-156.

Bea, F., et al. (1997) Pressure-dependence of rare earth element distribution in amphibolite- and granulite- grade garnets. A LA-ICP-MS study. *Geostandard Newsletter* 21, 253-270.

Becker, J.S., Pickhardt, C. and Dietze, H.-J., 2000. Laser ablation inductively coupled plasma mass spectrometry for determination of trace elements in geological glasses. *Mikrochimica Acta*, 135: 71-80.

L.P. Bédard, D.R. Baker and N. Machado (1997) A new technique for the synthesis of geochemical reference samples for laser ablation-ICP-MS analysis of zircons, *Chemical Geology*, 138: 1-7.

Bellotto, V.R. and Miekeley, N., 2000. Improvements in calibration procedures for the quantitative determination of trace elements in carbonate material (mussel shells) by laser ablation ICP-MS. *Fresenius Journal of Analytical Chemistry*, 367: 635-640.

Bleiner, D., Hametner, K. and Günther, D., 2000. Optimization of a laser ablation-inductively coupled plasma "time of flight" mass spectrometry system for short transient signal acquisition. *Fresenius J. Anal. Chem.*, 368: 37-44.

J. Blichert-Toft, C. Chauvel and F. Alabarède (1997) Separation of Hf and Lu for high-precision analysis of rock samples by magnetic sector-multiple collector ICP MS, *Contribution to Mineralogy and Petrology*, 127: 248-260.

Borisov, O.V., et al. (1999) Inductively coupled plasma mass spectrometric study of non-linear calibration behavior during laser ablation of binary Cu-Zn Alloys. *Spectrochimica Acta Part B-Atomic Spectroscopy* 54, 1351-1365.

Borisov, O.V., et al. (2000) Effect of crater development on fractionation and signal intensity during laser ablation inductively coupled plasma mass spectrometry. *Spectrochimica Acta Part B-Atomic Spectroscopy* 55, 1693-1704.

Bottrell S.H., Yardley B. and Buckley F. (1988) A modified crush-leach method for the analysis of fluid inclusion electrolytes, *Bulletin Mineralogique*, 111: 279-290.

Boué-Bigne, F., et al. (1999) A calibration strategy for LA-ICP-MS analysis employing aqueous standards having modified absorption coefficients. *Journal of Analytical Atomic Spectrometry* 14, 1665-1672.

Bryant, C.J., Arculus, R.J. and Eggins, S.M., 1999. Laser ablation-inductively coupled plasma-mass spectrometry and tephra: a new approach to understand arc-magma genesis. *geology*, 27: 1119-1122.

Bulanova, G.P., et al. (1996) Trace elements in sulfide inclusions from Yakutian diamonds. *Contribution to Mineralogy and Petrology* 124, 111-125.

Butler, I.B. and R.W. Nesbitt (1999) Trace element distributions in the chalcopyrite wall of a black smoker chimney: insights from laser ablation inductively coupled plasma mass spectrometry (LA-ICP-MS). *EPSL* 167, 335-345.

Campbell, A.J. and M. Humayun (1999) Trace element microanalysis in iron meteorites by laser ablation ICPMS. *Analytical Chemistry* 71, 939-946.

Chan, W.T., et al. (1998) Effects of gas environment on picosecond laser ablation. *Applied Surface Science* 129, 269-273.

Chan, G.C.Y., Chan, W.T., Mao, X.L. and Russo, R.E., 2000. Investigation of matrix effect on dry inductively coupled plasma conditions using laser ablation sampling. *Spectrochimica Acta Part B-Atomic Spectroscopy*, 55(3): 221-235.

D.M. Channer, DER and E.T.C. Spooner (1992) Analysis of fluid inclusion leachates from quartz by ion chromatography, *Geochimica et Cosmochimica Acta*, 56 PACROFI III Spec. Vol.:

Z.X. Chen, W. Doherty and D.C. Gregoire (1997) Application of laser sampling microprobe inductively coupled plasma mass spectrometry to the in situ trace element analysis of selected geological materials, *Journal of Analytical Atomic Spectrometry*, 12: 653-659.

Chen, Z. (1999) Inter-element fractionation and correction in laser ablation inductively coupled plasma mass spectrometry. *JAAS* 14, 1823-1828.

Chen, Z., Canil, D. and Longerich, H.P., 2000. Automated in situ trace element analysis of silicate materials by laser ablation inductively coupled plasma mass spectrometry. *Fresenius J. Anal. Chem.*, 368: 73-78.

S. Chenery, J. Cook, M. Styles and E.M. Cameron (1995) Determination of the three-dimensional distributions of precious metals in sulphide minerals by laser ablation microprobe - inductively coupled plasma-mass spectrometry (LAM-ICP-MS), *Chemical Geology*, 124: 55-65.

S. Chenery and J.M. Cook (1993) Determination of Rare Earth elements in single mineral grains by laser ablation microprobe - inductively coupled plasma mass spectrometry - preliminary study, *Journal of Analytical Atomic Spectrometry*, 8: 299-303.

S. Chenery, T. Williams, T.A. Elliott, P.L. Forey and L. Werdelin (1996) Determination of Rare Earth elements in biological and mineral apatite by EPMA and LAM-ICP-MS, *Mikrochimica Acta*, Suppl 13: 259-269.

Chin, C.-J., Wang, C.-F. and Jeng, S.-L., 1999. Multi-element analysis of airborne particulate matter collected on PTFE-membrane filters by laser ablation inductively coupled plasma mass spectrometry. *Journal of Analytical Atomic Spectrometry*, 14: 663-668.

J.N. Christensen, A.N. Halliday, D.C. Lee and C.M. Hall (1995) In situ Sr isotopic analysis by laser ablation, *Earth Planetary Science Letter*, 136: 79-85.

Ciocan, A.C., Mao, X.L., Borisov, O.V. and RE., R., 1998. optical emission spectroscopy studies of the influence of laser ablated mass on dry inductively coupled plasma conditions. *Spectrochimica Acta Part B-Atomic Spectroscopy*, 53: 463-470.

H. Cousin, A. Weber, B. Magyar, I. Abell and D. Günther (1995) An auto-focus system for reproducible focussing in laser ablation inductively coupled plasma mass spectrometry, *Spectrochimica Acta*, 50B: 63-66.

A. Cox, F. Keenan, M. Cooke and J. Appleton (1996) Trace element profiling of dental tissues using laser ablation inductively coupled plasma mass spectrometry, *Fresenius Journal of Analytical Chemistry*, 354: 254-258.

Craig, C.A., Jarvis, K.E. and Clarke, L.J., 2000. An assessment of calibration strategies for the quantitative and semi-quantitative analysis of calcium carbonate matrices by laser ablation-inductively coupled plasma-mass spectrometry (LA-ICP-MS). *Journal of Analytical Atomic Spectrometry*, 15: 1001-1008.

Cromwell, E.F. and Arrowsmith, P., 1995. Semiquantitative Analysis with Laser Ablation Inductively Coupled Plasma Mass Spectrometry. *Analytical Chemistry*, 67: 131-138.

C. Dalpé and D.R. Baker (1994) Partition coefficients for rare-earth elements between calcite amphibole and Ti-rich basanitic glass at 1.5 Gpa, 110°C, *Mineral Magazine*, 58A: 207-208.

C. Dalpé, D.R. Baker and S.R. Sutton (1995) Synchrotron X-ray-fluorescence and laser-ablation ICP-MS microprobes: useful instruments for analysis of experimental run-products, *Canadian Mineralogist*, 33: 481-498.

Davies, J.F., et al. (1998) Variations in REE and Sr-isotope chemistry of carbonate gangue, Castellanos Zn-Pb deposit, Cuba. *Chemical Geology* 144, 99-119.

E.H. De Carlo and E. Pruszkowski (1995) Laser ablation ICP-MS determination of alkaline and rare earth elements in marine ferro-manganese deposits, *Atomic Spectroscopy*, 16: 65-72.

E.R. Denoyer, K.J. Fredeen and J. Hager (1991) Laser Solid sampling for inductively coupled plasma mass spectrometry, *Analytical Chemistry*, 63: 445A-457A.

Denoyer, E.R. (1994) Optimization of transient signal measurements in ICP-MS. *Atomic Spectroscopy* 15, 7-16.

Devos, W., C. Moor, and P. Lienemann (1999) Determination of impurities in antique silver objects for authentication by laser ablation inductively coupled plasma mass spectrometry (LA-ICP-MS). *Journal of Analytical Atomic Spectrometry* 14, 621-626.

L.W. Diamond, D.D. Marshall, J.A. Jackman and G.B. Skippen (1990) Elemental analysis of fluid inclusions in minerals by secondary ion mass spectrometry (SIMS): Application to cation ratios of fluid inclusions in an Archean mesothermal gold-quartz vein, *Geochimica et Cosmochimica Acta*, 54: 545-552.

M. Ducreux-Zappa and J.-M. Mermet (1996) Analysis of glass by UV laser ablation inductively coupled plasma atomic emission spectrometry. Part1. Effects of the laser parameters on the amount of ablated material and the temporal behaviour of the signal for different types of laser, *Spectrochimica Acta*, 51B: 321-332.

S.F. Durrant (1994) Feasibility of improvement in analytical performance in laser ablation inductively coupled plasma-mass spectrometry (LA-ICP-MS) by addition of nitrogen to the argon plasma, *Fresenius Journal of Analytical Chemistry*, 349: 768-771.

S.F. Durrant and N.I. Ward (1994) Laser ablation-inductively coupled plasma mass spectrometry (LA-ICP-MS) for the multielemental analysis of biological materials: a feasibility study, *Food chemistry*, 49: 317-323.

Durrant, S.F. (1999) Laser ablation inductively coupled plasma mass spectrometry achievements, problems, prospects. *Journal of Analytical Atomic Spectrometry* 14, 1385-1403.

Durrant, S.F. (1993) Alternatives to all-argon plasmas in inductively coupled plasma mass spectrometry (ICP-MS): an overview. *Fresenius Journal of Analytical Chemistry* 347, 389-392.

S.M. Eggins, R.L. Rudnick and W.F. McDonough (1998) The composition of peridotites and their minerals: a laser-ablation ICP-MS study, *Earth and Planetary Science Letters*, 154: 53-71.

Eggins, S.M., L.P.J. Kinsley, and J.M.G. Shelley (1998) Deposition and element fractionation processes during atmospheric pressure laser sampling from analysis by ICP-MS. *Applied Surface Science* 129, 278-286.

R.D. Evans, P.M. Outridge and P. Richner (1994) Application of laser ablation inductively coupled plasma mass spectrometry to the determination of environmental contaminants in calcified biological structures, *Journal of Analytical Atomic Spectrometry*, 9: 985-989.

R.D. Evans, P. Richner and P.M. Outridge (1995) Micro-spatial variations of heavy metals in the teeth of Walrus as determined by laser ablation ICP-MS: the potential for reconstructing a history of metal exposure, *Archives of Environmental Contamination & Toxicology*, 28:

N.M. Evensen, P.J. Hamilton and R.K. O'Nions (1978) Rare-earth abundances in chondritic meteorites, *Geochimica et Cosmochimica Acta*, 42: 1199-1212.

Fabre, C., M.-C. Boiron, and A. Moissette (1999) Determination of ions in individual fluid inclusions by laser ablation optical emission spectroscopy: development and applications to natural fluid inclusions. *Journal of Analytical Atomic Spectrometry* 14, 913-922.

Falk, H.F., et al. (1998) Calibration of laser-ablation ICP-MS. Can we use synthetic standards with pneumatic nebulisation? *Fresenius Journal of Analytical Chemistry* 362, 468-472.

J.S. Federowich, J.C. Jain and R. Kerrich (1995) Trace-element analysis of garnet by laser-ablation microprobe ICP-MS, *Canadian Mineralogist*, 33: 469-480.

I. Feldmann, W. Tittes, N. Jakubowski and D. Stuewer (1994) Performance characteristics of inductively coupled plasma mass spectrometry with high mass resolution, *Journal of Analytical Atomic Spectrometry*, 9: 1007-1014.

R. Feng (1994) In situ trace element determination of carbonates by laserprobe inductively coupled plasma mass spectrometry using nonmatrix matched standardization, *Geochimica et Cosmochimica Acta*, 58: 1615-1623.

R. Feng, N. Machado and J. Ludden (1993) Lead geochronology of zircon by LaserProbe-Inductively Coupled Plasma Mass Spectrometry (LP-ICPMS), *Geochimica et Cosmochimica Acta*, 57: 3479-3486.

D. Figg, J. Cross and C. Brink (in press) More investigations into elemental fractionation resulting from laser ablation - inductively coupled plasma - mass spectrometry (LA-ICP-MS) on glass samples.

D. Figg and M.S. Kahr (1997) Elemental fractionation of glass using laser ablation inductively coupled plasma mass spectrometry, *Applied Spectroscopy*, 51: 1185-1192.

S.F. Foley, S.E. Jackson, B.J. Fryer, J.D. Greenough and G.A. Jenner (1996) Trace element partition coefficients for clinopyroxene and phlogopite in an alkaline lamprophyre from Newfoundland by LAM-ICP-MS, *Geochimica et Cosmochimica Acta*, 60: 629-638.

Foley, S.F., et al. (1996) Trace element partition coefficients for clinopyroxene and phlogopite in an alkaline lamprophyre from Newfoundland by LAM-ICP-MS. *Geochimica et Cosmochimica Acta* 60, 629-638.

J.D. Frantz, H.K. Mao, Y.G. Zhang, Y. Wu, A.C. Thompson, R. Underwood, J.H. Gaique, K.W. Jones and M.L. Rivers (1988) Analysis of fluid inclusions by X-ray fluorescence using synchrotron radiation, *Chemical geology*, 69: 235-244.

B.J. Fryer, S.E. Jackson and H.P. Longerich (1993) The application of laser ablation microprobe-inductively coupled plasma-mass spectrometry (LAM-ICP-MS) to in situ (U)-Pb geochronology, *Chemical Geology*, 109: 1-8.

B.J. Fryer, S.E. Jackson and H.P. Longerich (1995) The design, operation and role of the laser-ablation microprobe coupled with an inductively coupled plasma-mass spectrometer (LAM-ICP-MS) in the Earth Sciences, *Canadian Mineralogist*, 33: 303-312.

R. Fuge, T.J. Palmer, N.J.G. Pearce and W.T. Perkins (1993) Minor and trace element chemistry of modern shells: a laser ablation inductively coupled plasma mass spectrometry study, *Applied Geochemistry*, 2: 111-116.

Gastel, M., Becker, J.S., Küppers, G. and Dietze, H.-J., 1997. Determination of long-lived radionuclides in concrete matrix by laser ablation inductively coupled plasma mass spectrometry. *Spectrochimica acta part B*, 52: 2051-2059.

Gaegan, M. and J.M. Mermet (1998) Study of laser ablation of brass materials using inductively coupled plasma atomic emission spectrometric detection. *Spectrochimica Acta Part B* 53, 581-591.

Garofalo, P., Audétat, A., Günther, D., Heinrich, C.A. and Ridley, J., 2000. Estimation and testing of standard molar thermodynamic properties of tourmaline end-members using natural samples. *American Mineralogist*, 85: 78-88.

M. Gahderi, I.H. Campbell and P.J. Sylvester (1997) Eu anomalies in scheelite: implications for the oxidation state of hydrothermal gold mineralisation in Archaean greenstone belts, *RSES - Annual report*, 159-160.

Ghaderi, M., Palin, J.M., Campbell, I.H. and Sylvester, P.J., 1999. Rare earth element systematics in scheelite from hydrothermal gold deposits in the Kalgoorlie-Norseman region, Western Australia. *Economic Geology*, 94: 423-437.

C.-D. Garbe-Schönberg (1993) Simultaneous determination of thirty-seven trace elements in twenty-eight international rock standards by ICP-MS, *Geostandards Newsletter*, XVII: 81-98.

C.-D. Garbe-Schönberg (1994) In-situ micro-analysis of platinum and rare earths in ferromanganese crusts by laser ablation-ICP-MS (LAICPMS), *Fresenius Journal of Analytical Chemistry*, 350: 264-271.

C.-D. Garbe-Schönberg, C. Reimann and V.A. Pavlov (1997) Laser ablation ICP-MS analyses of tree-ring profiles in pine and birch from N Norway and NW Russia - a reliable record of the pollution history of the area, *Environmental Geology*, 32: 9-16.

Garbe-Schoenberg, C.D., C. Reimann, and V.A. Pavlov (1997) Laser ablation ICP-MS analyses of tree-ring profiles in pine and birch from N Norway and NW Russia; a reliable record of the pollution history of the area? *Environmental Geology* 32, 9-16.

Garbe-Schönberg, C.-D. and Arpe, T., 1997. High resolution-ICPMS in fast scanning mode: application for laser ablation analysis of zircon. *Fresenius J. Anal. Chem.*, 359: 462-464.

A.M. Ghazi, T.E. McCandless, D.A. Vanko and J. Ruiz (1996) New quantitative approach in trace elemental analysis of single fluid inclusions: applications of laser ablation inductively coupled plasma mass spectrometry (LA-ICP-MS), *Journal of Analytical Atomic Spectrometry*, 11: 667-674.

A.M. Ghazi, D.A. Vanko and R.C. Seeley (1993) Determination of rare earth elements in fluid inclusions by inductively coupled plasma-mass spectrometry (ICP-MS), *Geochimica et Cosmochimica Acta*, 57: 4513-4516.

Ghazi, A.M. (1994) Lead in Archaeological samples from North America: An application of laser ablation ICP-MS (LA-ICP-MS). *Applied Geochemistry* 9, 627-636.

Ghazi, A.M. and Shuttleworth, S., 2000. Trace element determination of single fluid inclusions by laser ablation ICP-MS: applications for halites from sedimentary basins. *Analyst*, 001: 205-210.

U. Giebmann and U. Greb (1994) High resolution ICP-MS - a new concept for elemental spectrometry, *Fresenius Journal of Analytical Chemistry*, 350: 186-193.

Glaser, S.M., S.F. Foley, and G. D. (1999) Trace element compositions of minerals in garnet and spinel peridotite xenoliths from the Vitim volcanic field, Transbaikalia, eastern Siberia. *Lithos* 48, 263-285.

P. Goodal, S.G. Johnson and E. Wood (1995) Laser ablation inductively coupled plasma atomic emission properties and analytical behavior, *Spectrochimica Acta*, 50B: 1823-1835.

A.L. Gray (1985) Solid sample introduction by laser ablation for inductively coupled plasma source mass spectrometry, *Analyst*, 110: 551-556.

D. Günther, A. Audetat, R. Frischknecht and C.A. Heinrich (1998) Quantitative analysis of major, minor and trace elements using laser ablation inductively coupled plasma mass spectrometry, *Journal of Analytical Atomic Spectrometry*, 13: 263-270.

D. Günther, R. Frischknecht, C.A. Heinrich and H.J. Kahlert (1997) Capabilities of an argon fluoride 193nm excimer laser for laser ablation inductively coupled plasma mass spectrometry microanalysis of geological materials, *Journal of Analytical Atomic Spectrometry*, 12: 939-944.

D. Günther, R. Frischknecht, H.-J. Müschenborn and C.A. Heinrich (1997) Direct liquid ablation: a new calibration strategy for laser ablation-ICP-MS microanalysis of solids and liquids, *Fresenius Journal of Analytical Chemistry*, 359: 390-393.

D. Günther, H.P. Longerich and S.E. Jackson (1995) A new enhanced sensitivity quadrupole inductively coupled plasma-mass spectrometer, *Canadian Journal of Applied Spectroscopy*, 40: 111-116.

D. Günther, H.P. Longerich, S.E. Jackson and L. Forsythe (1996) Effect of sample orifice on dry plasma inductively coupled plasma mass spectrometry (ICPMS) background, sensitivities and limit of detection using laser ablation sample introduction, *Fresenius Journal of Analytical Chemistry*, 355: 771-773.

Günther, D. and C.A. Heinrich (1999a) Enhanced sensitivity in laser ablation-ICP mass spectrometry using helium-argon mixtures as aerosol carrier. *Journal of Analytical Atomic Spectrometry* 14, 1363-1368.

Günther, D. and C.A. Heinrich (1999b) Comparison of the ablation behaviour of 266 nm Nd:YAG and 193 nm ArF excimer lasers for LA-ICP-MS analysis. *Journal of Analytical Atomic Spectrometry* 14, 1369-1374.

Günther, D., Horn, I. and Hattendorf, B., 2000. Recent trends and developments in laser ablation-ICP-Mass Spectrometry. *Fresenius J. Anal. Chem.*, 368: 4-14.

Guo, X. and F.E. Lichte (1995) Analysis of rocks, soils and sediments for the chalcophile elements by laser ablation-inductively coupled plasma mass spectrometry. *Analyst* 120, 2707-2711.

A.N. Halliday, D.-C. Lee, J.N. Christensen, A.J. Walder, P.A. Freedman, C.E. Jones, C.M. Hall, W. Yi and D. Teagle (1995) Recent developments in inductively coupled plasma magnetic sector multiple collector mass spectrometry, *International journal of Mass Spectrometry and ion Processes*, 146/147: 21-33.

D.L. Hamilton and T.C. Hopkins (1995) Preparation of glasses for use as chemical standards involving the coprecipitated gel technique, *Analyst*, 120: 1373-1377.

R.M. Hazen, R.M. Bell and H.K. Mao (1977) Comparison of adsorption spectra of lunar and terrestrial olivine, *Carnegie Inst Washington Yearbook*, 77: 853-855.

Heinrich, C.A., Gunther, D., Audetat, A., Ulrich, T. and Frischknecht, R., 1999. Metal fractionation between magmatic brine and vapor, determined by microanalysis of fluid inclusions. *Geology*, 27: 755-758.

Hemmerlin, M. and J.M. Mermet (1996) Determination of elements in polymers by laser ablation inductively coupled plasma atomic emission spectrometry: effect on the laser beam wavelength, energy and masking on the ablation threshold and efficiency. *Spectrochimica Acta* 51B, 579-589.

R.W. Hinton (1997) A brilliant future for microanalysis?, *Analyst*, 122: 1187-1192.

T. Hirata (1996) Lead isotopic analyses of NIST standard reference materials using multiple collector inductively coupled plasma mass spectrometry coupled with a modified external correction method for mass discrimination effect, *Analyst*, 121: 1407-1411.

T. Hirata (1997) In-situ osmium ratio analyses of oridosmines by laser ablation-multiple collector-inductively coupled plasma mass spectrometry, *Chemical Geology*,

T. Hirata (1997) Soft ablation technique for laser ablation inductively coupled plasma mass spectrometry, *Journal of Analytical Atomic Spectrometry*, 12: 1337-1342.

T. Hirata and R.W. Nesbitt (1995) U-Pb isotope geochronology of zircon: evaluation of the laser probe-inductively coupled plasma mass spectrometry technique, *Geochimica et Cosmochimica Acta*, 59: 2491-2500.

T. Hirata and R.W. Nesbitt (1997) Distribution of platinum group elements and rhenium between metallic phases of iron meteorites, *Earth and Planetary Science Letters*, 147: 11-24.

Hirata, T. (1997) Isotopic variations of germanium in iron and stony iron meteorites. *Geochimica et Cosmochimica Acta* 61, 4439-4448.

E. Hoffmann, C. Ludke, H. Scholze and H. Stephanowitz (1994) Analytical investigations of tree rings by laser ablation ICP-MS, *Fresenius Journal of Analytical Chemistry*, 350: 253-259.

E. Hoffmann, C. Ludke and H. Stephanowitz (1996) Application of laser-ICP-MS in environmental analysis, *Fresenius Journal of Analytical Chemistry*, 355: 900-903.

E. Hoffmann, C. Lüdle and H. Scholze (1997) Is laser ablation ICP-MS an alternative to solution analysis of solid samples, *Fresenius Journal of Analytical Chemistry*, 359: 394-398.

E. Hoffmann, H. Stephanowitz and J. Skole (1996) investigations of the migration of elements in tree rings by laser-ICP-MS, *Fresenius Journal of Analytical Chemistry*, 355: 690-693.

A.W. Hofmann (1988) Chemical differentiation of the Earth : the relationship between mantle, continental crust and oceanic crust, *Earth and Planetary Science Letters*, 90: 297-314.

Hoffmann, E., et al. (1999) Studies of the quantitative analysis of trace elements in single SiC crystals using laser ablation-ICP-MS. *Journal of Analytical Atomic Spectrometry* 14, 1679-1684.

Hoffmann, E., Lüdke, C., Skole, J., Stephanowitz, H. and Wagner, G., 1999. Studies of the quantitative analysis of trace elements in single SiC crystals using laser ablation-ICP-MS. *Journal of Analytical Atomic Spectrometry*, 14: 1679-1684.

K. Hollocher and J. Ruiz (1995) Major and trace element determinations on NIST glass standard reference Materials 611, 612, 614 and 1834 by Inductively Coupled plasma-Mass Spectrometry, *Geostandards Newsletter*, 19: 27-34.

Horn I., Foley S.F., Jackson S.E. and J. G.A. (1994) Experimentally determined partitioning of high field strength- and selected transition elements between spinel and basaltic melt, *Chemical Geology*, 117: 193-218.

I. Horn, R.W. Hinton, S.E. Jackson and H.P. Longrich (1997) Ultra-trace element analysis of NIST SRM 616 and 614 using laser ablation microprobe inductively coupled plasma mass spectrometry (LAM-ICP-MS): a comparison with secondary ion mass spectrometry (SIMS), *Geostandards Newsletter*, 21: 191-204.

N. Imai (1990) Quantitative analysis of original and powdered rocks and mineral inclusions by laser ablation inductively coupled plasma mass spectrometry, *Analytical Chimica Acta*, 235: 381-391.

N. Imai (1992) Microprobe analysis of geological materials by laser ablation inductively coupled plasma mass spectrometry, *Analytica Chimica Acta*, 269: 263-268.

N. Imai and K. Shimokawa (1993) ESR ages and trace element in a fossil mollusc shell, *Applied Radiation and isotopes*, 44: 161-165.

N. Imai and M. Yamamoto (1994) Direct analysis of laminated dolomite and zircon by laser ablation inductively coupled plasma mass spectrometry, *Microchemical Journal*, 50: 281-288.

Ionov, D. (1998) Trace element composition of mantle-derived carbonates and coexisting phases in peridotite xenoliths from alkali basalts. *Journal of Petrology* 39, 1931-1941.

J.J. Irwin and E. Roedder (1995) Diverse origins of fluid in magmatic inclusions at Bingham (Utah, USA), Butte (Montana, USA), St. Austell (Cornwall, UK), and Ascension Island (Mid-Atlantic, UK), indicate by laser microprobe analysis of Cl, K, I, Ba, Te, Ar, Kr, and Xe, *Geochimica et Cosmochimica Acta*, 59: 295-312.

S.E. Jackson, H.P. Longrich, G.R. Dunning and B.J. Fryer (1992) The application of laser-ablation microprobe-inductively coupled plasma-Mass Spectrometry (LAM-ICP-MS) to in situ trace-element determination in minerals, *Canadian Mineralogist*, 30: 1049-1064.

I. Jarvis and K.E. Jarvis (1992) Plasma spectrometry in the Earth Sciences: techniques, applications and future trends, *Chemical Geology*, 95: 1-33.

K.E. Jarvis (1990) A critical evaluation of two sample preparation techniques for low-level determination of some geologically incompatible elements by inductively coupled plasma-mass spectrometry, *Chemical Geology*, 83: 89-103.

K.E. Jarvis and J.G. Williams (1993) Laser ablation inductively coupled plasma spectrometry (LA-ICP-MS) : a rapid technique for the direct, quantitative determination of major, trace and rare earth elements in geological samples, *Chemical Geology*, 106: 251-262.

Jarvis, K.E., Williams, J.G., Parry, S.J. and Bertalan, E., 1995. Quantitative determination of platinum-group elements and gold using Ni S fire assay with laser ablation - inductively coupled plasma-mass spectrometry. *Chemical Geology*, 124: 37-46.

T.E. Jeffries, W.T. Perkins and N.J.G. Pearce (1995) Comparisons of infrared and ultraviolet laser probe microanalysis inductively coupled plasma mass spectrometry in mineral analysis, *Analyst*, 120: 1365-1371.

T.E. Jeffries, W.T. Perkins and N.J.G. Pearce (1995) Measurements of trace elements in basalts and their phenocrysts by LaserProbe micro-analysis inductively coupled plasma mass spectrometry, *Chemical Geology*, 121: 131-144.

Jeffries, T.E., S.E. Jackson, and H.P. Longerich (1998). Application of a frequency quintupled Nd-YAG source ($\lambda = 213 \text{ nm}$) for laser ablation inductively coupled plasma mass spectrometric analysis of minerals. *Journal of Analytical Atomic Spectrometry* 13, 935-940.

Jeffries, T.E., Pearce, N.J.G., Perkins, W.T. and Raith, A., 1996. Chemical fractionation during infrared and ultraviolet laser ablation inductively coupled plasma mass spectrometry - Implications for mineral microanalysis. *Analytical communications*, 33: 35-39.

Kanicky, V., Otruba, V. and Mermet, J., 2000. Analysis of tungsten carbide coatings by UV laser ablation inductively coupled plasma atomic emission spectrometry. *Spectrochimica Acta Part B-Atomic Spectroscopy*, 55(6): 575-586.

W.C. Kelly and P.A. Burgio (1983) Cryogenic scanning electron microscopy of fluid inclusions in ore and gangue minerals, *Economic Geology*, 87: 1262-1267.

L. Kinsley, J.M.G. Shelley and S.M. Eggins (1997) Processes affecting laser ablation sampling of materials for analysis by ICP-MS, RSES - Annual report, 137.

V.V. Kogan, M.W. Hinds and G.I. Ramendik (1994) The direct determination of trace emetals in gold and silver materials by laser ablation inductively coupled plasma mass spectrometry without matrix matched, *Spectrochimica Acta*, 49: 333-343.

D.J. Kontak and S. Jackson (1995) Laser-ablation ICP-MS micro-analysis of calcite cement from a Mississippi-valley-type Zn-Pb deposit, Nova Scotia: dramatic variability in REE content on macro- and micro-scales, *Canadian Mineralogist*, 33: 445-467.

Kontak, D.J. and S.J. Jackson (1999) Documentation of variable trace- and rare-earth-element abundances in carbonates from auriferous quartz veins in Meguma lode-gold deposits, Nova Scotia. *Canadian Mineralogist* 37, 469-488.

Kurat, G. and Dobosi, G., 2000. Garnet and diopside-bearing diamondites (framesites). *Mineralogy & Petrology*, 69: 143-159.

Y. Lahaye and N.T. Arndt (1996) Alteration of a komatiitic flow, Alexo, Ontario, Canada., *Journal of Petrology*, 37: 1261-1284.

Y. Lahaye, D. Lambert and S. Walters (1997) Ultraviolet laser sampling and high-resolution Inductively coupled plasma mass spectrometry, *Geostandard Newsletters*, 21: 205-214.

Leach, J.J., et al. (1999) Calibration of laser ablation inductively coupled plasma mass spectrometry using standard additions with dried solution aerosols. *Analytical Chemistry* 71, 440-445.

D.-C. Lee and A.N. Halliday (1995) Precise determinations of the isotopic compositions and atomic weights of molybdenum, tellurium, tin and tungsten using ICP magnetic sector multiple collector mass spectrometry, *International Journal of Mass spectrometry and ion Processes*, 146/147: 35-46.

Lee, K.M., et al. (1999) Use of laser ablation inductively coupled plasma mass spectrometry to provide element versus time profiles in teeth. *Analytica Chimica Acta* 395, 179-185.

Leung, A.P.K., et al. (1998) Influence of Gas environment on picosecond laser ablation sampling efficiency and ICP conditions. *Analytical Chemistry* 70, 4709-4716.

F.E. Lichte (1995) Determination of elemental content of rocks by laser ablation inductively coupled plasma mass spectrometry, *Analytical Chemistry*, 67: 2479-2485.

Liu, H.C., B.Q. Zhu, and Z.X. Zhang (1999) Single zircon dating by LAM-ICPMS technique. *Chinese Science Bulletin* 44, 182-186.

Liu, H.C., Mao, X.L., Yoo, J.H. and Russo, R.E., 1999. Early phase laser induced plasma diagnostics and mass removal during single-pulse laser ablation of silicon. *Spectrochimica Acta Part B*, 54: 1607-1624.

H.P. Longerich, S.E. Jackson, B.J. Fryer and D.F. Strong (1993) The laser ablation microprobe-inductively coupled plasma-mass spectrometer, *Geoscience Canada*, 20: 21-27.

H.P. Longerich, S.E. Jackson and D. Günther (1996) Laser ablation inductively coupled plasma mass spectrometric transient signal data acquisition and analyte concentration calculation, *Journal of Analytical Atomic Spectrometry*, 11: 899-904.

H.P. Longerich, G.A. Jenner, B.J. Fryer and S.E. Jackson (1990) Inductively coupled plasma mass spectrometry analysis of geological samples: a critical evaluation based on case studies, *Chemical Geology*, 83: 105-118.

R.R. Louks, S.M. Eggins, J.M.G. Shelley, L.P.J. Kinsley and N.G. Ware (1995) Development of the inductively-coupled-plasma mass spectrometry ultraviolet laser trace element micro-analyser (ICP-ULTEMA), *Research School of Earth Sciences - Annual report*, 138-140.

Loucks, R. and Mavrogenes, J., 1999. Gold solubility in supercritical hydrothermal brines measured in synthetic fluid inclusions. *Science*, 284: 2159-2163.

J.N. Ludden, R. Feng, G. Gauthier, J. Stix, L. Shi, D. Francis, N. Machado and G. Wu (1995) Applications of LAM-ICP-MS analysis to minerals, *Canadian Mineralogist*, 33: 419-434.

C. Lüdke, E. Hoffmann and J. Skole (1994) Comparative studies on metal determination in airborne particulates by LA-ICP-MS and furnace atomization non-thermal excitation spectrometry, *Fresenius Journal of Analytical Chemistry*, 350: 272-276.

N. Machado, A. Schrank, C.M. Noce and G. Gauthier (1996) Ages of detrital zircon from Archean-Paleoproterozoic sequences: implications for greenstone belt setting and evolution of a Transamazonian foreland basin in Quadrilatero Ferrífero, SE Brazil, *Earth and Planetary Science Letters*, 141: 259-276.

Mahoney, P.P., Li, G. and Hieftje, G.M., 1996. Laser ablation-inductively coupled plasma mass spectrometry with a time-of-flight mass analyser. *Journal of Analytical Atomic Spectrometry*, 11: 401-405.

Mank, A.J.G. and P.R.D. Mason (1999) A critical assessment of laser ablation ICP-MS as an analytical tool for depth analysis in silica-based glass samples. *Journal of Analytical Atomic Spectrometry* 14, 1143-1153.

X.L. Mao, W.T. Chan, M. Caetano, M.A. Shannon and R.E. Russo (1996) Preferential vaporization and plasma shielding during nano-second laser ablation, *Applied Surface Science*, 96: 126-130.

X.L. Mao, W.T. Chan and R.E. Russo (1997) Influence of sample surface condition on chemical analysis using laser ablation inductively coupled plasma atomic emission spectrometry, *Applied Spectroscopy*, 51: 1047-1054.

X.L. Mao, W.T. Chan, M.A. Shannon and R.E. Russo (1993) Plasma shielding during picosecond laser sampling of solid materials by ablation in He versus Ar atmosphere, *Journal of Applied Physics*, 74: 4915-4922.

Mao, X. and R.E. Russo (1997) Observation of plasma shielding by measuring transmitted and reflected laser pulse temporal profiles. *Applied Physics A* 64, 1-6.

Mao, X.L., O.V. Borisov, and R.E. Russo (1998) Enhancements in laser ablation inductively coupled plasma-atomic emission spectrometry based on laser properties and ambient environment. *Spectrochimica Acta Part B-Atomic Spectroscopy* 53, 731-739.

Mao, X.L., et al. (1998) Laser ablation processes investigated using inductively coupled plasma-atomic emission spectroscopy (ICP-AES). *Applied Surface science* 127-129, 262-268.

J. Marshall, J. Franks, I.D. Abell and C.T. Tye (1991) Determination of trace element in solid plastic materials by laser ablation - inductively coupled plasma mass spectrometry, *Journal of Analytical Atomic Spectrometry*, 6: 145-150.

Masters, B.J. and Sharp, B.L., 1997. Universal calibration strategy for laser ablation inductively coupled plasma mass spectrometry based on the use of aqueous standards with modified absorption coefficients. *Analytical Communications*, 34: 237-239.

Mason, P.R.D., Jarvis, K.E., Downes, H. and Vannucci, R., 1999. Determination of incompatible trace elements in mantle clinopyroxenes by LA-ICP-MS: A comparison of analytical performance with established techniques. *Geostandards Newsletter*, 23: 157-172.

T.E. McCandless, M.E. Baker and J. Ruiz (1997) Trace element analysis of natural gold by laser ablation ICPMS, *Geostandards Newsletter*, 21: 271-278.

T.E. McCandless, D.J. Lajack, J. Ruiz and A.M. Gahzi (1997) Trace element determination of single fluid inclusions in quartz by laser ablation ICP-MS, *Geostandard Newsletter*, 21: 271-278.

L. Moenke-Blankenburg (1989) *Laser ablation for direct elemental analysis of solid samples by inductively coupled plasma mass spectrometry*, Wiley, New York, 105 pp.

A. Moissette, T.J. Shepherd and S.R. Chenery (1996) Calibration strategies for the elemental analysis of individual aqueous fluid inclusions by laser ablation inductively coupled plasma mass spectrometry, *Journal of Analytical Atomic Spectrometry*, 11: 177-185.

Moore, L., A. Saint, and A. Gaal (1998) Improvement in inter-element and isotope ratio precision using laser ablation with a ICP Time-Of-Flight MS. *Laser ablation workshop Monash*.

Nolte, J., et al. (1999) The influence of true simultaneous internal standardization and background correction on repeatability for laser ablation and the slurry technique coupled to ICP emission spectrometry. *Journal of Analytical Atomic Spectrometry* 14, 597-602.

Motelica-Heino, M., et al. (1998) Macro and microchemistry of trace metals in vitrified domestic wastes by laser ablation ICP-MS and scanning electron microprobe X-ray energy dispersive spectroscopy. *Talanta* 46, 407-422.

C.A. Morrison, D.D. Lambert, R.J.S. Morrison, W.W. Ahlers and I.A. Nicholls (1995) Laser ablation-inductively coupled plasma-mass spectrometry: an investigation of elemental responses and matrix effects in the analysis of geostandard materials, *Chemical Geology*, 119: 13-29.

Narewski, U., Werner, G., Schulz, H. and Vogt, C., 2000. Application of laser ablation inductively coupled mass spectrometry (LA-ICP-MS) for the determination of major, minor, and trace elements in bark samples. *Fresenius Journal of Analytical Chemistry*, 366: 167-170.

R.W. Nesbitt, T. Hirata, I.B. Butler and J.A. Milton (1997) UV laser ablation ICP-MS: some applications in the Earth sciences, *Geostandard Newsletter*, 21: 232-244.

M. Norman (1988) Melting and metasomatism in the continental lithosphere: laser ablation ICPMS analysis of minerals in spinel lherzolites from Eastern Australia, *Contribution to Mineralogy and Petrology*, 130: 240-255.

M.D. Norman, N.J. Pearson, A. Sharma, W.L. Griffin and S. Shaw (1996) Quantitative analysis of trace elements in geological materials by laser ablation ICPMS: instrumental operation conditions and calibration values of NIST glasses, *Geostandards Newsletter*, 20: 247-261.

Norman, M.D., et al. (1998) Quantitative analysis of trace element abundances in glasses and minerals - a comparison of laser ablation inductively coupled plasma mass spectrometry,

solution inductively coupled plasma mass spectrometry, proton microprobe and electron microprobe data. *Journal of Analytical Atomic Spectrometry* 13, 477-482.

Ødegård, M. and M. Hamester (1997) Preliminary investigation into the use of a high resolution inductively coupled plasma mass spectro, meter with laser ablation for bulk analysis of geological materials fused with Li₂B₄O₇, *Geostandard Newsletter*, 21: 245-252.

Ødegård, M., et al. (1998) Application of a double-focussing magnetic sector inductively coupled plasma mass spectrometer with laser ablation for the bulk analysis of rare earth elements in rocks fused with Li₂B₄O₇. *Fresenius Journal of Analytical Chemistry* 362, 477-482.

Ødegård, M. (1998) Preparation of Oxidic calibration materials for the use in laser ablation-Inductively Coupled Plasma Mass Spectrometry and other Microtechniques for mineral analysis. - Preliminary results of experiments by direct fusion in high purity graphite electrodes. Laser ablation workshop Monash .

P.M. Outridge, W. Doherty and D.C. Gregoire (1996) The formation of trace element-enriched particulates during laser ablation of refractory materials, *Spectrochimica Acta Part B*, 51: 1451-1462.

P.M. Outridge, W. Doherty and D.C. Gregoire (1998) Determination of trace elemental signatures in placer gold by laser ablation-inductively coupled plasma-mass spectrometry as a potential aid for gold exploration, *Journal of Geochemical Exploration*, 60: 229-240.

P.M. Outridge and R.D. Evans (1995) Effect of laser parameters and tooth type on the ablation of trace metals from mammalian teeth, *Journal of Analytical Atomic Spectrometry*, 10: 595-600.

Outridge, P.M., Doherty, W. and Gregoire, D.C., 1997. Ablative transport fractionation of trace elements during laser sampling of glass and copper. *Spectrochimica Acta Part B*, 52: 2093-2102.

Paul, M., 1994. Analysis of solid samples by laser sampling ICP-MS. *Atomiv Spectrometry*, 9: 21-26.

N. Pearce and G. Schettler (1994) Trace element uptake by mussels in a recently decreased community, Lake Breitling, Germany - a laser ablation ICP-MS study, *Environmental Geochemistry & Health*, 16: 79.

N.J.G. Pearce, W.T. Perkins, I. Abell, G.A.T. Duller and R. Fuge (1992) Mineral microanalysis by laser ablation inductively coupled plasma mass spectrometry, *Journal of Analytical Atomic Spectrometry*, 7: 53-57.

N.J.G. Pearce, W.T. Perkins and R. Fuge (1992) Development in quantitative and semi-quantitative determination of trace elements in carbonates using laser ablation inductively coupled plasma mass spectrometry, *Journal of Analytical Atomic Spectrometry*, 7: 595-598.

N.J.G. Pearce, W.T. Perkins, J.A. Westgate, M.P. Gorton, S.E. Jackson, C.R. Neal and S.P. Chenery (1997) A compilation of new and published major and trace element data for NIST SRM 610 and NIST SRM 612 glass reference materials, *Geostandards Newsletter*, 21: 115-144.

W.T. Perkins, R. Fuge and N.J.G. Pearce (1991) Quantitative analysis of trace elements in carbonates using laser ablation inductively coupled plasma mass spectrometry, *Journal of Analytical Atomic Spectrometry*, 6: 445-449.

W.T. Perkins and N.J.G. Pearce (1995) Mineral microanalysis by laserprobe inductively coupled plasma mass spectrometry, Chapman & Hall, London, 291-325 pp.

W.T. Perkins, N.J.G. Pearce and R. Fuge (1992) Analysis of zircon by laser ablation and solution inductively coupled plasma mass spectrometry, *Journal of Analytical Atomic Spectrometry*, 7: 612-616.

W.T. Perkins, N.J.G. Pearce and T.E. Jeffries (1993) Laser ablation inductively coupled plasma mass spectrometry: a new technique for the determination of trace and ultra-trace elements in silicates, *Geochimica et Cosmochimica Acta*, 57: 475-482.

W.T. Perkins, N.J.G. Pearce and J.A. Westgate (1997) The development of laser ablation ICP-MS and calibration strategies: examples from the analysis of trace elements in volcanic glass shards and sulfide minerals, *Geostandards Newsletter*, 21: 175-190.

Pickhardt, C., Brenner, I.B., Becker, J.S. and Dietze, H.-J., 2000. Determination of trace elements in zeolites by laser ablation ICP-MS. *Fresenius J. Anal. Chem.*, 368: 79-97.

Poitrasson, F., Chenery, S. and Bland, D.J., 2000a. Contrasted monazite hydrothermal alteration mechanisms and their geochemical implications. *Earth and Planetary Science Letters*, 145: 79-96.

Poitrasson, F., Chenery, S. and Shepherd, T.J., 2000b. Electron microprobe and LA-ICP-MS study of monazite hydrothermal alteration: implications for U-Th-Pb geochronology and nuclear ceramics. *Geochimica Cosmochimica Acta*, 64: 3283-3297.

Price, G.D. and Pearce, N.J.G., 1997. Biomonitoring of pollution by cerastoderma edule from the British Isles: a laser ablation ICP-MS study. *Marine pollution bulletin*, 34: 1025-1031.

A. Raith and R.C. Hutton (1994) Quantification methods using laser ablation ICP-MS . Part 1: Analysis of powders, *Fresenius Journal of Analytical Chemistry*, 350: 242-246.

A. Raith, R.C. Hutton, I.D. Abell and J. Crighton (1995) Non-destructive sampling method of metals and alloys for laser ablation-inductively coupled plasma mass spectrometry, *Journal of Analytical Atomic Spectrometry*, 10: 591-594.

A. Raith, R.C. Hutton and J. Godfrey (1996) Quantitation methods using laser ablation ICP-MS . Part 2: Evaluation of new glass standards, *Fresenius Journal of Analytical Chemistry*, 354: 163-168.

Raith, A., Perkins, W.T., Pearce, N.J.G. and Jeffries, T.E., 1996. ENVIRONMENTAL MONITORING ON SHELLFISH USING UV LASER ABLATION ICP-MS. *Fresenius Journal of Analytical Chemistry*, 355: 789-792.

M.H. Ramsey, B.J. Coles, A.H. Rankin and J.J. Wilkinson (1992) Single fluid inclusion analysis by laser ablation-inductively coupled plasma-atomic emission.

A.H. Rankin, M.H. Ramsey, B. Coles, F. Van Langevelde and C.R. Thomas (1992) The composition of hypersaline, iron-rich granitic fluids based on laser-ICP and synchrotron-XRF microprobe analysis of individual fluid inclusions in topaz, Mole granite, eastern Australia, *Geochimica Cosmochimica Acta*, 56: 67-79.

Rauch, S., Morrison, G.M., Motelica-Heino, M., Donard, O.F.X. and Muris, M., 2000. Elemental association and fingerprinting of traffic related metals in road sediments. *Environmental Science & Technology*, 34: 3119-3123.

Reid, J.E., Horn, I., Longrich, H.P., Forsythe, L. and Jenner, G.A., 1999. Determination of Zr and Hf in a flux-free fusion of whole rock samples using laser ablation inductively coupled plasma-mass spectrometry (LA-ICP-MS) with isotope dilution calibration. *Geostandards Newsletter*, 23: 149-155.

Richner, P., Evans, D., Wahrenberger, C. and Dietrich, V., 1994. Applications of laser ablation and electrothermal vaporization as sample introduction techniques for ICP-MS. *Fresenius Journal of Analytical Chemistry*, 350: 235-241.

A.B.E. Rocholl, K. Simon, K.P. Jochum, F. Bruhn, R. Gehann, U. Kramar, W. Luecke, M. Molzahn, E. Pernicka, M. Seufert, B. Spettel and J. Stummeier (1997) Chemical characterisation of NIST silicate glass certified reference material SRM 610 by ICP-MS, TIMS, LIMS, SSMS, INAA and PIXE, *Geostandards Newsletter*, 21: 101-114.

Rodushkin, I., Axelsson, M.D. and Burman, E., 2000. Multielement analysis of coal by ICP techniques using solution nebulization and laser ablation. *Talanta*, 51(4): 743-759.

Rodushkin, I. and Axelsson, M.D., 2000. Application of double focusing sector field ICP-MS for multielemental characterization of human hair and nails. Part I. Analytical methodology. *Science of the Total Environment*, 250: 83-100.

Russo, R.E., X. Mao, and O.V. Borisov (1998) Laser ablation sampling. *Trends in Analytical Chemistry* 17, 461-469.

R.E. Russo (1995) Laser Ablation, *Applied Spectroscopy*, 49: A14-A28.

R.E. Russo, X. Mao, L.L., M. Caetano and M.A. Shannon (1996) Fundamental characteristics of laser-material interactions (ablation) in noble gases at atmospheric pressure using inductively coupled plasma-atomic emission spectroscopy, *Applied Surface Science*, 96: 144-148.

Russo, R.E., Mao, X.L., Liu, H.C., Yoo, J.H. and Mao, S.S., 1999. Time-resolved plasma diagnostics and mass removal during single-pulse laser ablation. *Appl. Phys.*, A69: S887-S894.

H. Scholze, E. Hoffmann, C. Ludke and A. Platalla (1996) Analysis of leaves by using the laser ICP-MS with isotope dissolution method, *Fresenius Journal of Analytical Chemistry*, 355: 892-894.

H. Scholze, H. Stephanowitz, E. Hoffmann and J. Skole (1994) Element analysis of inhomogeneous samples by laser ablation, *Fresenius Journal of Analytical Chemistry*, 350: 247-252.

Schroeder, E., M. Hamester, and M. Kaiser (1998) Properties and characteristics of a laser ablation ICP-MS system for the quantitative elemental analysis of glasses. *Applied Surface Science* 129, 292-298.

D.J. Scott and G. Gauthier (1996) Comparison of TIMS (U-Pb) and laser ablation microprobe ICP-MS (Pb) techniques for age determination of detrital zircons from Paleoproterozoic metasedimentary rocks from northeastern Laurentia, Canada, with tectonic implications, *Chemical Geology*, 131: 127-142.

Scott, D.J. (1999) U-Pb geochronology of the eastern Hall Peninsula, southern Baffin Island, Canada: a northern link between the Archean of West Greenland and the Paleoproterozoic Torngat Orogen of northern Labrador. *Precambrian Research* 93, 5-26.

Shaohai, C., et al. (1998) Trace element characteristics in the diopsides of peridotite xenoliths; a laser ablation-inductively coupled plasma-mass spectrometry study. *Chinese Science Bulletin* 43, 579-583.

T.J. Sheppherd and S.R. Chenery (1995) Laser ablation ICP-MS elemental analysis of individual fluid inclusions: An evaluation study, *Geochimica Cosmochimica Acta*, 59: 3997-4007.

Shibata, Y., Yoshinaga, J. and Morita, M., 1993. Micro-laser ablation system combined with inductively coupled plasma mass spectrometry for the determination of elemental composition in the micron range. *Analytical Sciences*, 9: 129-131.

Shibuya, E.K., et al. (1998) Determination of platinum group elements and gold in geological materials using an ultraviolet laser ablation high-resolution inductively coupled plasma mass spectrometric technique. *Journal of Analytical Atomic Spectrometry* 13, 941-944.

Shuttleworth, S. and D.T. Kremser (1998) Assessment of laser ablation and sector field inductively coupled plasma mass spectrometry for elemental analysis of solid samples. *Journal of Analytical Atomic Spectrometry* 13, 697-699.

Siddaiah, N.S. and A. Masuda (1997) Preconcentration of noble metals in geological and environmental samples: a nickel sulfide Mini-bead technique. *Proceedings of the Japan Academy Series B-Physical & Biological Sciences* 73 B, 13-18.

Sie, S.H. (1997) Nuclear microprobe in geological applications - where do we go from here. *Nuclear instrument and methods in Physics Research* 130B, 592-607.

D.J. Sinclair and M.T. McCulloch (1997) The coral record of terrestrial fluxes into the Great Barrier Reef: Analysis of trace elements in inshore corals by laser-ablation ICP-MS, RSES - Annual report, 138-139.

Sinclair, D.J., L.P.J. Kinsley, and M.T. McCulloch (1998) High resolution analysis of trace elements in corals by laser ablation ICP-MS. *Geochimica et Cosmochimica Acta* 62, 1889-1901.

R. Stalder, S.F. Foley, G.P. Brey, L.M. Forsythe and I. Horn (1997) First results from a new experimental technique to determine fluid/solid trace element partition coefficients using diamond aggregate extraction traps, *N Jb Miner Abh*, 172: 117-132.

Stix, J., G. Gauthier, and J. Ludden (1995) A critical look at quantitative-laser-ablation ICP-MS analysis of natural and synthetic glasses. *Canadian Mineralogist* 33, 435-444.

S.J. Stotesbury, J.M. Pickering and M.A. Grifferty (1989) Analysis of lithium and Boron by inductively coupled plasma mass spectrometry, *Journal of Analytical Atomic Spectrometry*, 4: 457-460.

P. Sylvester and M. Ghaderi (1997) Trace element analysis of scheelite by excimer laser ablation-inductively coupled plasma-mass spectrometry (ELA-ICP-MS) using a synthetic silicate glass standard, *Chemical Geology*, 141: 49-65.

P.J. Sylvester (1997) New technique using laser ablation blasts into geochemical labs, *EOS Trans Am Geophys Union*, 78: 117-120.

P.J. Sylvester and S.M. Eggins (1997) Analysis of re, Au, Pd, Pt and Rh in NIST glass certified reference materials and natural basalt glasses by laser ablation ICP-MS, *Geostandard Newsletter*, 21: 215-230.

Tanaka, S., et al. (1998) Rapid and simultaneous multi-element analysis of atmospheric particulate matter using inductively coupled plasma mass spectrometry with laser ablation sample introduction. *Journal of Analytical Atomic Spectrometry* 13, 135-140.

P.D.P. Taylor, P. De Bièvre, A.J. Walder and A. Entwistle (1995) Validation of the analytical linearity and mass discrimination correction model exhibited by a multiple collector inductively coupled plasma mass spectrometer by means of a set of synthetic uranium isotope mixtures, *Journal of Analytical Atomic Spectrometry*, 10: 395-398.

R.P. Taylor, S.E. Jackson, H.P. Longerch and J.D. Webster (1997) In situ trace-element analysis of individual silicate melt inclusions by laser ablation microprobe-inductively coupled plasma-mass spectrometry (LAM-ICP-MS), *Geochimica et Cosmochimica Acta*, 61: 2559-2567.

Taylor, M.E., Blaney, D.L. and Cardell, G., 2000. Elemental fractionation in ultraviolet laser ablation sampling of igneous silicate minerals relevant to Mars. *Applied Surface Science*, 165: 166-177.

M.F. Thirlwall and A.J. Walder (1995) In situ hafnium isotope ratio analysis of zircon by inductively coupled plasma multiple collector mass spectrometry, *Chemical Geology*, 122: 241-247.

M. Thompson, S. Chenery and L. Brett (1990) Nature of particulate matter produced by laser ablation-Implications for tandem analytical systems, *Journal of Analytical Atomic Spectrometry*, 5: 49-55.

Thompson, G.M. and Malpas, J., 2000. Mineral/melt partition coefficients of oceanic alkali basalts determined on natural samples using laser ablation-inductively coupled plasma-mass spectrometry (LAM-ICP-MS). *Mineralogical Magazine*, 64: 85-94.

Thorrold, S.R. and Shuttleworth, S., 2000. In situ analysis of trace elements and isotope ratios in fish otoliths using laser ablation sector field inductively coupled plasma mass. *Canadian Journal of Fisheries & Aquatic Sciences*, 57(6): 1232-1242.

M. Totland, I. Jarvis and K.E. Jarvis (1992) An assessment of dissolution techniques for the analysis of geological samples by plasma spectrometry, *Chemical Geology*, 95: 35-62.

K. Ulens, L. Moens, R. Dams, S. Vanwinckel and L. Vandeveldel (1994) Study of element distributions in weathered marble crusts using laser ablation inductively coupled plasma mass spectrometry, *Journal of Analytical Atomic Spectrometry*, 9: 1243-1248.

Ulrich, T., D. Günther, and C.A. Heinrich (1999) Gold concentrations of magmatic brines and the metal budget of porphyry copper deposits. *Nature* 399, 676-679.

Van Achterbergh, E., C.G. Ryan, and W.L. Griffin (1998) GLITTER: On-line interactive data reduction for the LA-ICPMS microprobe. Laser ablation workshop Monash .

A.A. Van Heuzen and J.B.W. Morsink (1991) Analysis of solids by laser ablation - inductively coupled plasma - mass spectrometry (LA-ICP-MS) - II. Matching with a pressed pellet, *Spectrochimica Acta*, 46B: 1819-1928.

D.A. Vanko, S.R. Sutton, M.L. Rivers and R.J. Bodnar (1993) Major-element ratios in synthetic fluid inclusions by synchrotron X-ray fluorescence microprobe, *Chemical geology*, 107: 125-134.

Vander Putten, E., Dehairs, F., Keppens, E. and Baeyens, W., 2000. High resolution distribution of trace elements in the calcite shell layer of modern *Mytilus edulis*: Environmental and biological controls. *Geochimica et Cosmochimica Acta*, 64: 997-1011.

A.J. Walder, I.D. Abell, I. Platzner and P.A. Freedman (1993) Lead isotope ratio of NIST 610 glass by laser ablation inductively coupled plasma mass spectrometry, *Spectrochimica Acta*, 48B: 397-402.

A.J. Walder and N. Furuta (1993) High-precision lead isotope ratio measurement by inductively coupled plasma multiple collector mass spectrometry, *Analytical Sciences*, 9: 675-680.

A.J. Walder, D. Koller, N.M. Reed, R.C. Hutton and P.A. Freedman (1993) Isotope ratio measurement by inductively coupled plasma multiple collector mass spectrometry incorporating a high efficiency nebulization system, *Journal of Analytical Atomic Spectrometry*, 8: 1037-1041.

A.J. Walder, I. Platzner and P.A. Freedman (1993) Isotope ratio measurement of lead, neodymium and neodymium-samarium mixtures, hafmium and hafmium-lutetium mixtures with a double focussing multiple collector inductively coupled plasma mass spectrometer, *Journal of Analytical Atomic Spectrometry*, 8: 19-23.

Watling, R.J. (1998) In-line mass transport measurement cell for improving quantification in sulfide mineral analysis using laser ablation inductively coupled plasma mass spectrometry. *Journal of Analytical Atomic Spectrometry* 13, 927-934.

R.C. Watling, H.K. Herbert and I.D. Abell (1995) The application of laser ablation - inductively coupled plasma mass spectrometry (LA-ICP-MS) to the analysis of selected sulphide minerals, *Chemical Geology*, 124: 67-81.

R.J. Watling, H.K. Herbert, I.S. Barrow and A.G. Thomas (1995) Analysis of diamond and indicator minerals for diamond exploration by laser ablation-inductively coupled plasma mass spectrometry, *Analyst*, 120: 1357-1364.

R.J. Watling, H.K. Herbert, D. Delev and I.D. Abell (1994) Gold fingerprinting by laser ablation inductively coupled mass spectrometry, *Spectrochimica Acta*, 49B: 205-291.

S.A. Watmough, T.C. Hutchinson and R.D. Evans (1997) Application of laser ablation inductively coupled plasma-mass spectrometry in dendrochemical analysis, *Environmental Science & Technology*, 114-118.

Watmough, S.A., T.C. Hutchinson, and R.D. Evans (1998) The quantitative analysis of sugar maple tree rings by laser ablation in conjunction with ICP-MS. *Journal of Environmental Quality* 27, 1087-1094.

Watmough, S.A., T.C. Hutchinson, and R.D. Evans (1998) Development of solid calibration standards for trace elemental analyses of tree rings by laser ablation inductively coupled plasma-mass spectrometry. *Environmental Science & Technology* 32, 2185-2190.

J.A. Westgate, W.T. Perkins, R. Fuge, N.J.G. Pearce and A.G. Wintle (1994) Trace element analysis of volcanic glass shards by LA-ICP-MS: application to tephrochronological studies, *Applied Geochemistry*, 9: 323-335.

M. Wiedenbeck, P. Allé, F. Corfu, W.L. Griffin, M. Meier, F. Oberli, A. Von Quadt, J.C. Roddick and W. Spiegel (1995) Three natural zircon standards for U-Th-Pb, Lu-Hf, trace element and REE analyses, *Geostandards Newsletter*, 19: 1-23.

D. Wiederin and M. Hamster (1997) Order of improvement in sector-field ICP-MS performance using a Pt Guard Electrode, Winter Plasma conference.

J.J. Wilkinson, A.H. Rankin, S.C. Mulshaw, J. Nolan and M.H. Ramsey (1994) Laser ablation-ICP-AES for the determination of metals in fluid inclusions: An application to the study of magmatic fluids, *Geochimica et Cosmochimica Acta*, 58: 1133-1146.

Wolf, R.E., C. Thomas, and A. Bohlke (1998) Analytical determinations of metals in industrial polymers by laser ablation ICP-MS. *Applied Surface Science* 129, 299-303.

G. Wu and C. Hillaire-Marcel (1995) Application of LP-ICP-MS to benthic foraminifers, *Geochimica et Cosmochimica Acta*, 59: 409-414.

Yang, P., T. Rivers, and S.E. Jackson (1999) Crystal-chemical and thermal controls on trace-element partitioning between coexisting garnet and biotite in metamorphic rocks from western Labrador. *Canadian Mineralogist* 37, 443-468.

Yang, P.S. and Rivers, T., 2000. Trace element partitioning between coexisting biotite and muscovite from metamorphic rocks, Western Labrador: Structural, compositional and thermal controls. *Geochimica et Cosmochimica Acta*, 64: 1451-1472.

Yoon, Y.Y., Kim, T.S., Chung, K.S., Lee, K.Y. and Lee, G.H., 1997. Application of laser induced plasma spectroscopy to the analysis of rock samples. *The Analyst*, 122: 1223-1227.

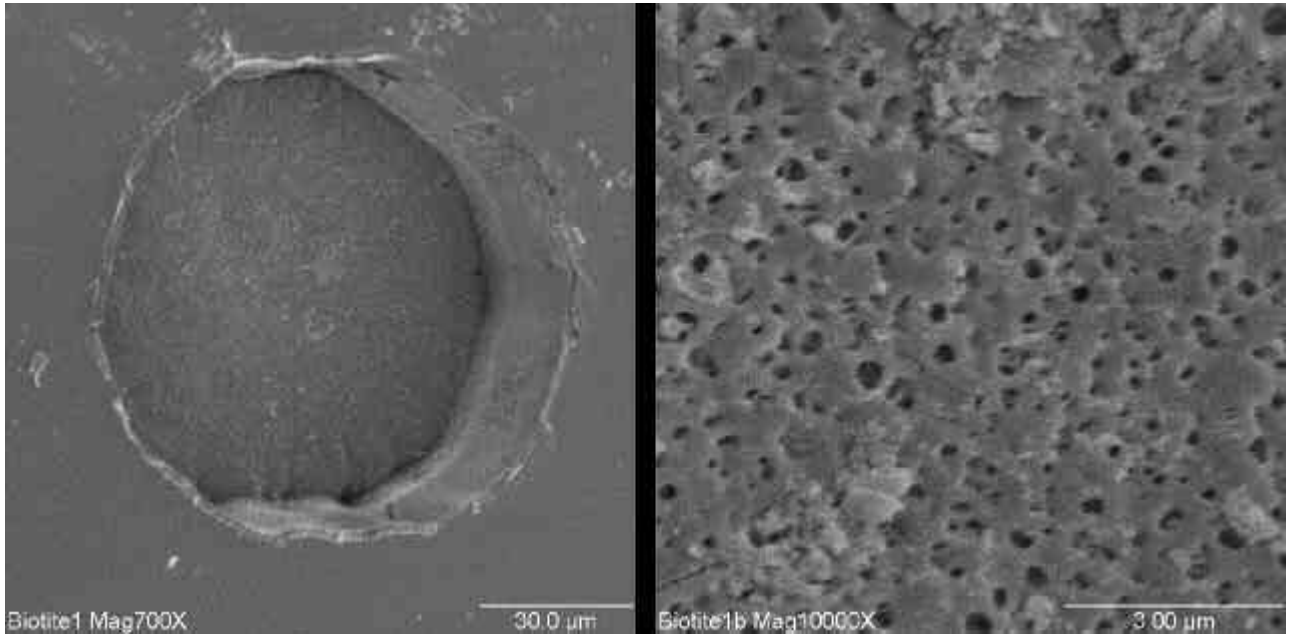
T. Zack, S.F. Foley and G.A. Jenner (1997) A consistent partition coefficient set for clinopyroxene, amphibole and garnet from laser ablation microprobe analysis of garnet pyroxenites from Kakanui, New Zealand, *N Jb Miner Mh*, 172: 23-41.

Laser Ablation Pits on Minerals

The morphology of the pits will depend on the optical properties and the chemistry of the mineral which will generate different power density per volume on different matrix at the same fluence.

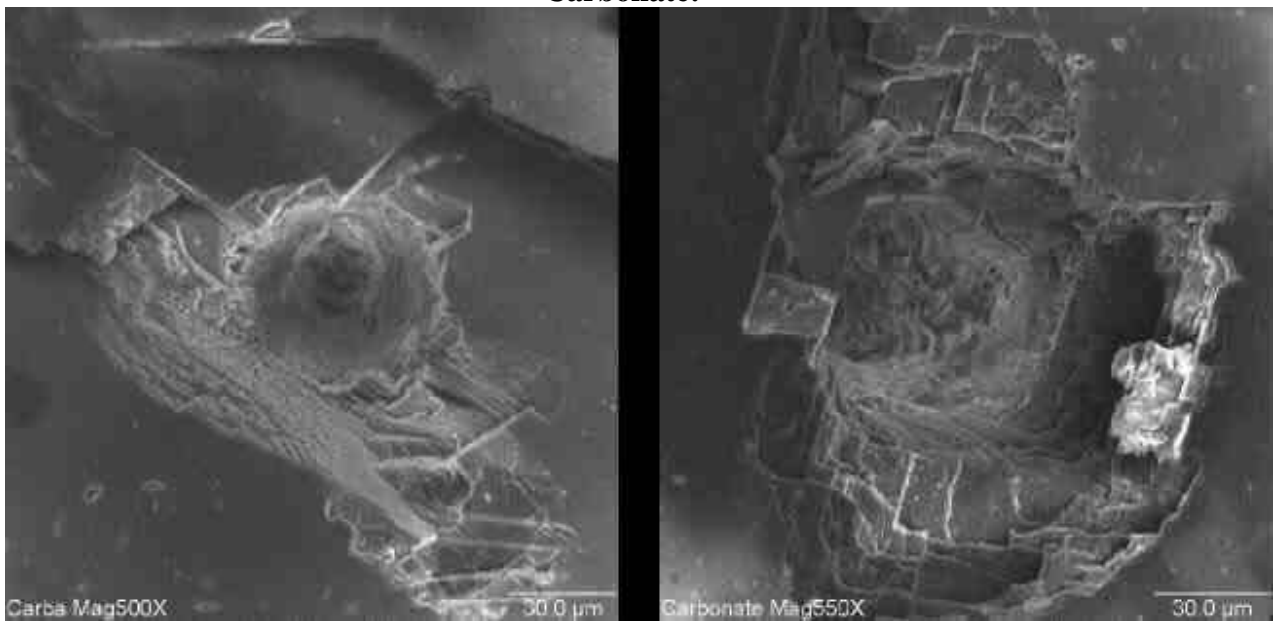
See for example the differences between the dark biotite and the transparent carbonate.

Biotite:



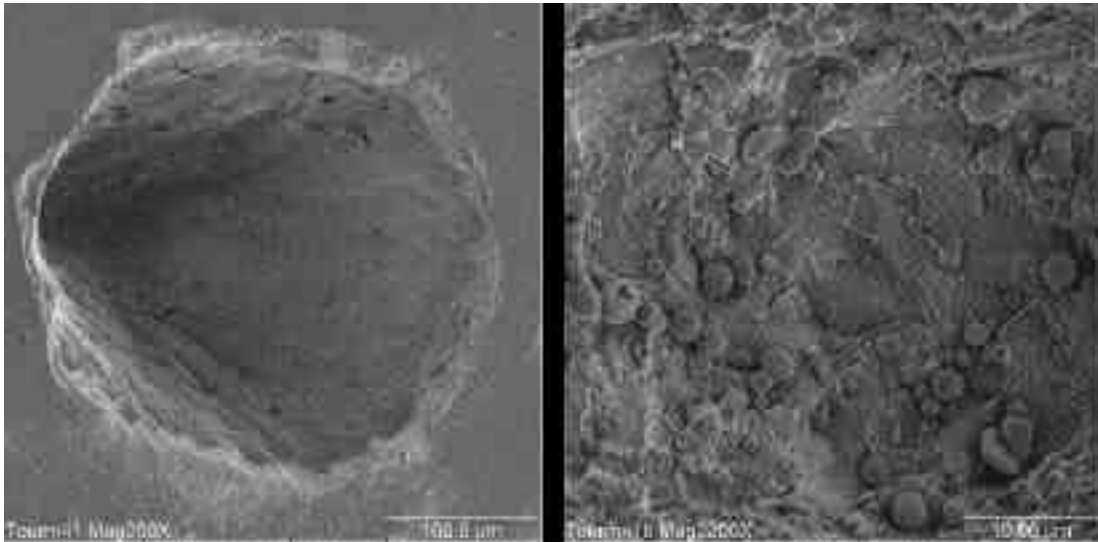
OUTSIDE-----INSIDE

Carbonate:



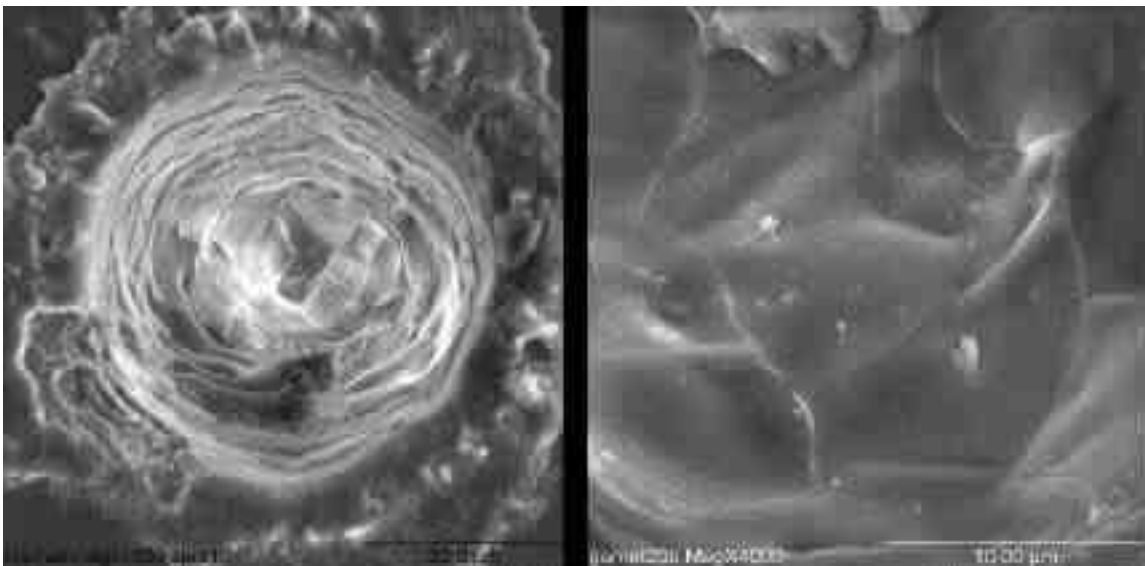
OUTSIDE-----INSIDE

Apatite:



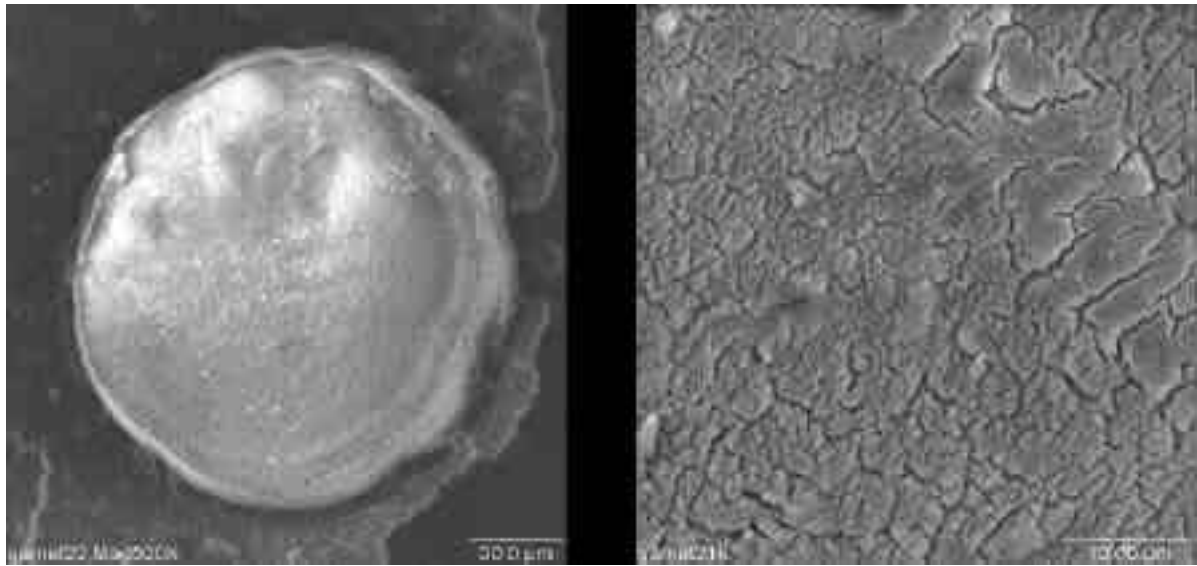
OUTSIDE-----INSIDE

Garnet 1 (transparent):



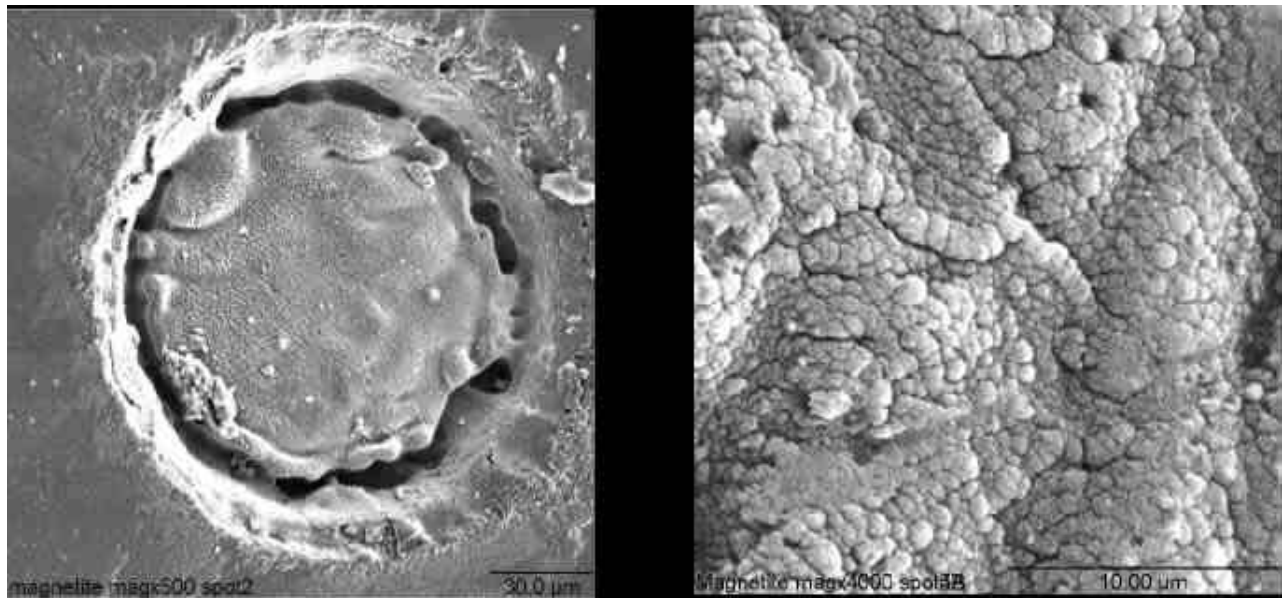
OUTSIDE-----INSIDE

Garnet 1 (dark):



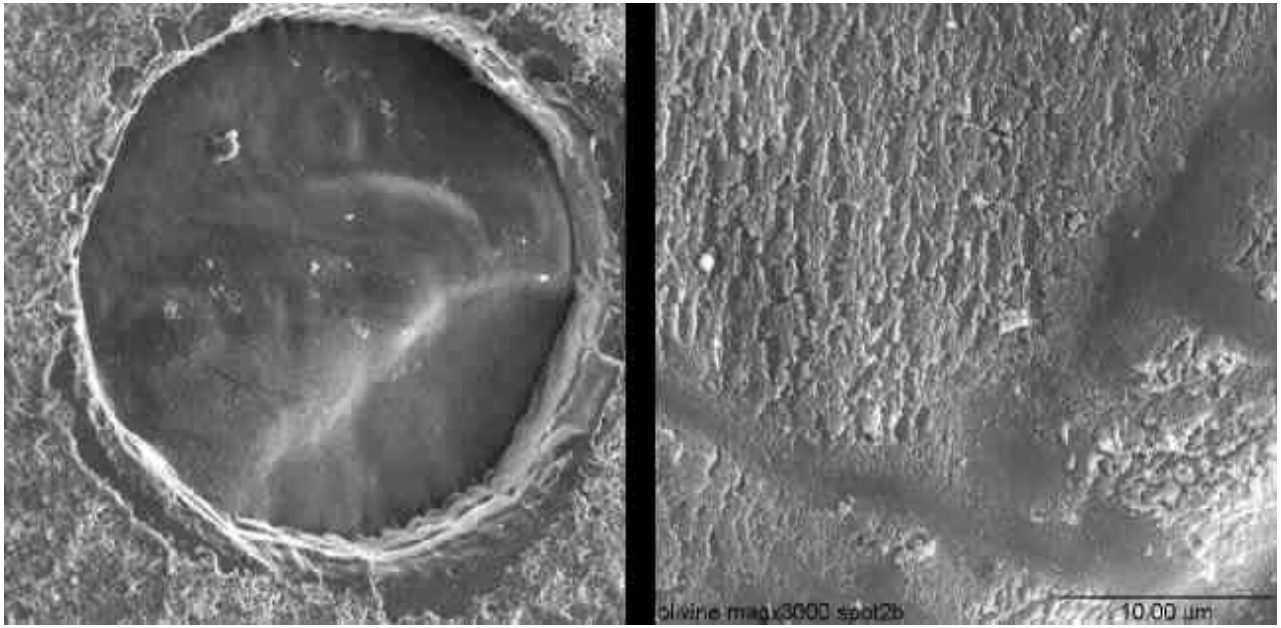
OUTSIDE-----INSIDE

Magnetite:



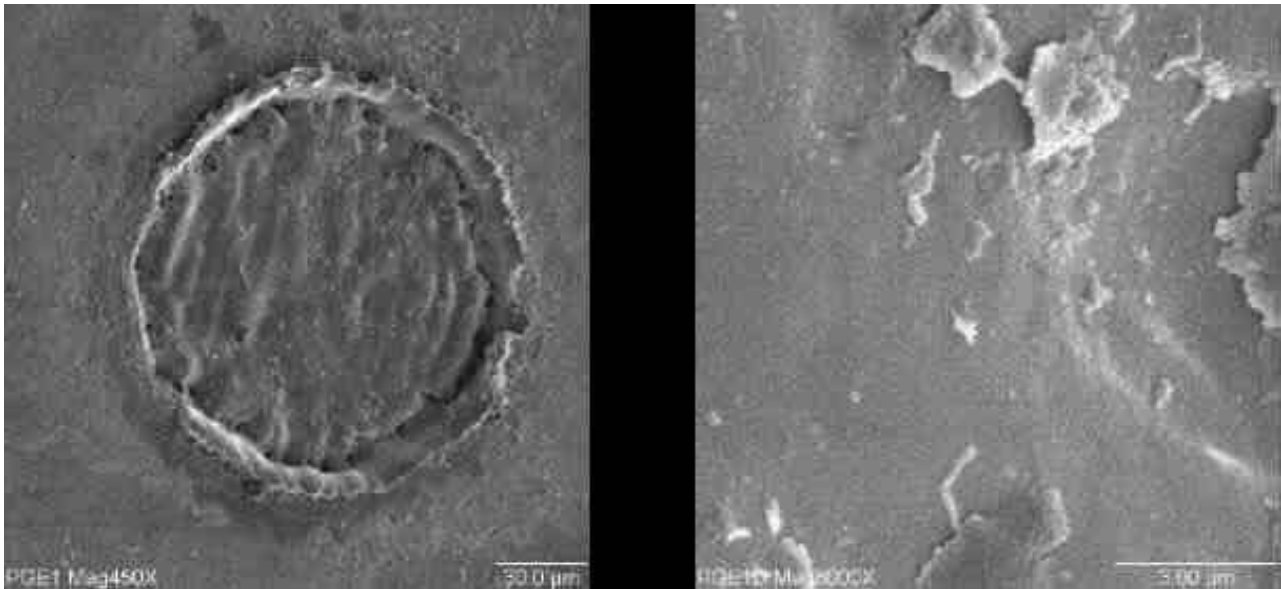
OUTSIDE-----INSIDE

Olivine:



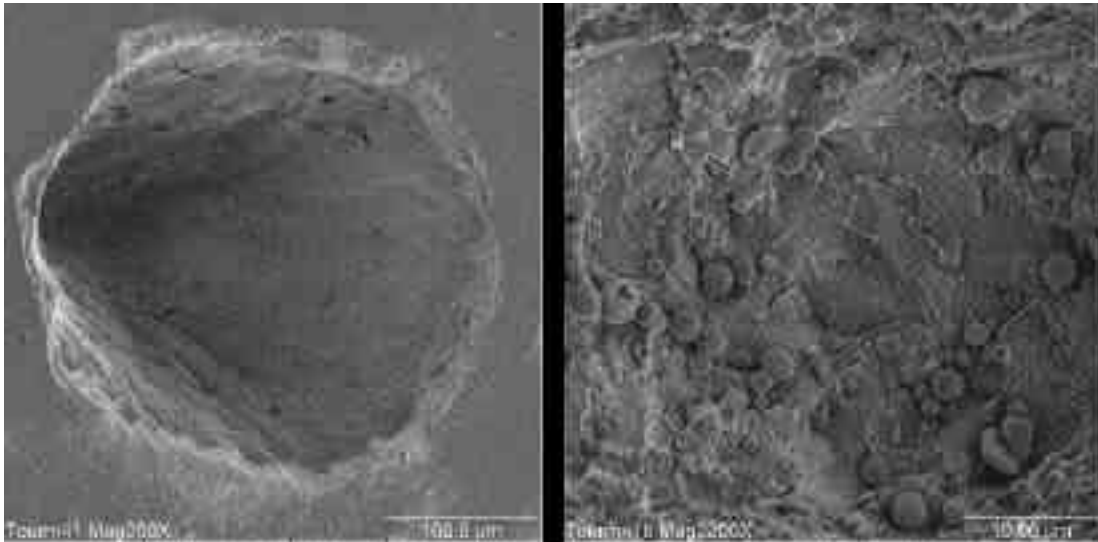
OUTSIDE-----INSIDE

Sulphide:



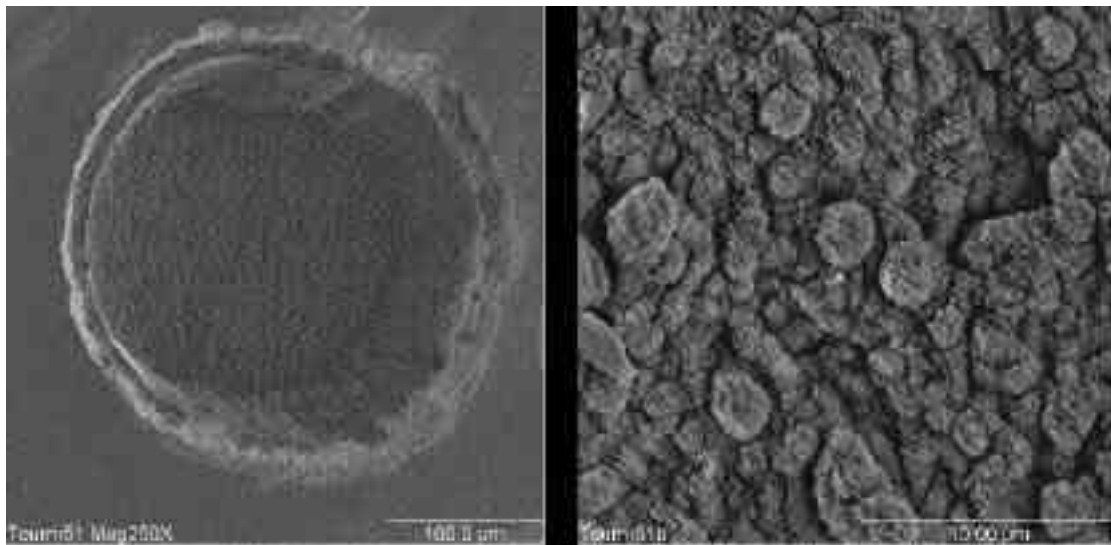
OUTSIDE-----INSIDE

Tourmaline 1 (transparent):



OUTSIDE-----INSIDE

Tourmaline 1 (dark):



OUTSIDE-----INSIDE